

International  
Progress Report

**IPR-06-35**

# Äspö Hard Rock Laboratory

## Canister Retrieval Test

Sensors data report  
(Period 001026-060501)  
Report No:12

Reza Goudarzi  
Lennart Börgesson  
Clay Technology AB

Kennert Röshoff  
Martin Edelman

BBK

May 2006

***Svensk Kärnbränslehantering AB***

Swedish Nuclear Fuel  
and Waste Management Co  
Box 5864  
SE-102 40 Stockholm Sweden  
Tel 08-459 84 00  
+46 8 459 84 00  
Fax 08-661 57 19  
+46 8 661 57 19



**Äspö Hard Rock  
Laboratory**



Report no.  
**IPR-06-35**

Author  
**Reza Goudarzi**  
**Lennart Börgesson**  
**Kennert Röshoff**  
**Martin Edelman**

Checked by  
**Lennart Börgesson**

Approved  
**Anders Sjöland**

No.  
**F69K**

Date  
**May 2005**

Date  
**2007-01-10**

Date  
**2007-01-25**

# Äspö Hard Rock Laboratory

## Canister Retrieval Test

### Sensors data report (Period 001026-060501) Report No:12

Reza Goudarzi  
Lennart Börgesson  
Clay Technology AB

Kennert Röshoff  
Martin Edelman

BBK

May 2006

**Keywords:** Buffer, Bentonite, Rock, Temperature, Stress, Strain, Test, Measurements, Swelling, Full scale, In-situ

This report concerns a study which was conducted for SKB. The conclusions and viewpoints presented in the report are those of the author(s) and do not necessarily coincide with those of the client.



## Abstract

This report presents data from the measurements in the Canister Retrieval Test from 001026 to 060501. It is the final data report from this test, since the test was interrupted and the bentonite excavated during spring 2006.

The following measurements were made in the bentonite: Temperature was measured in 32 points, total pressure in 27 points, pore water pressure in 14 points and relative humidity in 55 points. Temperature was also measured by all relative humidity gauges. The positions of the measuring points in the bentonite are related to a coordinate system in the deposition hole.

The following measurements were made in the rock: Temperature was measured in 40 points, stresses were measured in 8 points and strain was measured in 9 points. Stresses and strains were also measured in the rock around the empty deposition hole located 6 m south of the test hole.

The following measurements were made in the canister: Temperature was measured every meter along two fiber optic cables and strain was measured in 76 points on the surface of the copper envelop. Temperature was measured in the steel insert in 18 points.

The following measurements were made on the plug: Force was measured in 3 of the 9 anchors and vertical displacement was measured in three points.

The water inflow to the filter mats on the rock surface was also measured.

The general conclusion is that the measuring systems and transducers worked well except for the heaters, the transducers inside the canister and Kulite pressure transducers in the bentonite. The strain measurements in the canister are not reported due to question marks regarding the relevance of the results.

Most Vaisala relative humidity transducers stopped yielding results due to full water saturation. Four out of six Kulite total pressure transducers seem to have yielded erroneous results. All temperature sensors inside the canister stopped functioning at an early stage.

The heat power of the canister was successively reduced due to failure of heaters. After the latest failure in March 2005 only 4 out of 36 heaters were still working and the power was kept constant at about 1150 W. On October 11 2005 (day 1811) the power was switched off in order to prepare for the dismantling, excavation and retrieval of the test, which started in the beginning of 2006.

The water pressure in the mats attached to the wall of the deposition hole was reduced to atmospheric in March 2005 in order to try to keep the last heaters alive, which resulted in that the water inflow stopped as well as the increase in force acting on the plug.

The plug was dismounted 060116 (day 1908) and the excavation of the buffer started shortly after. The manual excavation and sampling was finished 060316. Testing of the heaters was done in April (days 1979-2002) by applying a power of 2000 W. The retrieval of the canister with salt water flushing was done in May.



# Sammanfattning

I denna rapport presenteras data från mätningar i Återtagsprojektet under perioden 001026-060501. Det är den sista datarapporten eftersom försöket avbröts och bentoniten grävdes ur under våren 2006.

Följande mätningar gjordes i bentoniten: Temperaturen mättes i 32 punkter, totaltryck i 27 punkter, porvattentryck i 14 punkter och relativa fuktigheten i 55 punkter. Temperaturen mättes även i alla relativa fuktighetsmätare. Varje mätpunkt relateras till ett koordinatsystem i deponeringshålet.

Följande mätningar gjordes i berget: Temperaturen mättes i 40 punkter, bergspänningar mättes i 8 punkter och töjningar i 9 punkter. Bergspänningar och töjningar mättes också i berget runt det tomma deponeringshålet 6 m söder om försökshålet.

Följande mätningar gjordes på ytan i kapselns kopparhölje: Temperaturen mättes varje meter längs två fiberoptiska kablar och töjning mättes i 76 punkter. Temperaturen mättes i stålinsatsen i kapseln i 18 punkter.

Följande mätningar gjordes på pluggen: Kraften mättes i 3 av de 9 stagen och vertikala förskjutningen mättes i tre punkter.

Vatteninflödet till filtermattorna mättes också.

En generell slutsats är att mätsystemen och givarna tycks ha fungerat bra förutom värmarna, givarna inuti kapseln och Kulites givare. Töjningsmätningarna i kapseln har inte redovisats p. g. a frågetecken beträffande mätresultatens relevans.

De flesta av Vaisalas relativa fuktighetsmätare, hade slutat fungera innan brytningen p. g. a. hög vattenmättnadsgrad. Fyra av sex Kulite totaltrycksgivare tycks ha gett felaktiga resultat. Alla temperaturgivare inuti kapseln hade slutat fungera tidigt.

Värmeeffekten i kapseln reducerades succesivt p.g.a. att värmarna gick sönder. Efter det sista avbrottet som skedde i mars 2005 fungerade bara 4 av 36 värmare och effekten hölls sedan dess konstant till c:a 1150 W. Den 11 oktober 2005 (dag 1811) stängdes effekten av för att förbereda för brytning av försöket och demonstration av återtaget. Brytningen startade i början av 2006.

Vattentrycket i bevättningsmattorna på deponeringshållsväggen sänktes till atmosfärstryck i mars 2005 i ett försök att hålla de sista värmarna vid liv, vilket fick till följd att vatteninflödet upphörde liksom ökningen av krafterna på pluggen.

Pluggen demonterades 060116 (dag 1908) och urgrävningen av bufferten started strax därefter. Den manuella urgrävningen och provtagningen ner till halva kapseln var klar 060316. Test av värmarnas funktion utfördes i april (dagarna 1979-2002) genom att effekten 2000 W lades på. Återtaget av kapseln med spolning av saltlösning utfördes i maj.





# Contents

<b>1</b>	<b>Introduction</b>	<b>9</b>
<b>2</b>	<b>Comments</b>	<b>11</b>
2.1	General	11
2.2	Total pressure, Geokon (App. A pages 35-38)	12
2.3	Total Pressure, Kulite (App. A page 39)	12
2.4	Suction, Wescore Psychrometers (App. A pages 40-49)	12
2.5	Relative humidity, Vaisala (App. A pages 50-54)	13
2.6	Pore water pressure, Geokon (App. A pages 55-56)	13
2.7	Pore water pressure, Kulite (App. A page 57)	13
2.8	Water flow into the filters (App. A page 58)	13
2.9	Forces on the plug (App. A page 59)	14
2.10	Displacement of the plug (App. A page 60)	14
2.11	Canister power (App. A page 61)	14
2.12	Temperature in the buffer (App. A pages 62-66)	14
2.13	Temperature in the rock (App. A pages 67-70)	15
2.14	Temperature on the canister surface, Optical fiber cables (App. A pages 71-72)	15
2.15	Temperature inside the canister (App. A pages 73-75)	15
2.16	Strain in the canister	15
2.17	Rock stresses and strains	15
<b>3</b>	<b>Geometry</b>	<b>17</b>
<b>4</b>	<b>Location of instruments</b>	<b>19</b>
4.1	Brief description of the instruments	19
	Measurements of temperature	19
	Measurement of total pressure in the buffer	19
	Measurement of pore water pressure in the buffer	19
	Measurement of the water saturation process	20
	Measurements of strain in the Canister	20
	Measurements of stresses and strain in the rock	20
	Measurements of forces on the plug	20
	Measurements of plug displacement	20
	Measurement of water flow into the permeable mats	20
4.2	Strategy for describing the position of each device	20
4.3	Position of each instrument in the bentonite	21
4.4	Instruments in the rock	26
	Temperature measurements	26
	Stress and strain measurements	26
4.5	Instruments in the canister	27
4.6	Instruments at the plug	30
	<b>References</b>	<b>31</b>
	<b>Appendix A: Results</b>	<b>33</b>
	<b>Appendix B: Stress and strain measurements of the rock mass</b>	<b>77</b>



# 1 Introduction

The installation of the Canister Retrieval Test was made during autumn 2000. In general the data in this report are presented in diagrams covering the time period 2000-10-26 to 2005-11-01. The time axis in the diagrams represents days from 2000-10-26. The diagrams are attached in Appendix A. The stress and strain measurements in the rock are reported separately by BBK. That report is attached as Appendix B.

A test overview with the positions of the measuring points and a brief description of the instruments is also presented in this report (chapters 3 and 4).

General comments concerning the collected data are given in chapter 2.



## 2 Comments

### 2.1 General

In this chapter short comments on general trends in the measurements are given. Sensors that were not delivering reliable data or no data at all are noted and comments on the data in general are given.

The slot between rock and bentonite block was filled with bentonite pellets and water on 001026. This date is also marked as start date. 1 m water head in the water supply tank was connected to the filters on 001102.

The heating of the canister started with an initially applied constant power of 700 W at 001027 that is one day after test start. The power was raised to 1700 W on 001113. The power was further raised to 2600 W on 010213.

At the end of 2001 two of the 36 electrical heaters failed due to short circuit to earth and no power was generated during one day between November 5 and 6, 2001 (day 375). The heaters were also shut off during one week between March 4 and 11 2002 (days 495 to 502) for control measurements. The water pressure in the mats was stepwise increased to 800 kPa in the period 5/9 – 10/10 2002 (days 687-713). The power of the heaters in the canister was reduced to 2100 W on day 683 (10/9 –02) and to 1600 W on day 1135 (4/12 –03). The later reduction was done after another heater failure that took place on day 1134.

There have been additional problems with the heaters resulting in failure of heaters and short power interruptions. The latest occurred on 2005-02-20 (day 1578) and 2005-03-10 (day 1596), after which only 4 heaters were still functioning. Consequently the power in the canister had to be reduced from 1600 W to about 1150 W on day 1596 (10/3- 05).

The water pressure in the mats attached to the deposition hole wall was temporarily reduced to 100 kPa during the period 5/12 2002 – 9/1 2003 (days 770-805) and to 400 kPa during the period 9/1 2003 – 23/1 2003 (days 805-819). The water pressure was reduced to atmospheric in March 2005 (day ~1600) in order to try to keep the last heaters alive.

On October 11 (day 1811) the power was switched off in order to prepare for the dismantling, excavation and retrieval of the test, which started in the beginning of 2006.

The mats were flushed on July 19 2005 (day 1727).

It should also be mentioned that the actual power from start until day 1135 had been higher than indicated by the measurements. See chapter 2.11.

The eleventh report covered the period up to 051101. This report is the twelfth and final one and covers the results up to 060501.

## **2.2 Total pressure, Geokon (App. A pages 35-38)**

The pressure has decreased in three steps. At first it decreased due to the reduction in water pressure in the filters on day ~1600 and then slowly increased but did not regain the original values. It is interesting to note that there is a sudden pressure increase on July 19, the same day as the mats were flushed. On day 1811 the pressure decreased dramatically again after turning off the heaters. Then the pressure has at first increased due to reestablishment of the pore water pressure and then decreased again due to the release of the plug and stepwise excavation of the buffer.

Sensor P104 was not installed. U106 was originally intended to be a pore pressure sensor but was replaced by a total pressure sensor. One of 21 sensors was out of order.

## **2.3 Total Pressure, Kulite (App. A page 39)**

Six Kulite total pressure transducers were installed in the bentonite blocks. Unfortunately they never worked properly. The reason for the malfunction is probably brakeage of the transducer connections at high pressures.

One sensor (P221) did not work from start, 3 stopped working earlier and the two remaining transducers had problems and did not yield reliable values during one year period. Only one transducer worked until excavation.

## **2.4 Suction, Wescor Psychrometers (App. A pages 40-49)**

Wescor psychrometers are only working at suction below 5000 kPa, which correspond to high relative humidity (above about 96%). 24 out of 26 transducer yielded values that could be evaluated and had thus a high relative humidity at termination of the test. 9 out of these 24 were drowned meaning that the sensors were probably filled with water. The remaining two sensors (of all 26) had not a high enough relative humidity to yield readable values.

The interpretation of the values should be done with care since the evaluation was done with an automatic technique and the plateau required for proper evaluation not always formed. This explains why most transducers start their appearance from very low value. These low values are not correct but only an indication of that the relative humidity or suction is getting close to the measuring range. All diagrams are included (also diagrams with no evaluated values).

In Ring 5 eight out of 9 transducers indicated a high relative humidity (measurable suction), which confirm the total pressure measurements. In ring 10 all eight transducers indicated a high relative humidity.

The temperature and water pressure reduction have resulted in a change in suction for some transducers.

## **2.5 Relative humidity, Vaisala (App. A pages 50-54)**

Relative humidity and temperature were also measured with Vaisala transducers. The relative humidity results and the temperature results in ring 10 have been split into two diagrams (pages 52 and 53) since the data were interfering with each other.

All transducers in Cyl.1 and Ring5 have stopped to work before excavation. In Ring 10 the two transducers placed above the canister yielded a continuing increase in RH (after the initial drying) until the water pressure in the mats was decreased.

The reason for the successive malfunction is not clear but the transducers do not work very well at high relative humidity. All transducers between the rock and the canister in rings 5 and 10 indicate a high degree of saturation, which confirm the results of the Wescor psychrometers.

18 out of 25 sensors were out of order at start excavation. The main reason for malfunction is high degree of saturation.

## **2.6 Pore water pressure, Geokon (App. A pages 55-56)**

The reduced water pressure and reduced power and subsequent temperature decrease were reflected in a strong reduction of pore pressure, which remained at very low values due to the low water pressure in the mats.

U106 was replaced by a total pressure sensor.

1 out of 11 sensors was out of order at start excavation.

## **2.7 Pore water pressure, Kulite (App. A page 57)**

There were only one sensor of this type in Ring 10 and one in Cylinder 4. None of them have shown any increase in pore pressure.

## **2.8 Water flow into the filters (App. A page 58)**

Measurement of water inflow into the filters started at 001102. The total inflow to the filters has since that date been 672 liter.

The inflow strongly increased after start pressurizing the water in the mats at 020905 (day 678) and ceased after the pressurization was stopped on 050304 (day 1590).

## **2.9 Forces on the plug (App. A page 59)**

The forces on the plug have been measured since 001106. The total force was about 8800 kN when disconnected at 060109 (day 1901). It had steadily increased until the water pressure was reduced. Very little increase in force has been measured after that date.

During the first about 50 days the plug was only fixed with 3 rods. When the total force exceeded 1500 kN the rest of the 9 rods were fixed in a prescribed manner. This procedure took place 12-14 December 2000 that is 46-48 days after test start. From that time only every third anchor is measured and the results should thus be multiplied with 3. The diagram shows both the actual measurements and after multiplication with 3.

## **2.10 Displacement of the plug (App. A page 60)**

One transducer shows a logical steady upwards displacement of the plug, while two transducers act strangely due to an error in the measuring equipment.

## **2.11 Canister power (App. A page 61)**

There were problems with the heaters at several occasions and the power has successively been reduced. The power was switched off 2005-10-11 (day 1811).

Days 600-1100 the power 2100 W was measured by direct measurement regularly. However, an alternative technique for measuring the power showed for some canisters in the Prototype Repository a deviating power. This technique, which consists in measurement of the entire energy consumed by the canister, was used to measure the average power of the canister in CRT during four weeks (at day ~1000). The result was a conclusion that the average power was not 2100 W as plotted but 2220 W. This difference seems to have endured up to the latest power failure. After reduction in power to 1600W the two techniques agree. The new equipment for continuous measurement and calculation of the entire energy consumed by the canister was installed on 2004-01-28 and has been used in the data plot from that date (day ~1200).

At around day 2000 the power 2000 W was temporarily applied in order to test the function of the heaters.

## **2.12 Temperature in the buffer (App. A pages 62-66)**

All temperature sensors have worked well during the entire test. The temperature decreased after turning off the heaters to between 20 and 25 degrees. The final drop took place when the sensors were uncovered. The temporary increase around day 2000 is related to the canister test.



### **2.13 Temperature in the rock (App. A pages 67-70)**

The temperature in the rock was measured until the final date 060501. The temperature dropped to between 20 and 30 degrees after the heaters were turned off. The canister test is also seen as increased temperatures.

There was an almost complete axial symmetry of the temperature measured in the rock until day 880. The change of this trend with mainly increasing temperature in direction A (north) is caused by the neighboring experiment TBT that started its heating at 030326.

### **2.14 Temperature on the canister surface, Optical fiber cables (App. A pages 71-72)**

The first diagram shows the maximum temperature plotted as a function of time. The maximum temperature measured on the canister surface was about 27 °C in the last measurement at 2006-02-07 (day 1931). The second diagram shows the distribution of the temperature along the cables at 06-02-07. The length of the cable on the canister surface is only about 20 m and close to the entrances the lower surrounding temperatures have an influence on the measured temperature.

### **2.15 Temperature inside the canister (App. A pages 73-75)**

All sensors have been lost.

### **2.16 Strain in the canister**

Continuous measurements have been made but so far no results have been produced due to evaluation problems.

### **2.17 Rock stresses and strains**

Rock stresses and strains are reported in Appendix B.



### 3 Geometry

The test installation consists of a full-scale deposition hole, a copper canister equipped with electrical heaters and bentonite blocks (cylindrical and ring shaped). A plug of concrete and steel is anchored to the rock on top of the bentonite.

The saturation of the bentonite is attained artificially by vertical filter stripes. 16 stripes with a width of 0.1 meters and a length of 5.5 meters are applied on the surrounding rock.

Measurements are made in four vertical sections A, B, C and D according to Figure 3-1. Direction A-B is parallel to the tunnels axial with A headed almost against north.

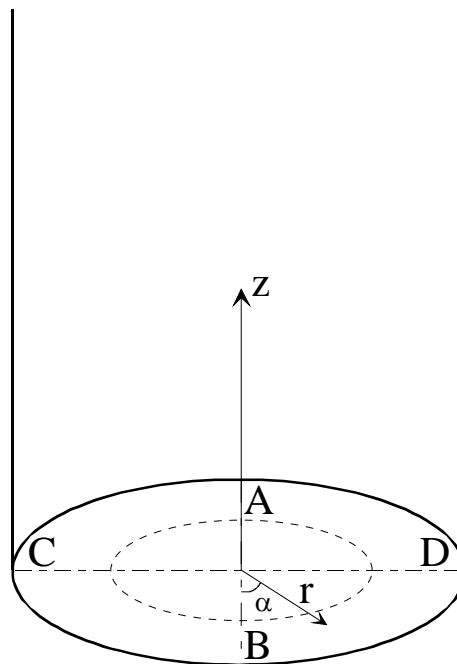


**Figure 3-1.** Figure describing the instrument planes (A-D) and the coordinate system used when describing the instrument positions.



## 4 Location of instruments

### 4.1 Brief description of the instruments

The different instruments that are used in the experiment are briefly described in this chapter.

#### Measurements of temperature

##### *Buffer*

Thermocouples from BICC have been installed for measuring temperature in the buffer. Measurements are done in 32 points in the test hole. In addition, temperature gauges are built in into the capacitive relative humidity sensors (29 sensors) as well as in the pressure gauges of vibrating wire type (13 gauges). Temperature is also measured in the psychrometers.

##### *Canister*

Temperature is measured inside the canister (on the insert) in 19 points with PT-100 gauges. In addition temperature is measured on the surface of the canister with optical fiber cables. An optical measuring system called FTR (Fiber Temperature Laser Radar) from BICC is used.

##### *Rock*

Temperature in the rock and on the rock surface of the hole is measured in 40 points with thermocouples from BICC.

#### Measurement of total pressure in the buffer

Total pressure is the sum of the swelling pressure and the pore water pressure. It is measured with the following instrument types:

- Geocon total pressure cells with vibrating wire transducers. 15 cells of this type have been installed.
- Kulite total pressure cells with piezo resistive transducers. 6 cells of this type have been installed.

#### Measurement of pore water pressure in the buffer

Pore water pressure is measured with the following instrument types:

- Geocon pore pressure cells with vibrating wire transducer. 13 cells of this type have been installed.
- Kulite pore pressure cells with piezo resistive transducer. 2 cells of this type have been installed.

### **Measurement of the water saturation process**

The water saturation process is recorded by measuring the relative humidity in the pore system, which can be converted into water ratio or total suction (negative water pressure). The following techniques and devices are used:

- Vaisala relative humidity sensor of capacitive type. 29 cells of this type have been installed. The measuring range is 0-100 % RH.
- Wescor psychrometers model PST-55. The devices measure the relative humidity in the pore system. The measuring range is 95.5-99.6 % RH corresponding to the pore water pressure -0.5 to -6MPa. 26 cells of this type have been installed.

### **Measurements of strain in the Canister**

These measurements are not reported.

### **Measurements of stresses and strain in the rock**

These measurements are not reported.

### **Measurements of forces on the plug**

The force on the plug caused by the swelling pressure of the bentonite is measured in 3 of the 9 anchors. The force transducers are of the type GLÖTZL.

### **Measurements of plug displacement**

Due to straining of the anchors the swelling pressure of the bentonite will cause not only a force on the plug but also displacement of the plug. The displacement is measured in three points with transducers of the type LVDT with the range 0 – 50 mm.

### **Measurement of water flow into the permeable mats**

Water is supplied to the bentonite with filter strips attached to the rock surface. The water flow into these mats is measured by measuring the water volume in the supply tank with a differential pressure transmitter that measures the difference in pressure between the nitrogen in the top of the tank and the water in the bottom of the tank.

## **4.2 Strategy for describing the position of each device**

Every instrument is named with a short unique name consisting of 1-2 letters describing the type of measurement and 3 figures numbering the device. Every instrument position in the buffer and rock is described with three coordinates according to Figure 3-1.

The r-coordinate is the horizontal distance from the center of the hole and the z-coordinate is the height from the bottom of the hole (the block height is set to 500 mm). The  $\alpha$ -coordinate is the angle from the vertical direction B (almost south).

The short description of the positions in the diagrams differs between the buffer and the rock.

**Buffer:** Three positions with the following meaning: (bentonite block or cylinder number counted from the bottom \ direction A, B, C, or D \ radius in mm from center line)

**Rock:** Three positions with the following meaning: (distance in meters from the bottom \  $\alpha$  according to Fig 3-1 \ distance in meters from the hole surface)

The bentonite blocks are called cylinders and rings. The cylinders are numbered C1-C4 and the rings R1-R10 respectively (Figure 4-1).

### **4.3 Position of each instrument in the bentonite**

Measurements are done in four vertical sections A, B, C and D according to Figure 3-1. Direction A and B are placed in the tunnels axial direction.

An overview of the positions of the instruments is shown in Fig 4-1. Exact positions are described in Tables 4-1 to 4-4.

The instruments are located in two main levels in the blocks, 50 mm and 160 mm, from the upper surface. The thermocouples have mostly placed in the 50mm level and the other gauges in the 160 mm level.

- pore water pressure + temp.
- total pressure + temp.
- × temp.
- △ relative humidity (+ temp.)

1m

A

B+C

D

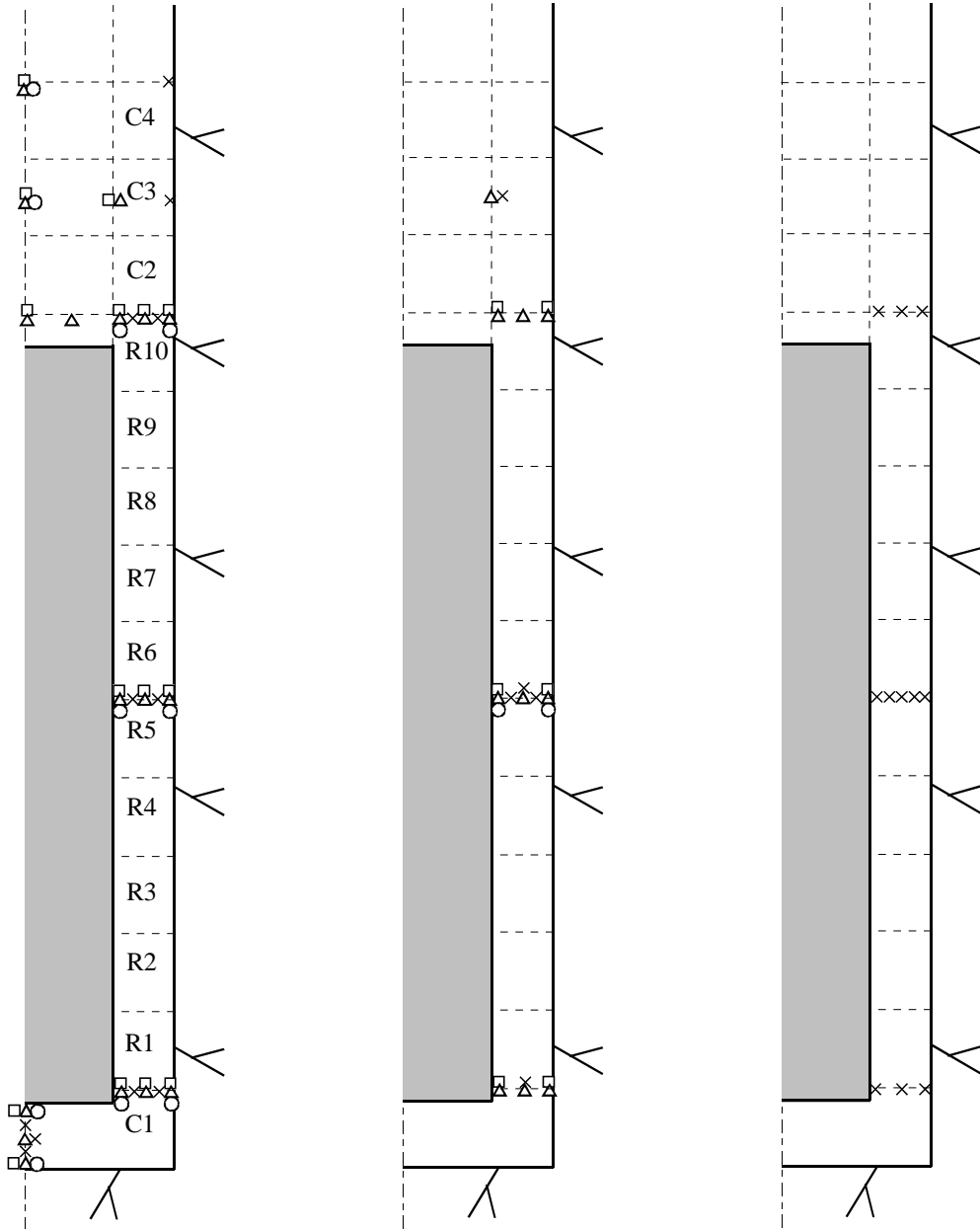


**Figure 4-1.** Schematic view over the instruments in four vertical sections and the block designation.



**Table 4-1. Numbering and position of instruments for measuring temperature (T).**

Type and number	Block	Instrument position in block				Cable pos.		Fabricate	Remark
		Direction	$\alpha$	r	Z	$\alpha$			
T101	Cyl. 1	Center	90	50	50	242	BICC		
T102	Cyl. 1	Center	90	50	250	238	BICC		
T103	Cyl. 1	Center	90	50	450	230	BICC		
T104	Cyl. 1	A	180	635	450	206	BICC		
T105	Cyl. 1	A	180	735	450	202	BICC		
T106	Cyl. 1	B	365	685	450	38	BICC		
T107	Cyl. 1	C	275	685	450	274	BICC		
T108	Cyl. 1	D	90	585	450	96	BICC		
T109	Cyl. 1	D	90	685	450	94	BICC		
T110	Cyl. 1	D	90	785	450	92	BICC		
T111	Ring 5	A	180	635	2950	224	BICC		
T112	Ring 5	A	180	735	2950	218	BICC		
T113	Ring 5	B	360	610	2950	318	BICC		
T114	Ring 5	B	360	685	2950	322	BICC		
T115	Ring 5	B	360	735	2950	324	BICC		
T116	Ring 5	C	270	610	2950	258	BICC		
T117	Ring 5	C	270	685	2950	260	BICC		
T118	Ring 5	C	270	735	2950	262	BICC		
T119	Ring 5	D	90	585	2950	44	BICC		
T120	Ring 5	D	90	635	2950	46	BICC		
T121	Ring 5	D	90	685	2950	48	BICC		
T122	Ring 5	D	90	735	2950	50	BICC		
T123	Ring 5	D	90	785	2950	52	BICC		
T124	Ring 10	A	180	635	5450	200	BICC		
T125	Ring 10	A	180	735	5450	194	BICC		
T126	Ring 10	D	90	585	5450	54	BICC		
T127	Ring 10	D	90	685	5450	56	BICC		
T128	Ring 10	D	90	785	5450	58	BICC		
T129	Cyl. 3	A	180	785	6250	166	BICC		
T130	Cyl. 3	B	365	585	6250	358	BICC		
T131	Cyl. 3	C	275	585	6250	280	BICC		
T132	Cyl. 4	A	180	785	6950	66	BICC		

**Table 4-2. Numbering and position of instruments for measuring total pressure (P).**

Type and number	Block	Instrument position in block			Z(mm)	Cable pos.		Fabricate	Remark
		Direction	$\alpha$	r(mm)		$\alpha$			
P101	Cyl. 1	Center	180	50	0	244	Kulite		
P102	Cyl. 1	Center	180	50	450	232	Kulite		
P103	Cyl. 1	A	185	585	340	208	Geokon		
P104	Cyl. 1	A	185	685	340	204	Geokon		
P105	Cyl. 1	A	185	785	340	186	Geokon		
P106	Cyl. 1	B	365	585	340	40	Geokon		
P107	Cyl. 1	B	365	785	340	2	Geokon		
P108	Cyl. 1	C	275	585	340	278	Geokon		
P109	Cyl. 1	C	275	785	340	270	Geokon		
P110	Ring 5	A	185	585	2840	228	Geokon		
P111	Ring 5	A	185	685	2840	222	Geokon		
P112	Ring 5	A	185	785	2840	188	Geokon		
P113	Ring 5	B	365	535	2840	36	Geokon		
P114	Ring 5	B	365	825	2840	16	Geokon		
P115	Ring 5	C	275	585	2840	296	Geokon		
P116	Ring 5	C	275	785	2840	290	Geokon		
P117	Ring 10	Center	180	50	5340	24	Kulite		
P118	Ring 10	A	180	585	5340	216	Geokon		
P119	Ring 10	A	180	685	5340	198	Geokon		
P120	Ring 10	A	180	785	5340	192	Geokon		
P121	Ring 10	B	365	585	5340	20	Kulite		
P122	Ring 10	B	365	785	5340	18	Kulite		
P123	Ring 10	C	275	585	5340	286	Kulite		
P124	Ring 10	C	275	785	5340	284	Kulite		
P125	Cyl. 3	Center	180	50	6250	158	Geokon		
P126	Cyl. 3	A	180	585	6250	162	Geokon		
P127	Cyl. 4	Center	180	50	6840	64	Kulite		

**Table 4-3. Numbering and position of instruments for measuring pore water pressure (U).**

Type and number	Block	Instrument position in block			Z(mm)	Cable pos.		Fabricate	Remark
		Direction	$\alpha$	r(mm)		$\alpha$			
U101	Cyl. 1	Center	270	50	50	246	Geokon		
U102	Cyl. 1	Center	270	50	450	236	Geokon	Horizontal	
U103	Cyl. 1	A	175	585	340	126	Geokon		
U104	Cyl. 1	A	175	785	340	178	Geokon		
U105	Ring 5	A	175	585	2840	138	Geokon		
U106	Ring 5	A	175	785	2840	180	Geokon		
U107	Ring 5	B	355	535	2840	314	Geokon	In the slot	
U108	Ring 5	B	355	825	2840	348	Geokon	In the slot	
U109	Ring 5	C	265	585	2840	256	Geokon		
U110	Ring 5	C	265	825	2840	264	Geokon	In the slot	
U111	Ring 10	A	175	585	5340	146	Geokon		
U112	Ring 10	A	175	785	5340	152	Geokon		
U113	Cyl. 3	Center	270	50	6250	156	Geokon		
U114	Cyl. 4	Center	270	50	6950	62	Kulite		

**Table 4-4. Numbering and position of instruments for measuring water content (W).**

Type and number	Block	Instrument position in block				Cable pos.		Fabricate	Remark
		Direction	$\alpha$	r	Z	$\alpha$			
W101	Cyl. 1	Center	360	50	50	248	Vaisala		
W102	Cyl. 1	Center	360	400	160	240	Vaisala		
W103	Cyl. 1	Center	360	50	450	234	Vaisala	Horizontal	
W104	Cyl. 1	A	180	585	340	128	Vaisala		
W105	Cyl. 1	A	180	685	340	132	Vaisala		
W106	Cyl. 1	A	180	785	340	184	Vaisala		
W107	Cyl. 1	A	170	585	340	124	Wescor		
W108	Cyl. 1	A	170	685	340	130	Wescor		
W109	Cyl. 1	A	170	785	340	134	Wescor		
W110	Cyl. 1	B	360	585	340	304	Vaisala		
W111	Cyl. 1	B	360	785	340	360	Vaisala		
W112	Cyl. 1	B	360	685	340	308	Vaisala		
W113	Cyl. 1	B	355	585	340	302	Wescor		
W114	Cyl. 1	B	355	685	340	306	Wescor		
W115	Cyl. 1	B	355	785	340	310	Wescor		
W116	Cyl. 1	C	270	585	340	250	Wescor		
W117	Cyl. 1	C	270	685	340	252	Wescor		
W118	Cyl. 1	C	270	785	340	254	Vaisala		
W119	Ring 5	A	180	585	2840	226	Vaisala		
W120	Ring 5	A	180	685	2840	220	Vaisala		
W121	Ring 5	A	180	785	2840	182	Vaisala		
W122	Ring 5	A	170	585	2840	136	Wescor		
W123	Ring 5	A	170	685	2840	140	Wescor		
W124	Ring 5	A	170	785	2840	142	Wescor		
W125	Ring 5	B	360	535	2840	316	Vaisala	In the slot	
W126	Ring 5	B	360	685	2840	34	Vaisala		
W127	Ring 5	B	360	785	2840	350	Vaisala		
W128	Ring 5	B	350	535	2840	312	Wescor	In the slot	
W129	Ring 5	B	350	685	2840	320	Wescor		
W130	Ring 5	B	350	785	2840	346	Wescor		
W131	Ring 5	C	270	585	2840	294	Wescor	In the slot	
W132	Ring 5	C	275	685	2840	292	Wescor		
W133	Ring 5	C	270	785	2840	288	Wescor		
W134	Ring 10	Center	360	50	5340	22	Vaisala		
W135	Ring 10	A	180	262	5340	26	Vaisala		
W136	Ring 10	A	180	585	5340	214	Vaisala		
W137	Ring 10	A	180	685	5340	196	Vaisala		
W138	Ring 10	A	180	785	5340	190	Vaisala		
W139	Ring 10	A	170	585	5340	144	Wescor		
W140	Ring 10	A	170	685	5340	148	Wescor		
W141	Ring 10	A	170	785	5340	150	Wescor		
W142	Ring 10	B	360	585	5340	328	Vaisala		
W143	Ring 10	B	360	685	5340	332	Vaisala		
W144	Ring 10	B	360	785	5340	336	Vaisala		
W145	Ring 10	B	355	585	5340	326	Wescor		
W146	Ring 10	B	355	685	5340	330	Wescor		
W147	Ring 10	B	355	785	5340	334	Wescor		
W148	Ring 10	C	270	585	5340	266	Wescor		
W149	Ring 10	C	270	685	5340	268	Wescor		
W150	Ring 10	C	270	785	5340	272	Vaisala		
W151	Cyl. 3	Center	360	50	6250	154	Vaisala		
W152	Cyl. 3	A	180	585	6250	160	Vaisala		
W153	Cyl. 3	B	360	585	6250	356	Vaisala		
W154	Cyl. 3	C	270	585	6250	276	Wescor		
W155	Cyl. 4	Center	360	50	6840	60	Vaisala		

## 4.4 Instruments in the rock

### Temperature measurements

40 thermocouples are placed in the rock and on the rock surface of the deposition hole. Holes have been bored in three directions on three levels and one additional hole has been bored in the bottom of the deposition hole i.e. totally 10 holes. They are led from the rock, over the gap between rock and bentonite and up along the bentonite block periphery. The position of the thermocouples in the rock is shown in Table 4-5.

**Table 4-5. Numbering and positions of thermocouples in the rock.**

Type and number	Level	Direction	Distance from rock surface	Cable pos. $\alpha$	Fabricate	Remark
TR101	0	Center	0.000	70°-90°	BICC	
TR102	0	Center	0.375	70°-90°	BICC	
TR103	0	Center	0.750	70°-90°	BICC	
TR104	0	Center	1.500	70°-90°	BICC	
TR105	0.61	10°	0.000	4°-14°	BICC	
TR106	0.61	10°	0.375	4°-14°	BICC	
TR107	0.61	10°	0.750	4°-14°	BICC	
TR108	0.61	10°	1.500	4°-14°	BICC	
TR109	0.61	80°	0.000	70°-90°	BICC	
TR110	0.61	80°	0.375	70°-90°	BICC	
TR111	0.61	80°	0.750	70°-90°	BICC	
TR112	0.61	80°	1.500	70°-90°	BICC	
TR113	0.61	170°	0.000	168°-176°	BICC	
TR114	0.61	170°	0.375	168°-176°	BICC	
TR115	0.61	170°	0.750	168°-176°	BICC	
TR116	0.61	170°	1.500	168°-176°	BICC	
TR117	3.01	10°	0.000	4°-14°	BICC	
TR118	3.01	10°	0.375	4°-14°	BICC	
TR119	3.01	10°	0.750	4°-14°	BICC	
TR120	3.01	10°	1.500	4°-14°	BICC	
TR121	3.01	80°	0.000	70°-90°	BICC	
TR122	3.01	80°	0.375	70°-90°	BICC	
TR123	3.01	80°	0.750	70°-90°	BICC	
TR124	3.01	80°	1.500	70°-90°	BICC	
TR125	3.01	170°	0.000	168°-176°	BICC	
TR126	3.01	170°	0.375	168°-176°	BICC	
TR127	3.01	170°	0.750	168°-176°	BICC	
TR128	3.01	170°	1.500	168°-176°	BICC	
TR129	5.41	10°	0.000	4°-14°	BICC	
TR130	5.41	10°	0.375	4°-14°	BICC	
TR131	5.41	10°	0.750	4°-14°	BICC	
TR132	5.41	10°	1.500	4°-14°	BICC	
TR133	5.41	80°	0.000	70°-90°	BICC	
TR134	5.41	80°	0.375	70°-90°	BICC	
TR135	5.41	80°	0.750	70°-90°	BICC	
TR136	5.41	80°	1.500	70°-90°	BICC	
TR137	5.41	170°	0.000	168°-176°	BICC	
TR138	5.41	170°	0.375	168°-176°	BICC	
TR139	5.41	170°	0.750	168°-176°	BICC	
TR140	5.41	170°	1.500	168°-176°	BICC	

### Stress and strain measurements

See Appendix B .

## 4.5 Instruments in the canister

The canister is instrumented with optical fiber cables on the copper surface, thermocouples in the steel insert and strain gauges on the inner and outer surface of the copper envelop in canister.

### Optical fiber cables

Figure 4-2 shows how the two optical fiber cables are placed on the canister surface. Both ends of a cable are used for measurements. This means that the two cables are used as four measuring channels as described in Table 4-6.

With this laying the cable will enter and exit the surface at almost the same position. Curvatures are shaped as a quarter circle with a radius of 20 cm. The cable is placed in a milled out channel on the surface. The channel has a width and a depth of just above 2 mm

**Table 4-6. Combination of cables and channels.**

Channel 1	Outlet of cable 1
Channel 2	Inlet of cable 1
Channel 3	Outlet of cable 2
Channel 4	Inlet of cable 2

Figure 4-3 shows the location of the thermocouples on the steel insert inside the canister.

### Thermocouple, PT100

Temperature in the steel insert measured at 18 point of measuring with. thermocouple of type PT100. Figure 4-4 shows how these thermocouple are placed

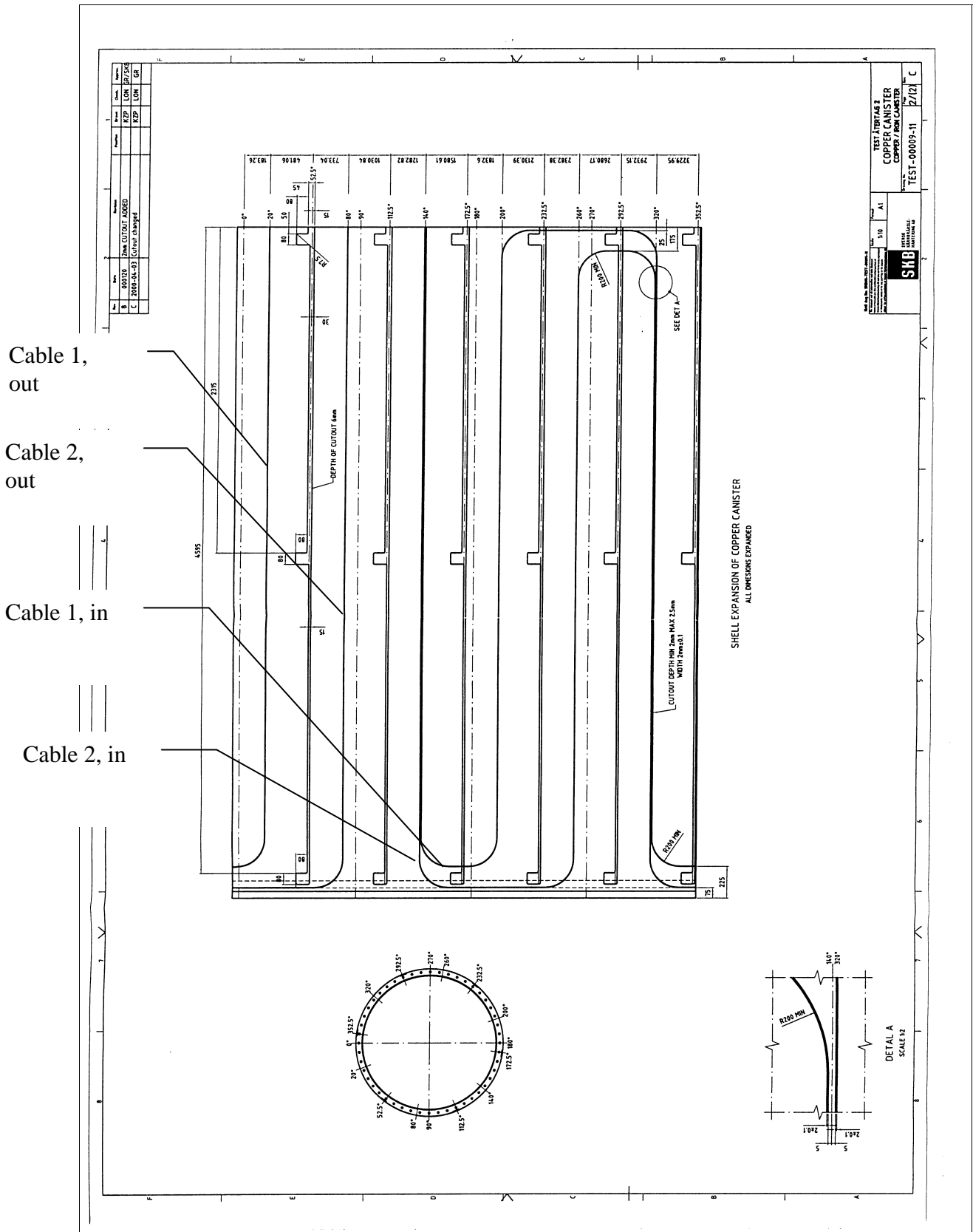


**Figure 4-2.** Laying of two optical fibre cables with protection tube of Inconel 625 (outer diameter 2 mm) for measurement of the canister surface temperature (surface unfolded).

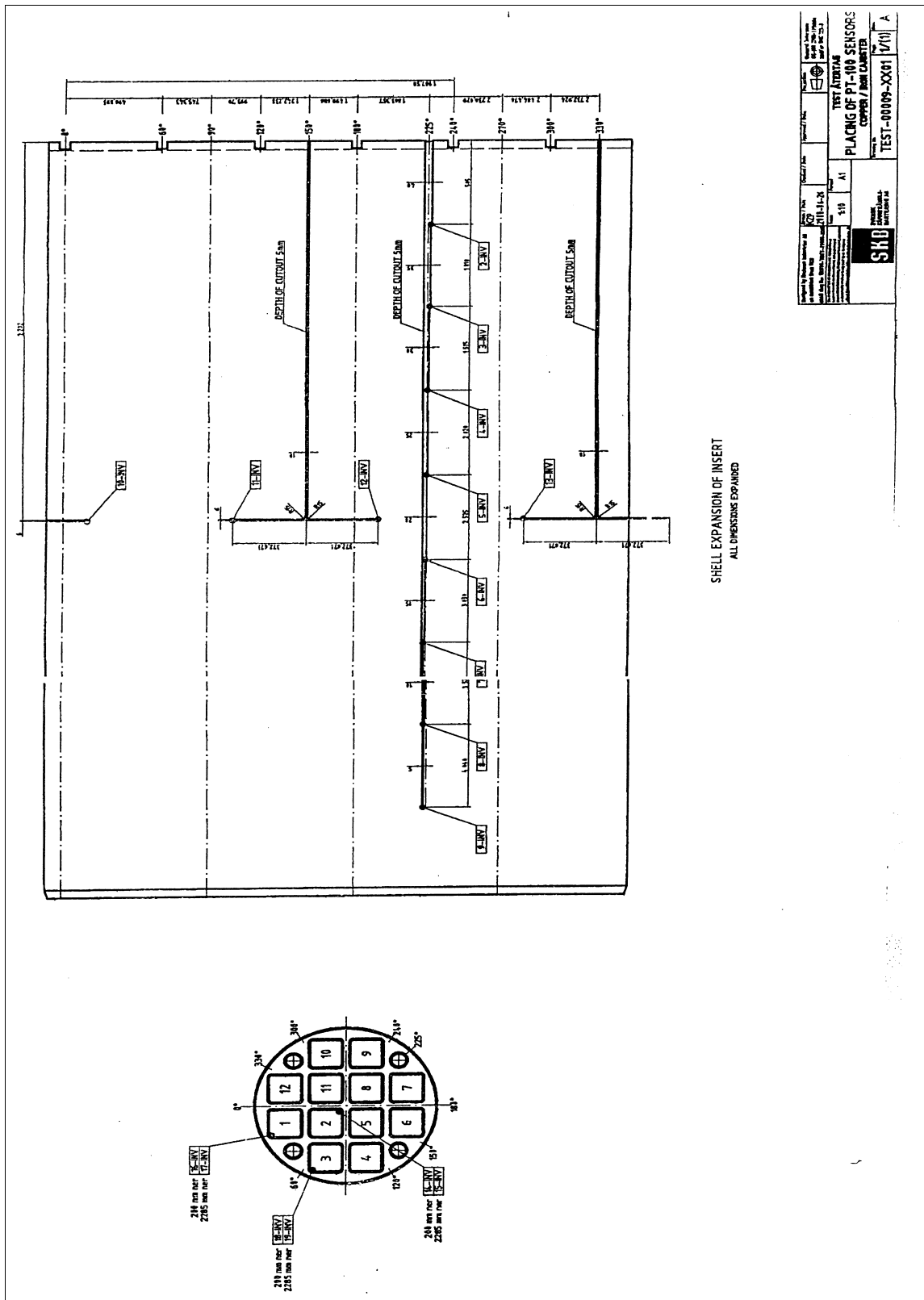
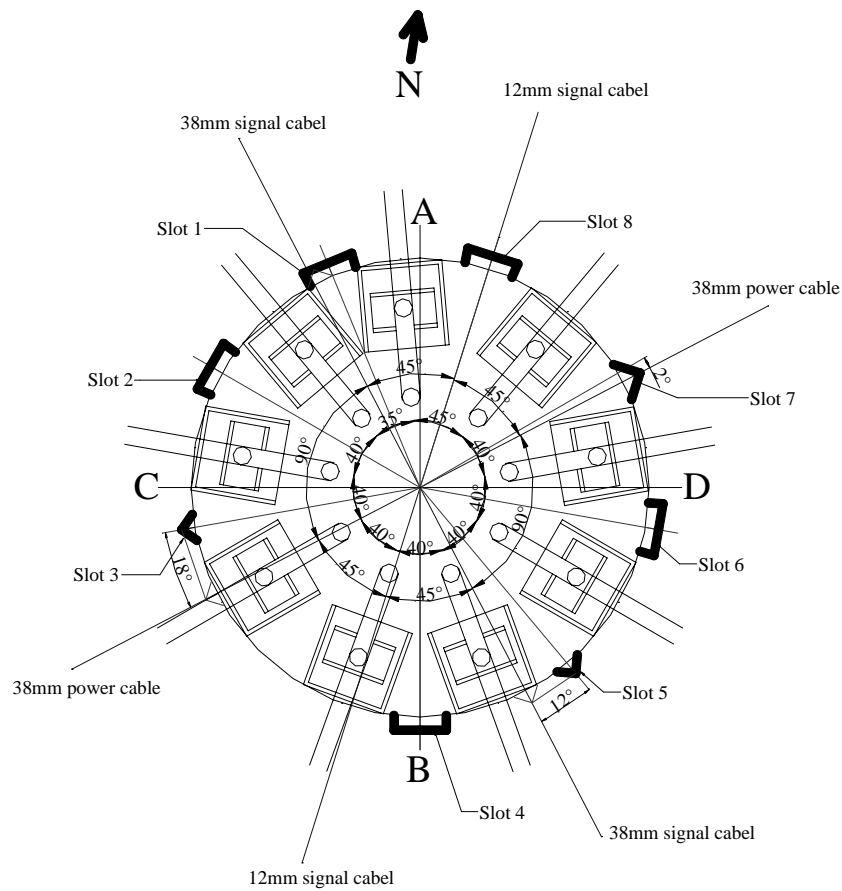


Figure 4-3. Location of thermocouples inside the canister

## 4.6 Instruments at the plug

Three force transducers and three displacement transducers have been placed on the plug to measure the force of the anchors and the displacement of the plug. The location of these transducers can be described in relation to Fig 4-4, which shows a schematic view of the plug with the slots, rods and cables.

The rods are numbered 1-9 anti-clockwise and number 1 is assumed to be the northern rod in direction A. The force transducers are placed on rods 3, 6, and 9. The displacement transducers are placed between the rods 5 cm from the rock surface of the hole and according to Table 4-6. They are fixed on the rock surface and measure thus the displacement relative the rock.



**Figure 4-4.** Schematic view of the deposition hole, showing the position of the slots, the rods and the cables from the canister.

**Table 4-6. Location of displacement transducers.**

TransducerNo.	Located between rods No.
1	4 and 5
2	7 and 8
3	1 and 2



## References

/1-1/ **Sanden T, Börgesson L.** Report on instrument positions and preparation of bentonite blocks for instruments and cables May 2000. SKB IPR-00-14

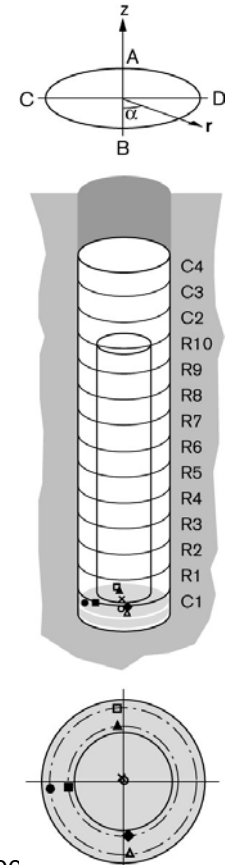
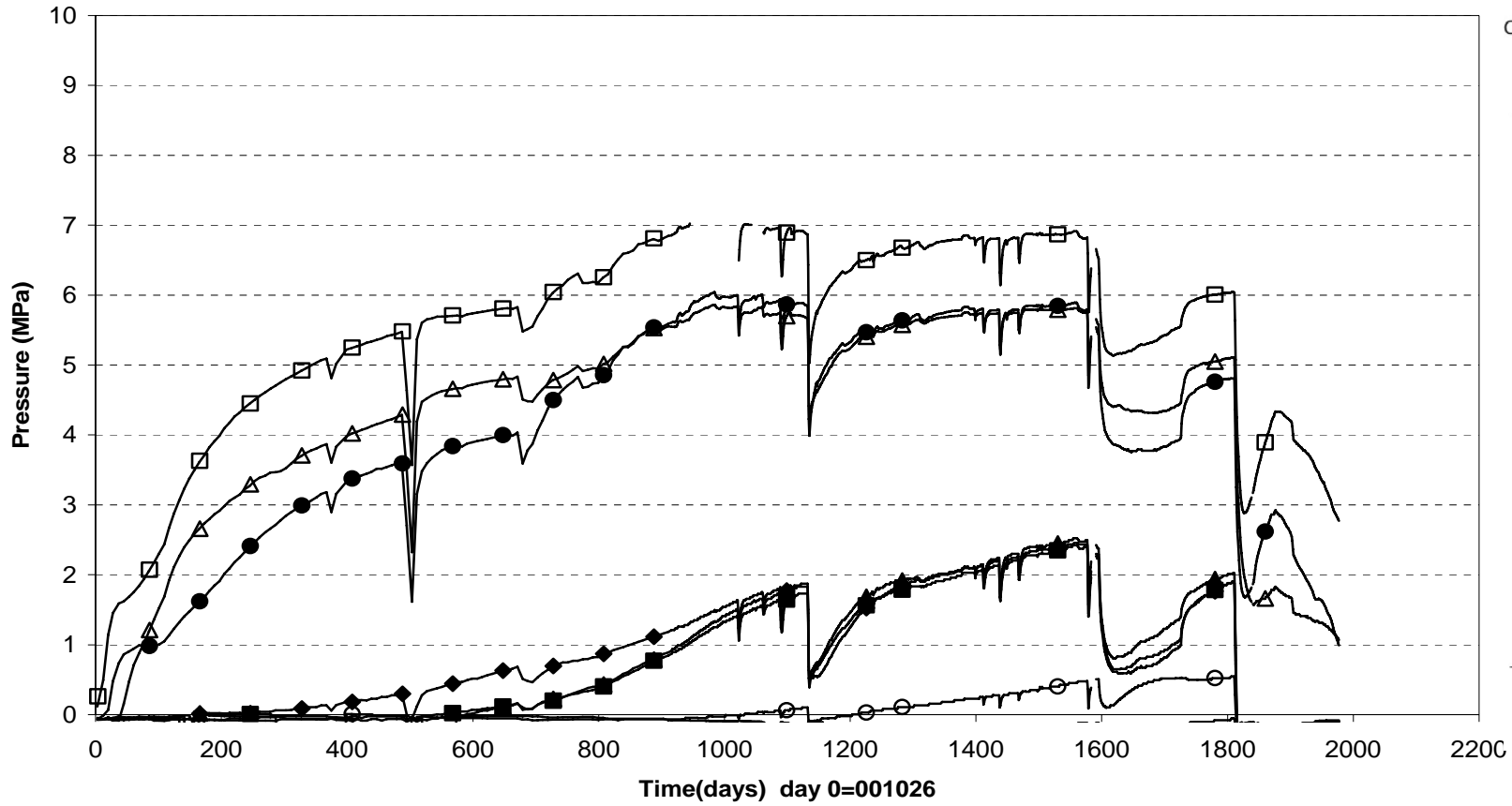


# Appendix A

## Measured data

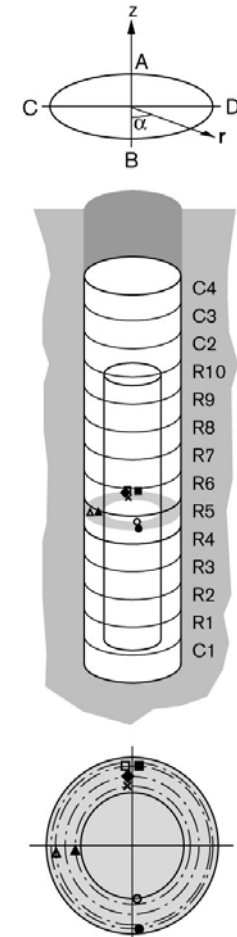
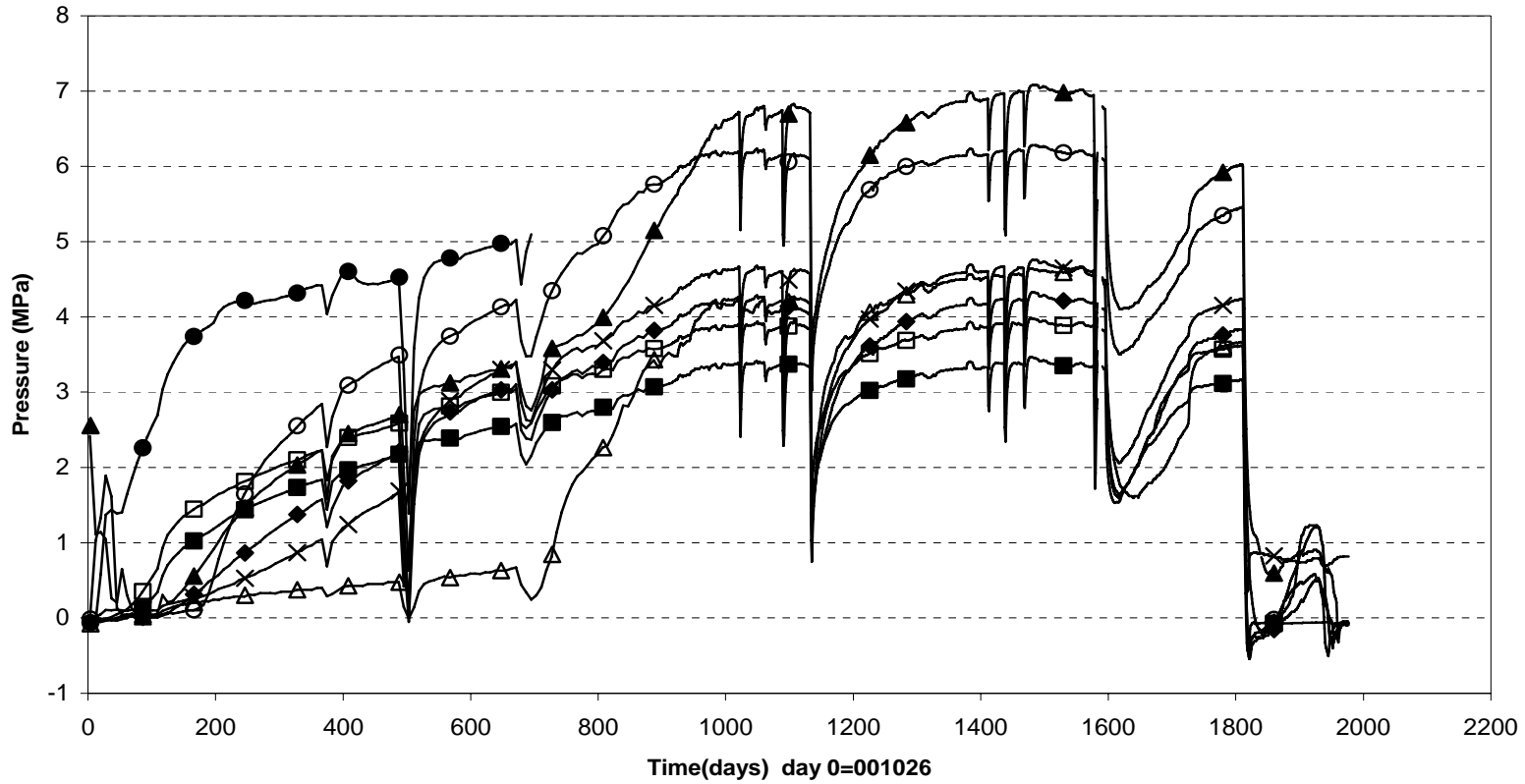


**Total pressure - Cylinder 1 (001026-060501)  
Geokon**



- |                         |                         |                     |                     |                     |
|-------------------------|-------------------------|---------------------|---------------------|---------------------|
| ○ P101(Cyl.1\center\50) | × P102(cyl.1\center\50) | ▲ P103(Cyl.1\A\585) | ◆ P106(Cyl.1\B\585) | ■ P108(Cyl.1\C\585) |
| □ P105(Cyl1\A\785)      | △ P107(Cyl.1\B\785)     | ● P109(Cyl1\C\785)  |                     |                     |

Total pressure - Ring 5 (001026-060501)  
Geokon

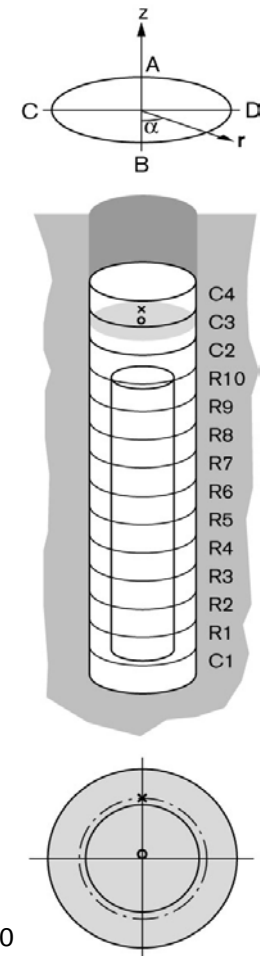
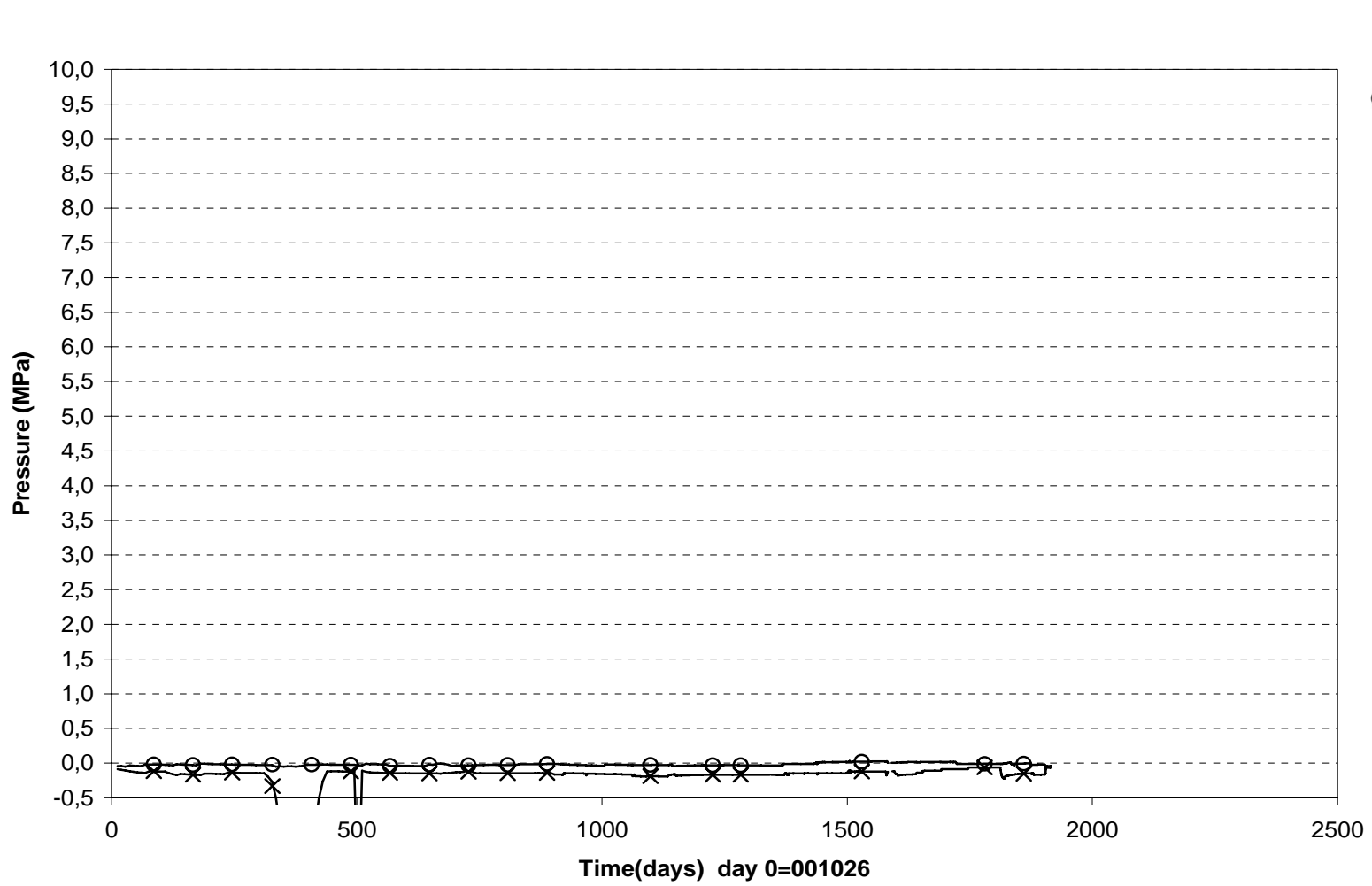


- |                     |                     |                          |                          |
|---------------------|---------------------|--------------------------|--------------------------|
| ○ P113(Ring5\B\535) | × P110(Ring5\A\585) | ▲ P115(Ring5\C\585)      | ◆ P111(Ring5\A\685)      |
| ■ U106(Ring5\A\785) | □ P112(Ring5\A\785) | △ P116(Ring5\C\785\slot) | ● P114(Ring5\B\815\slot) |

**Total pressure - Ring 10 (001026-060501)  
Geokon**



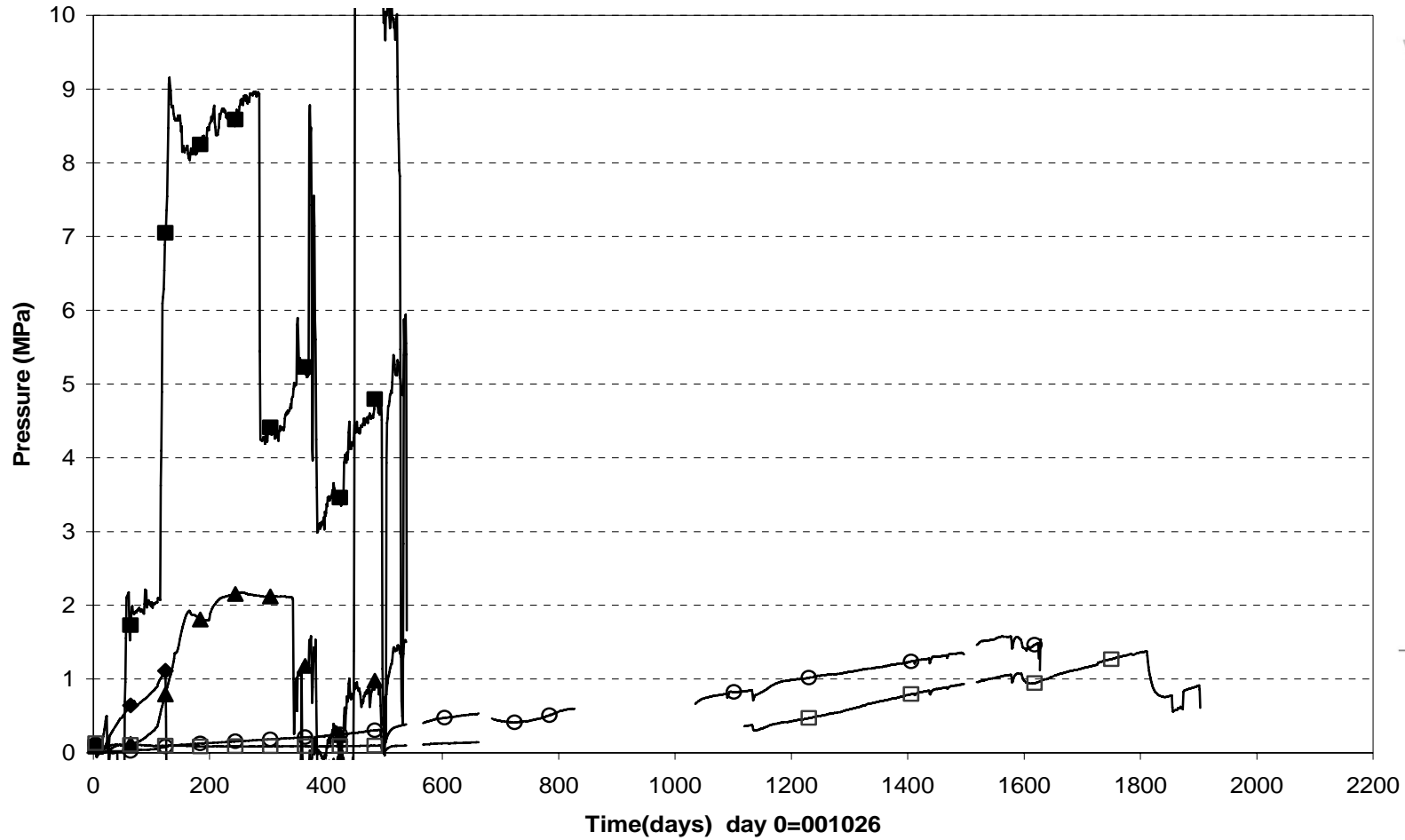
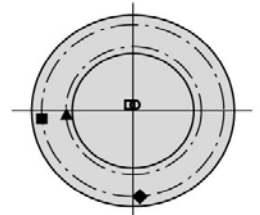
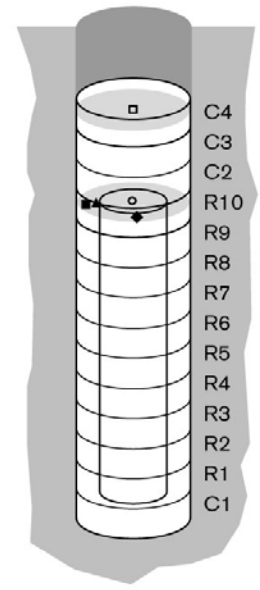
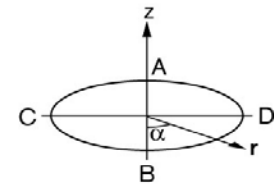
**Total pressure - Cylinder 3 (001026-060501)  
Geokon**



○ P125(Cyl.3\center\50) × P126(Cyl.3\VA\585)

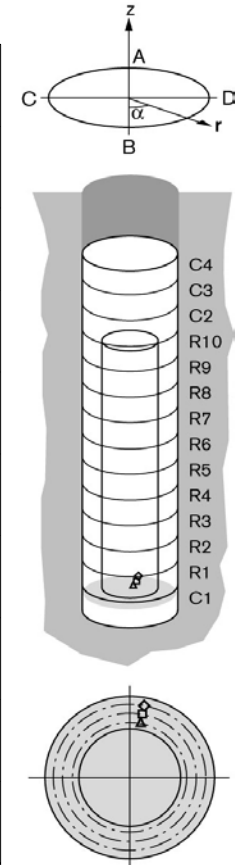
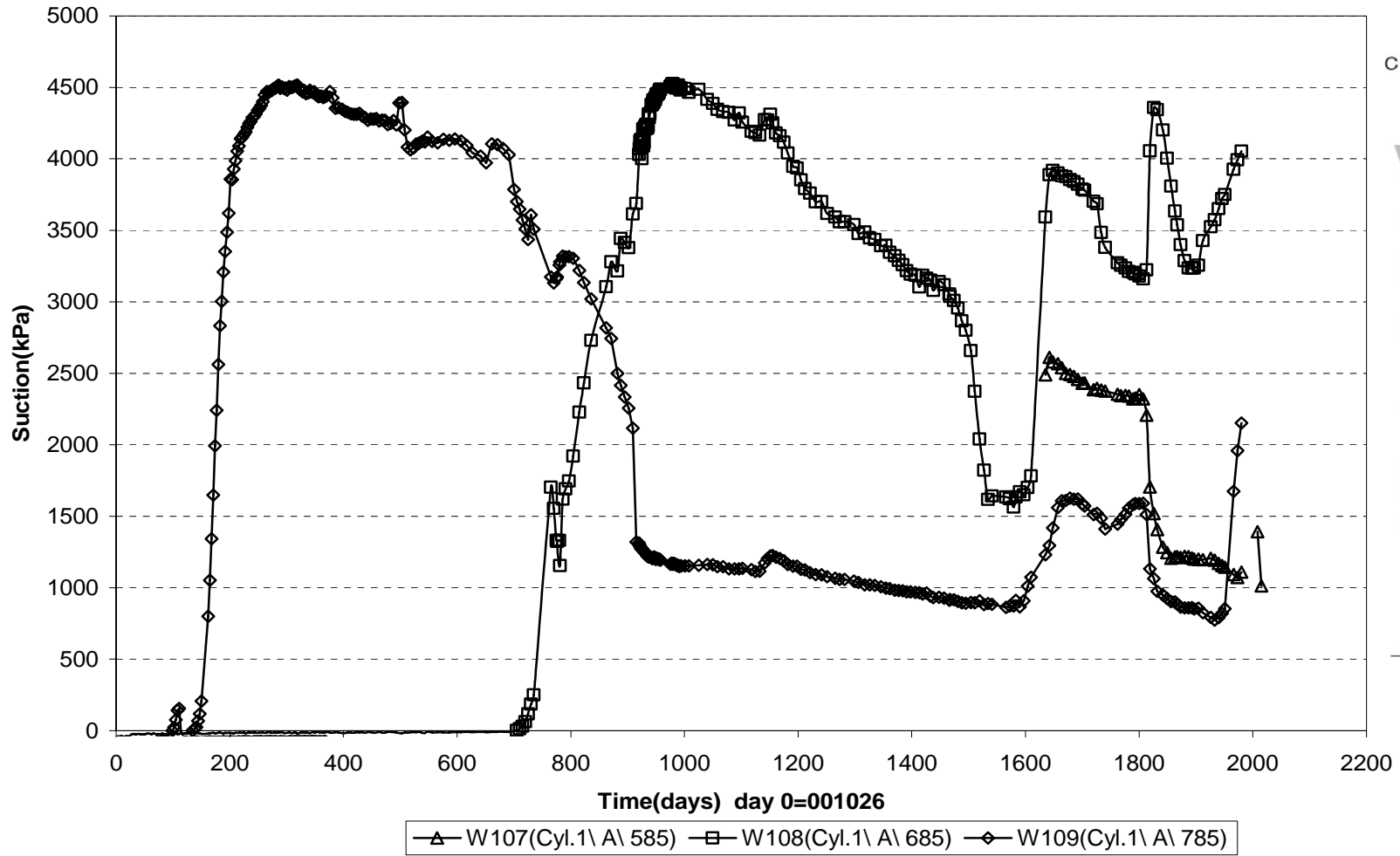


**Total pressure - Ring 10 (001026-060501)  
Kulite**

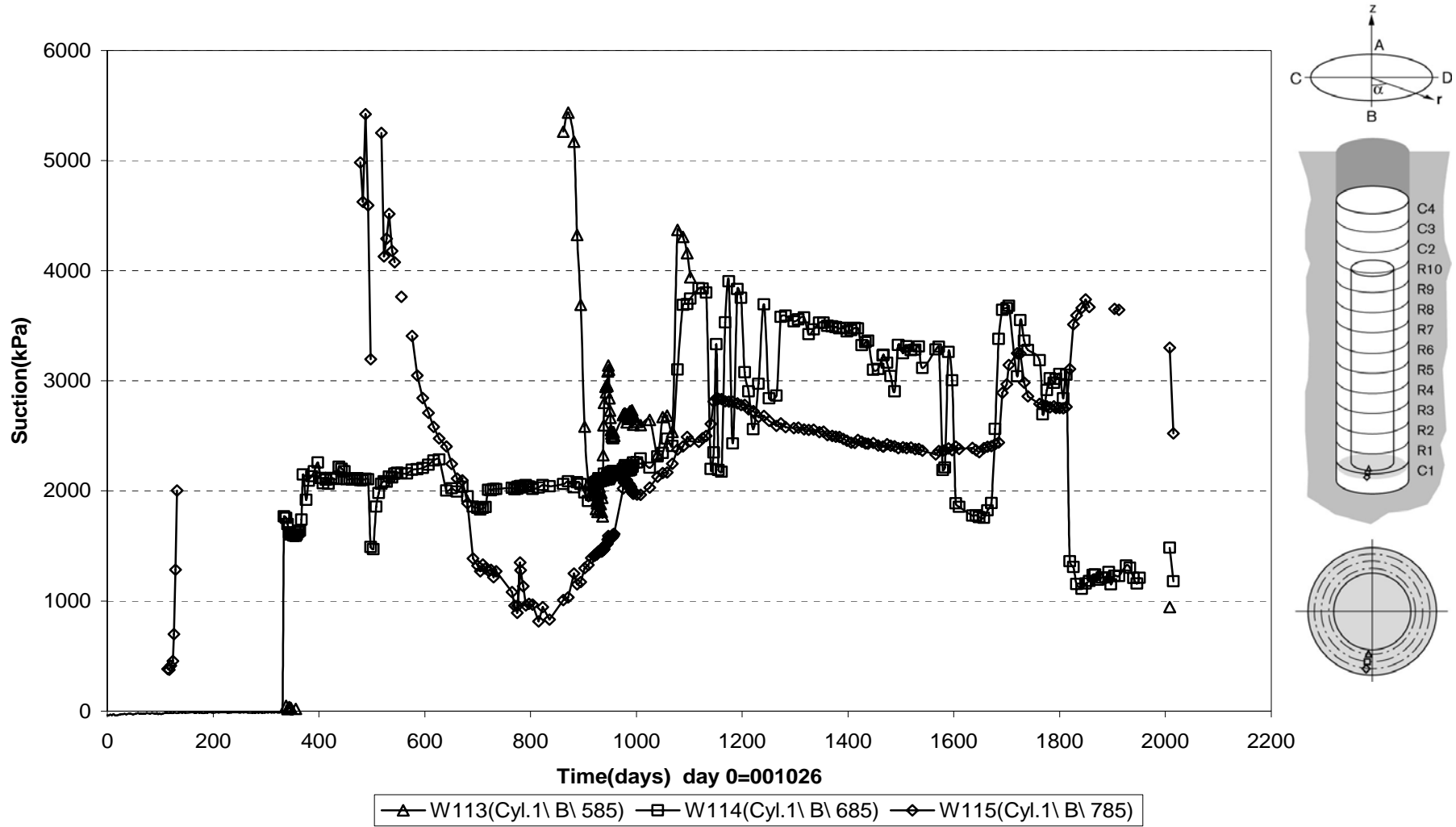


○ P217(Ring10-center-50) ▲ P223(Ring10-C-585) ◆ P222(Ring10-B-785) ■ P224(Ring10-C-785) □ P227(Cyl.4-center-50)

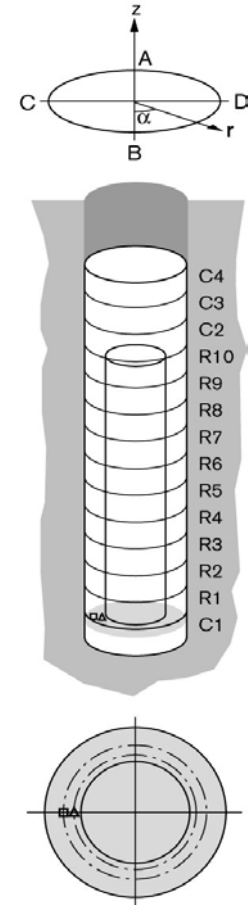
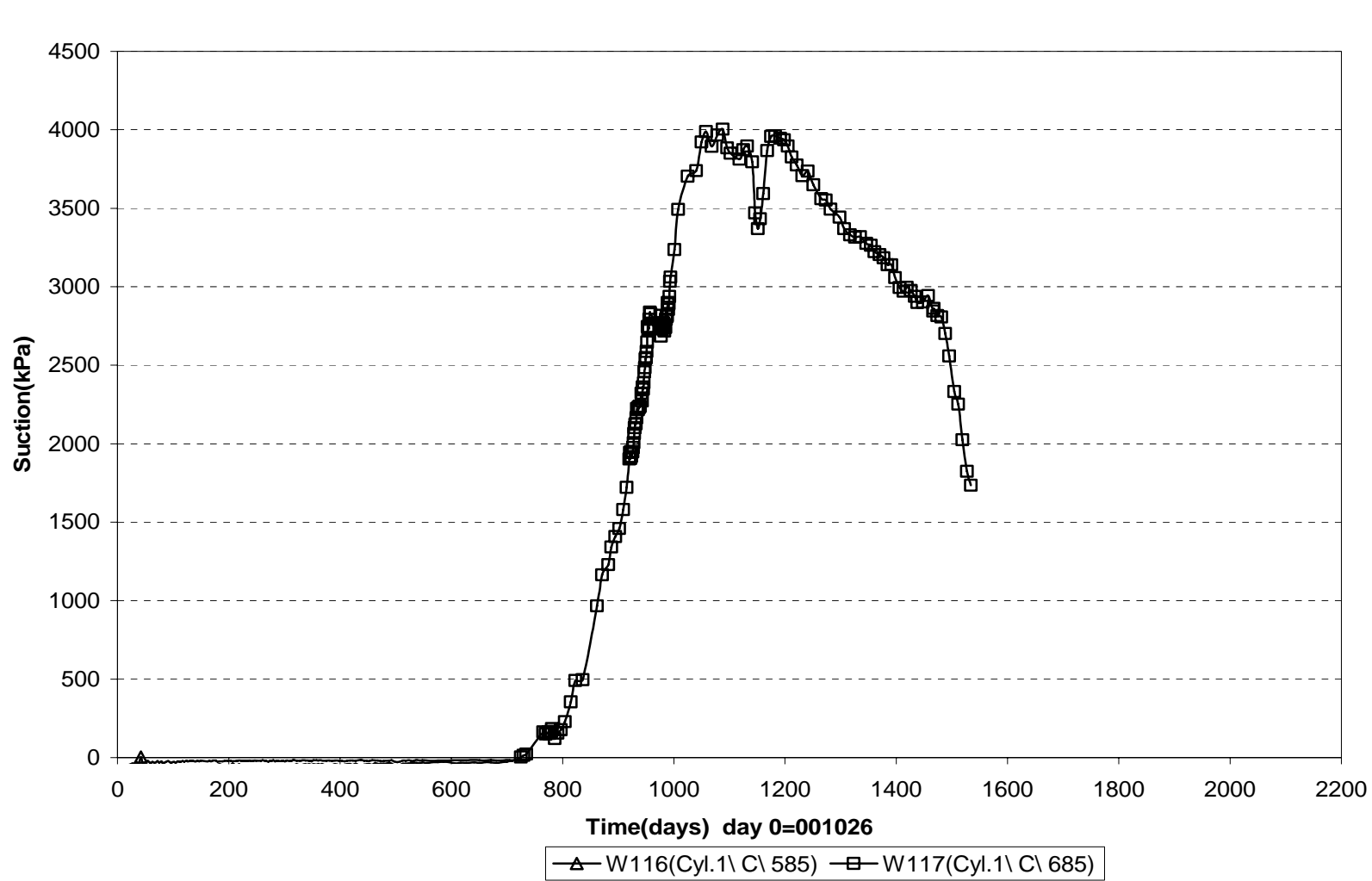
Suction in the buffer - Cyl.1 (001026-060501)  
Wescor



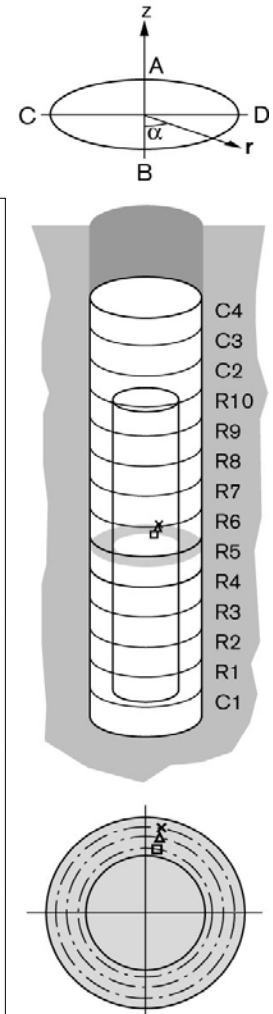
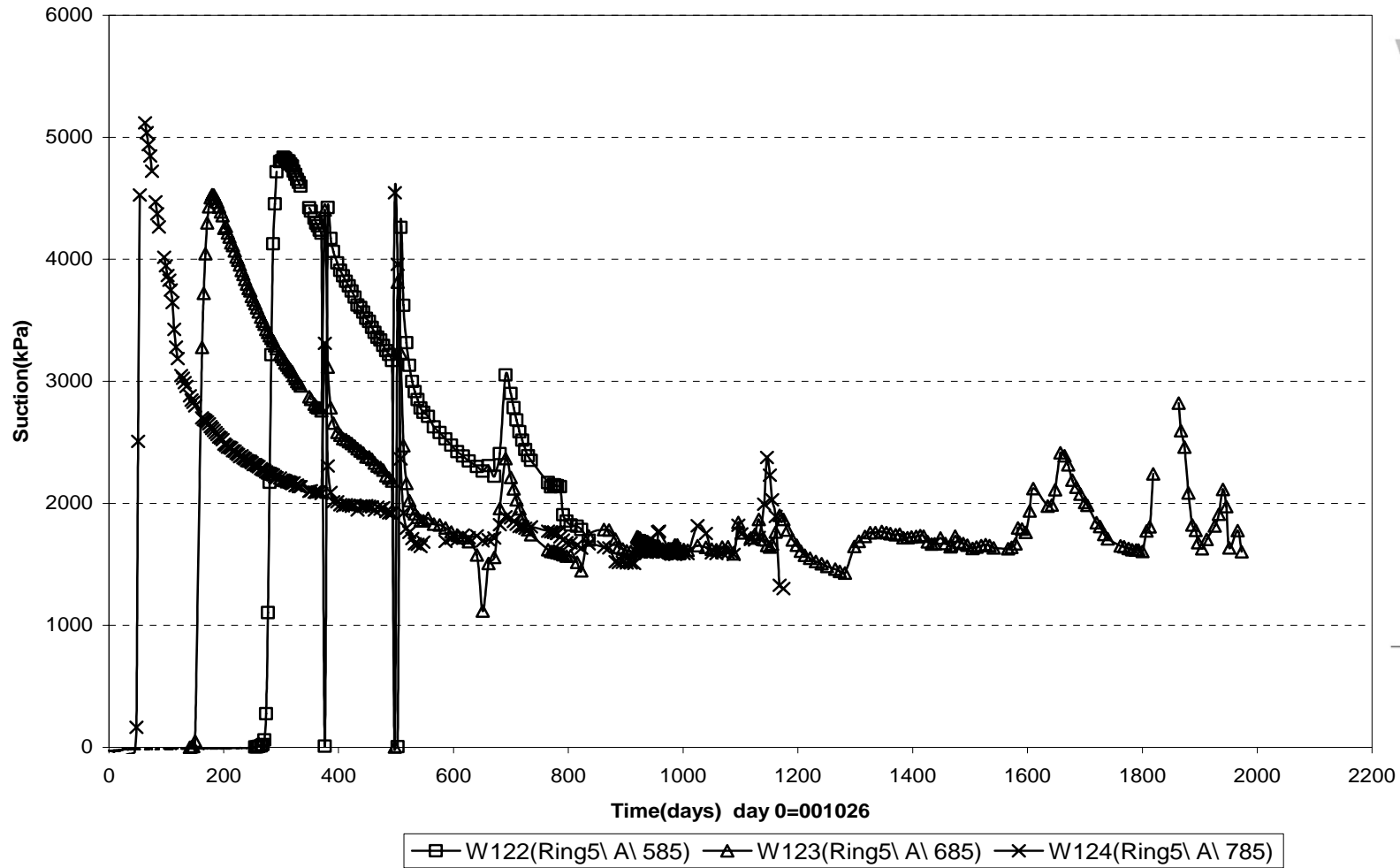
Suction in the buffer - Cyl.1 (001026-060501)  
Wescor



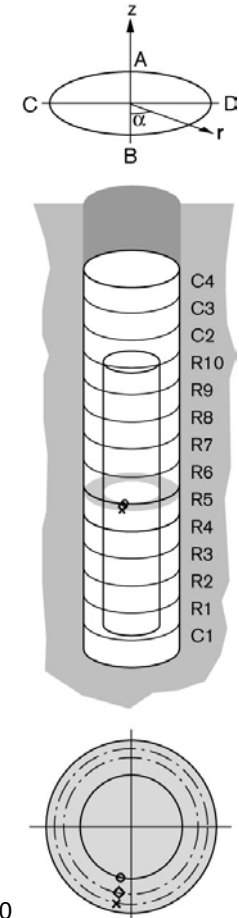
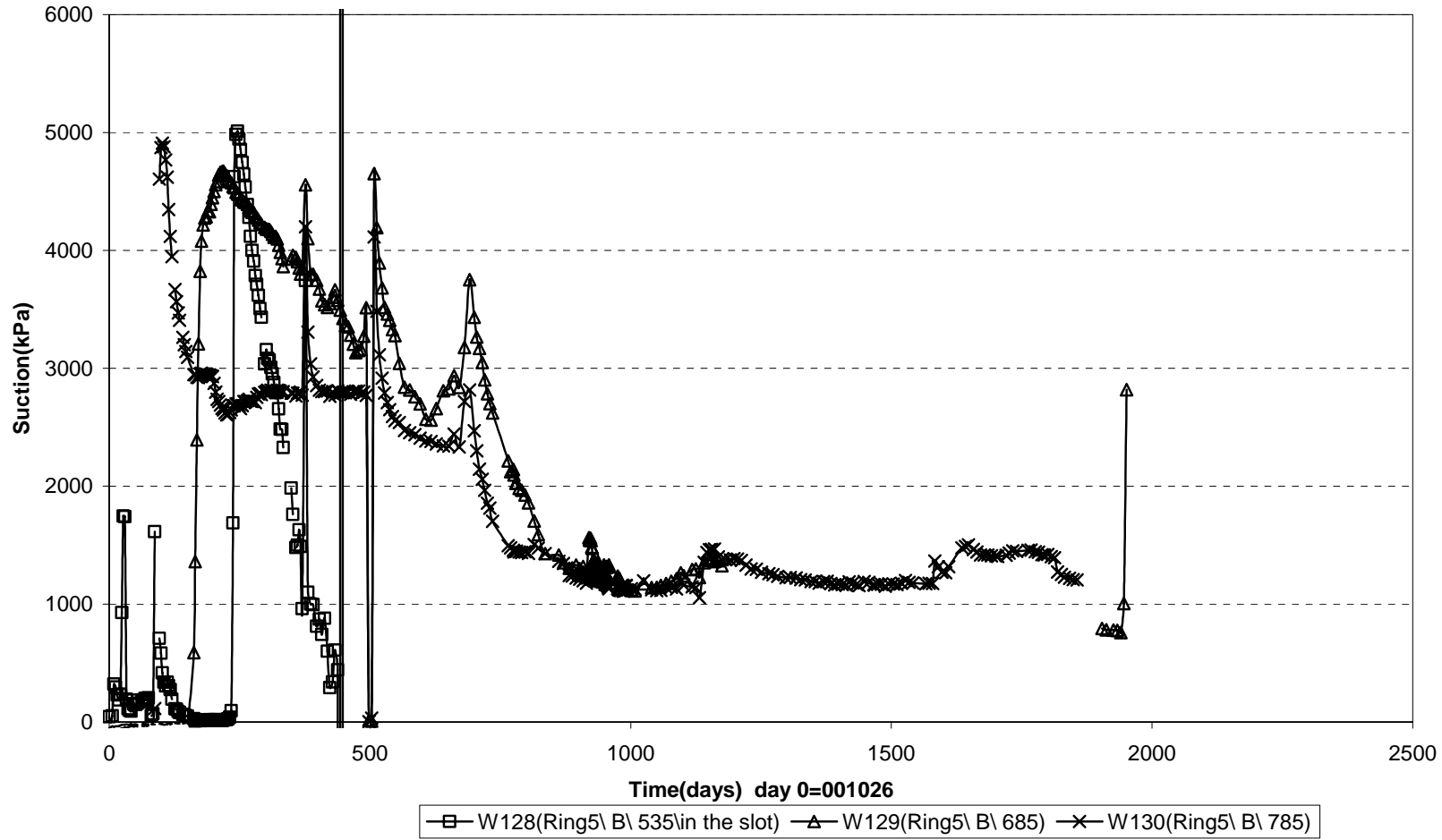
Suction in the buffer - Cyl.1 (001026-060501)  
Wescor



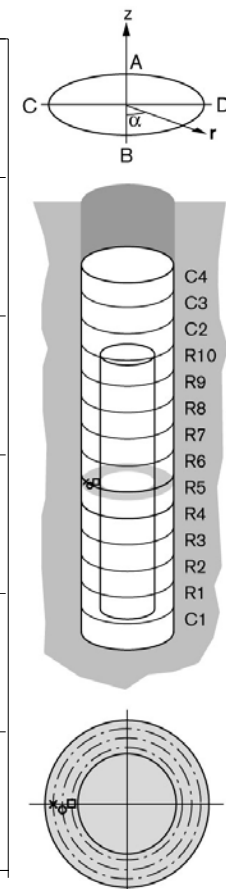
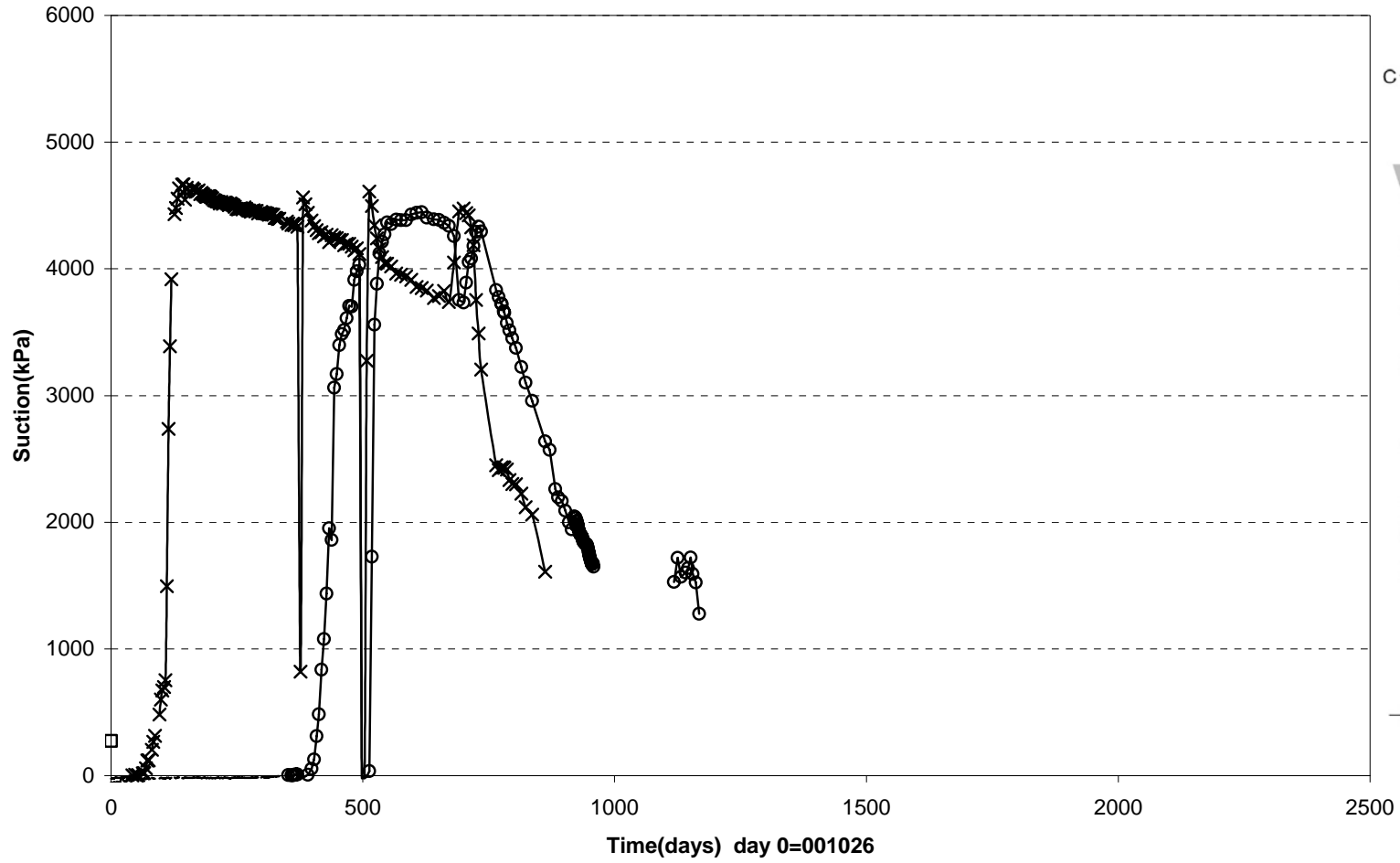
Suction in the buffer - Ring 5 (001026-060501)  
Wescor



Suction in the buffer - Ring 5 (001026-060501)  
Wescor

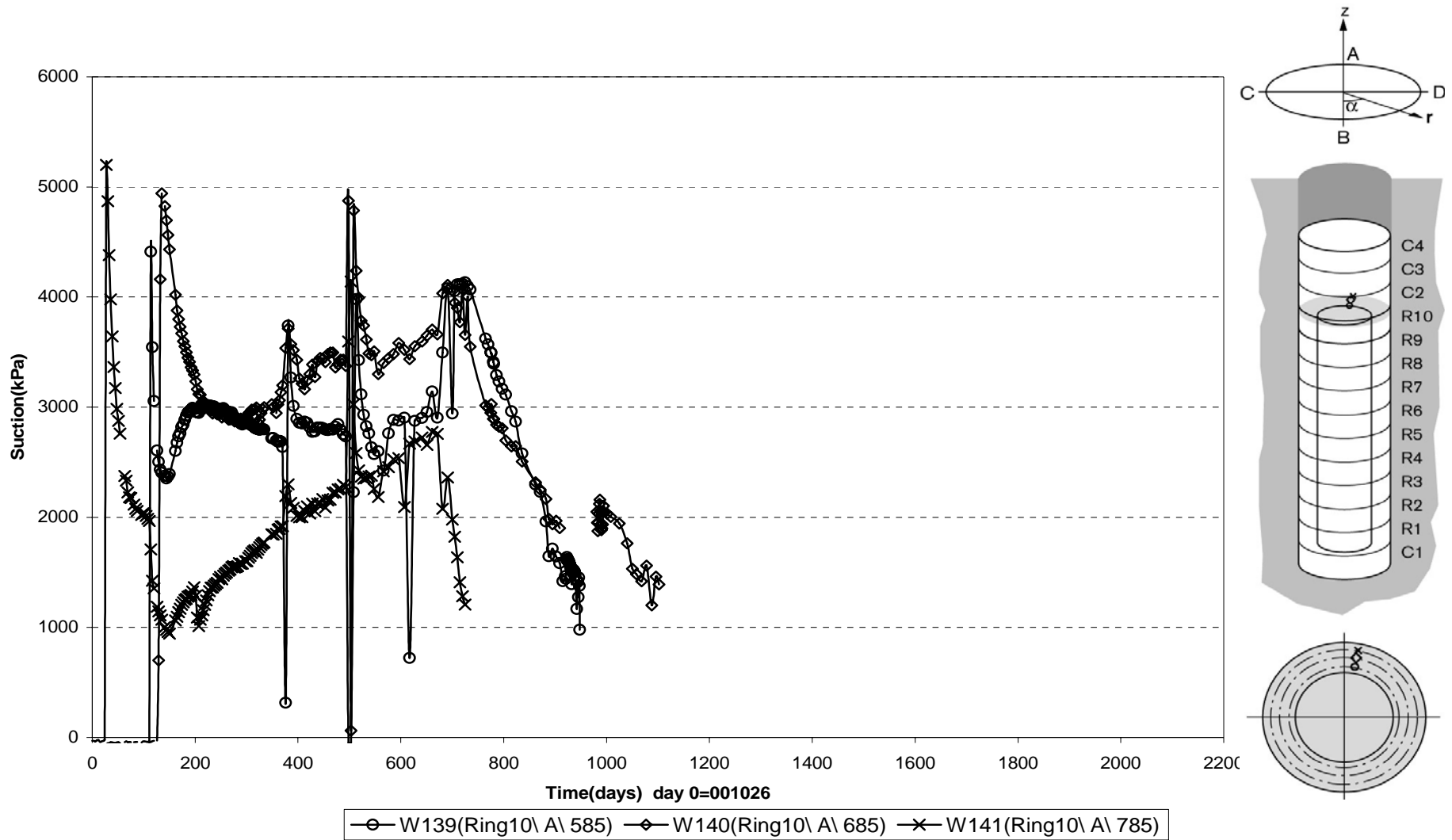


Suction in the buffer - Ring 5 (001026-060501)  
Wescor



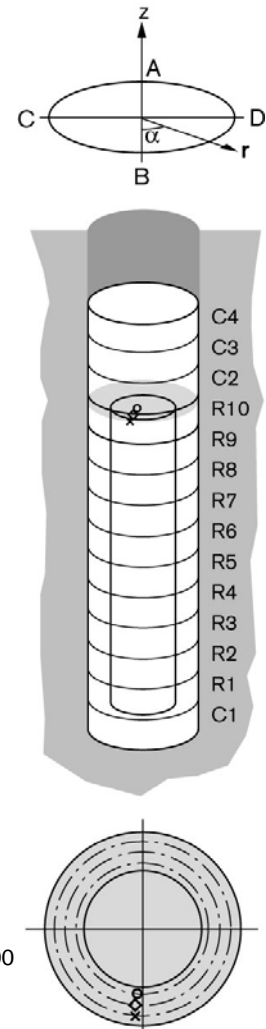
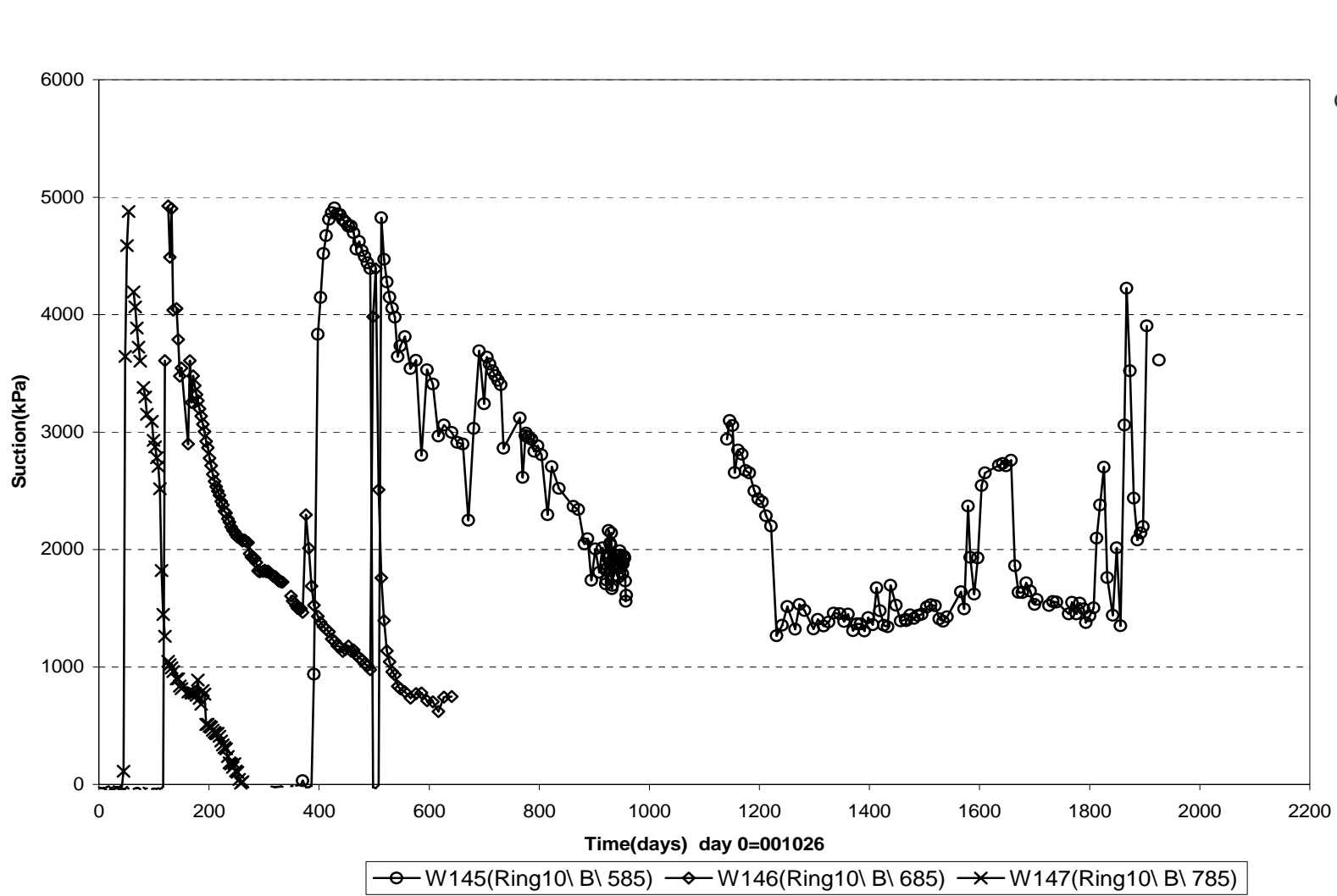
□ W131(Ring5\C\ 535\in the slot)   
 ○ W132(Ring5\C\ 685)   
 × W133(Ring5\C\ 785)

Suction in the buffer - Ring 10 (001026-060501)  
Wescor

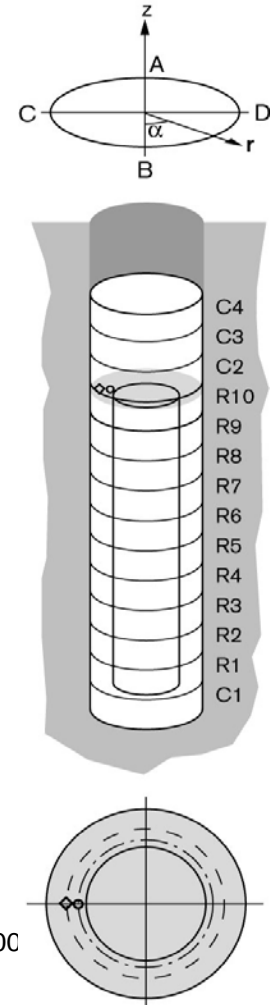
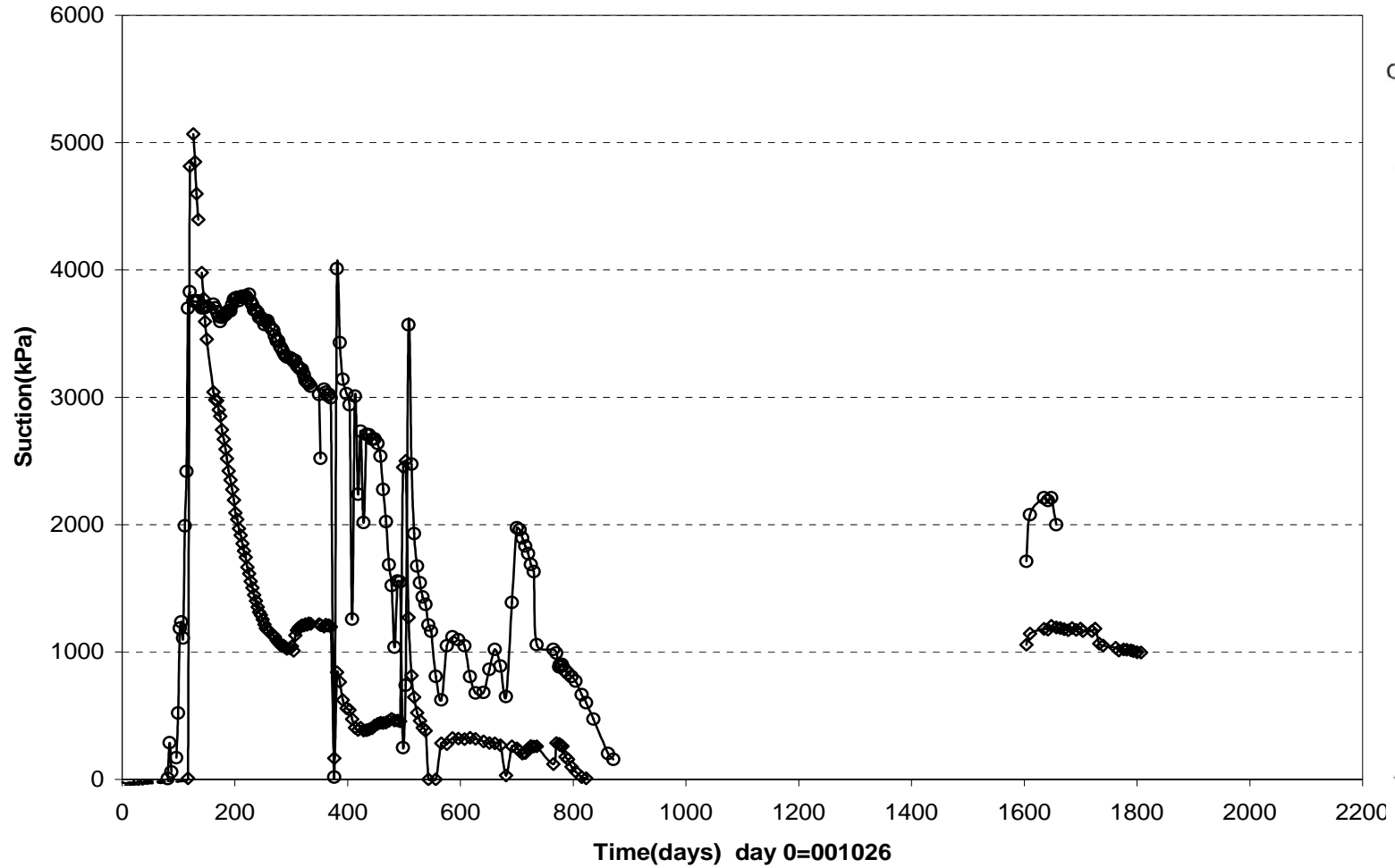




Suction in the buffer - Ring 10 (001026-060501)  
Wescor

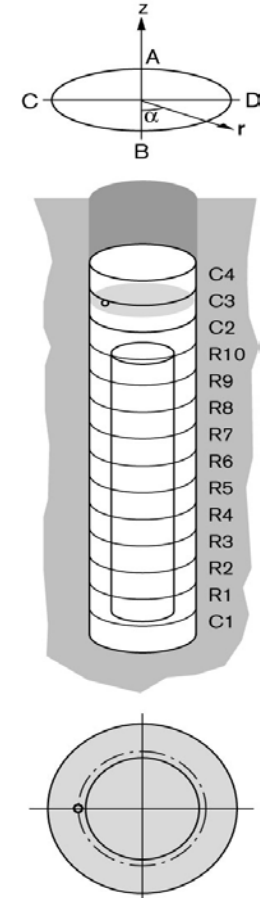
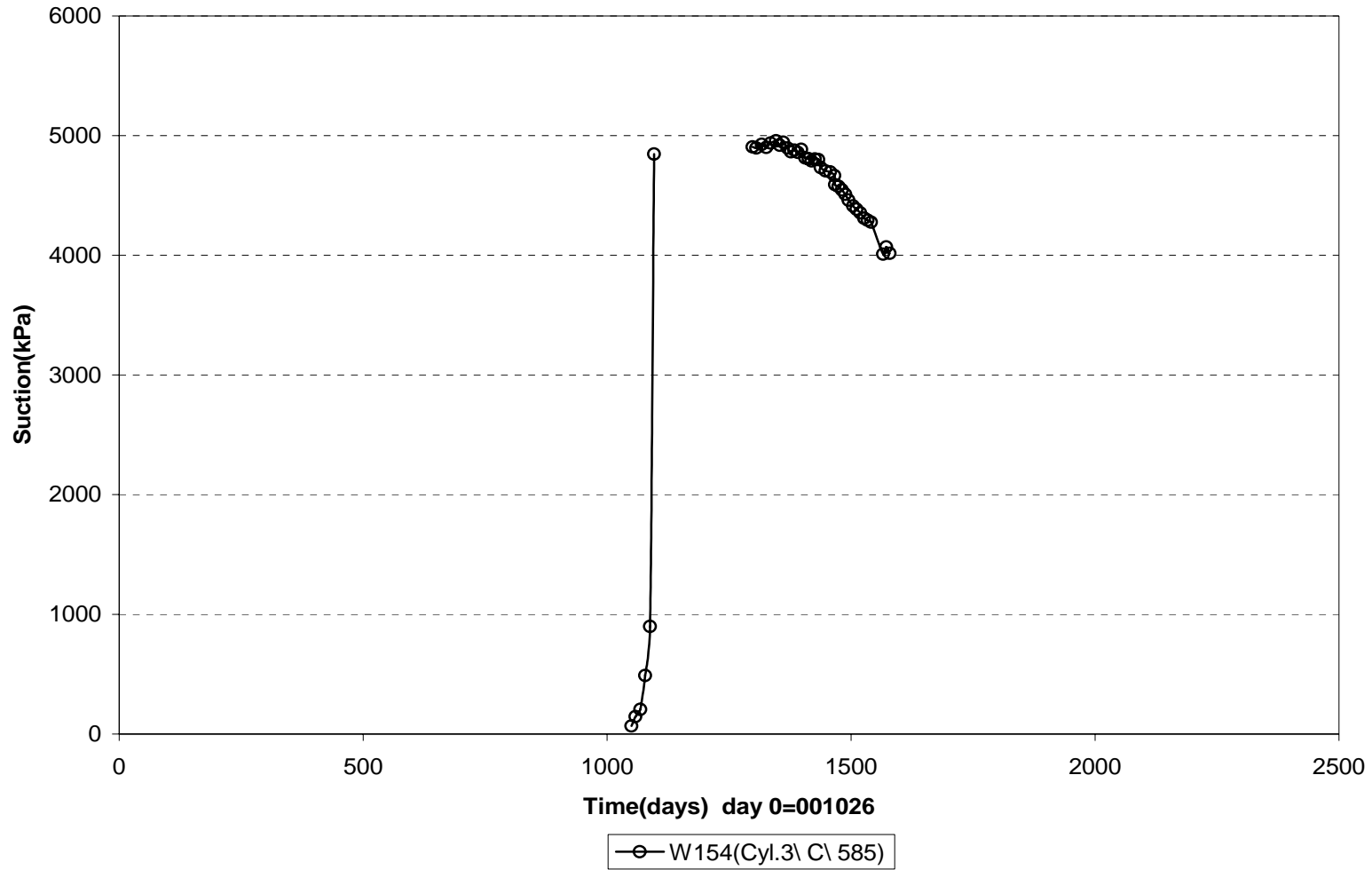


Suction in the buffer - Ring 10 (001026-060501)  
Wescor

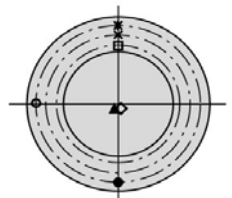
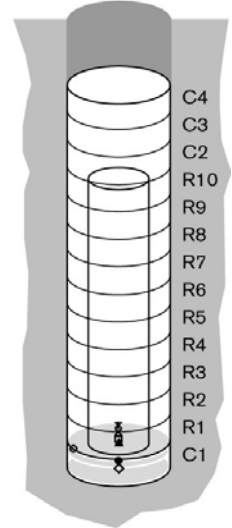
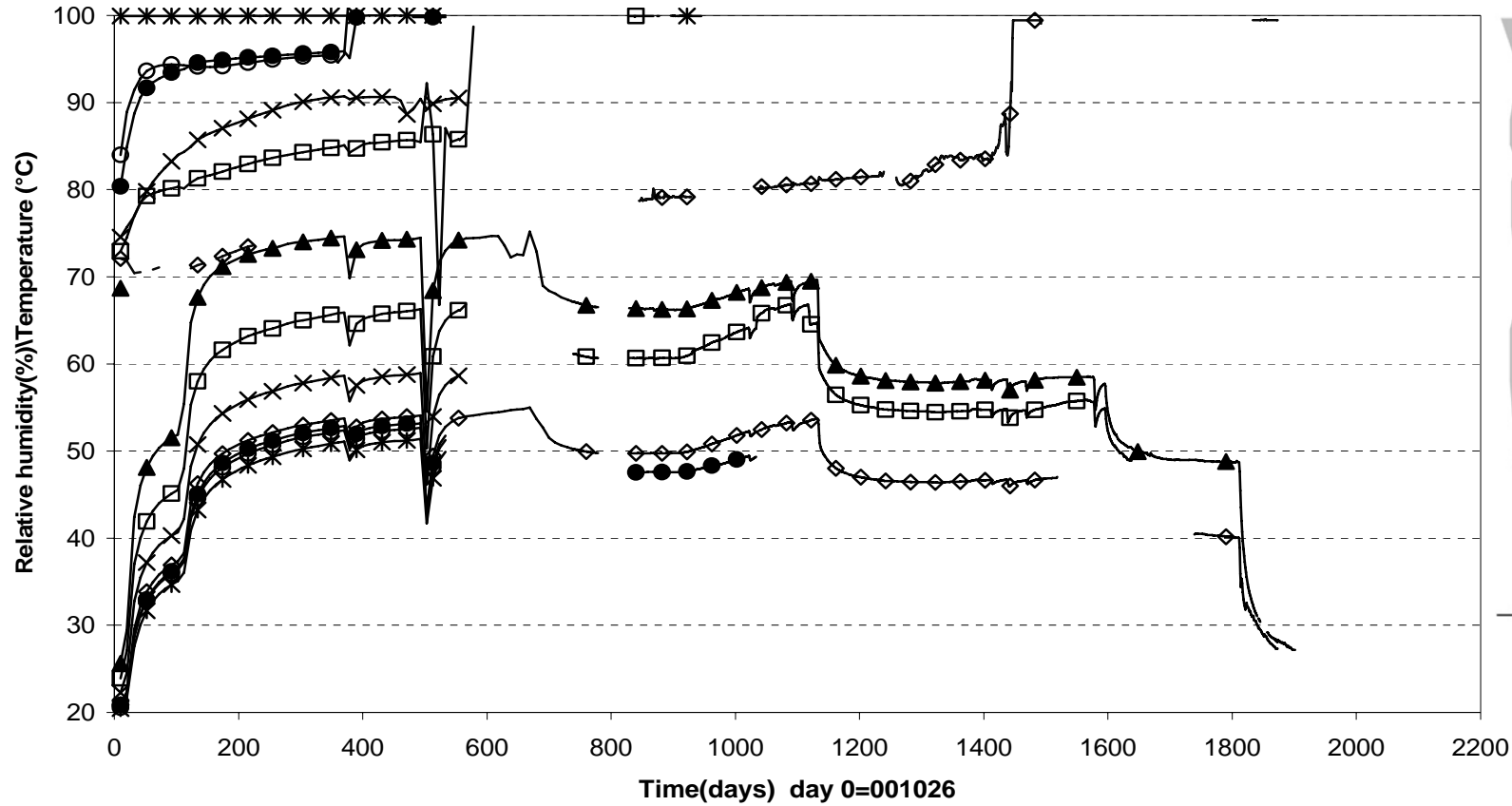
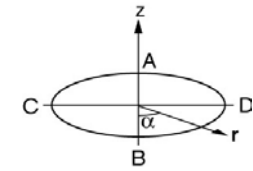


—○— W148(Ring10\C\ 585) —◇— W149(Ring10\C\ 685)

Suction in the buffer - Cyl.3 (001026-060501)  
Wescor

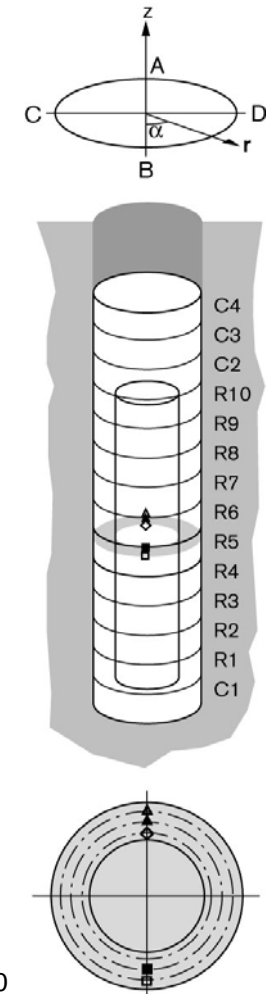
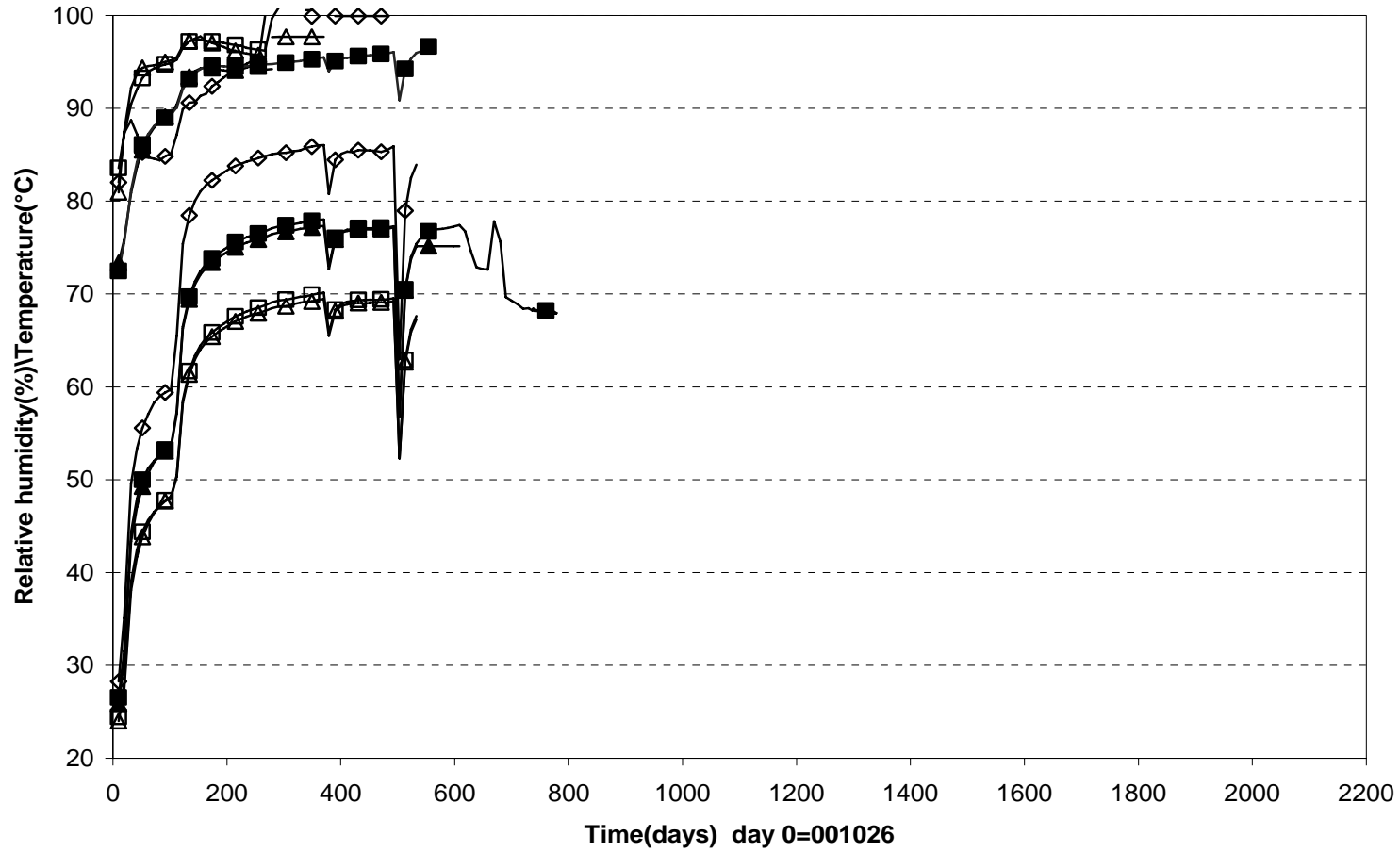


Relative humidity - Cylinder 1 (001026-060501)  
Vaisala



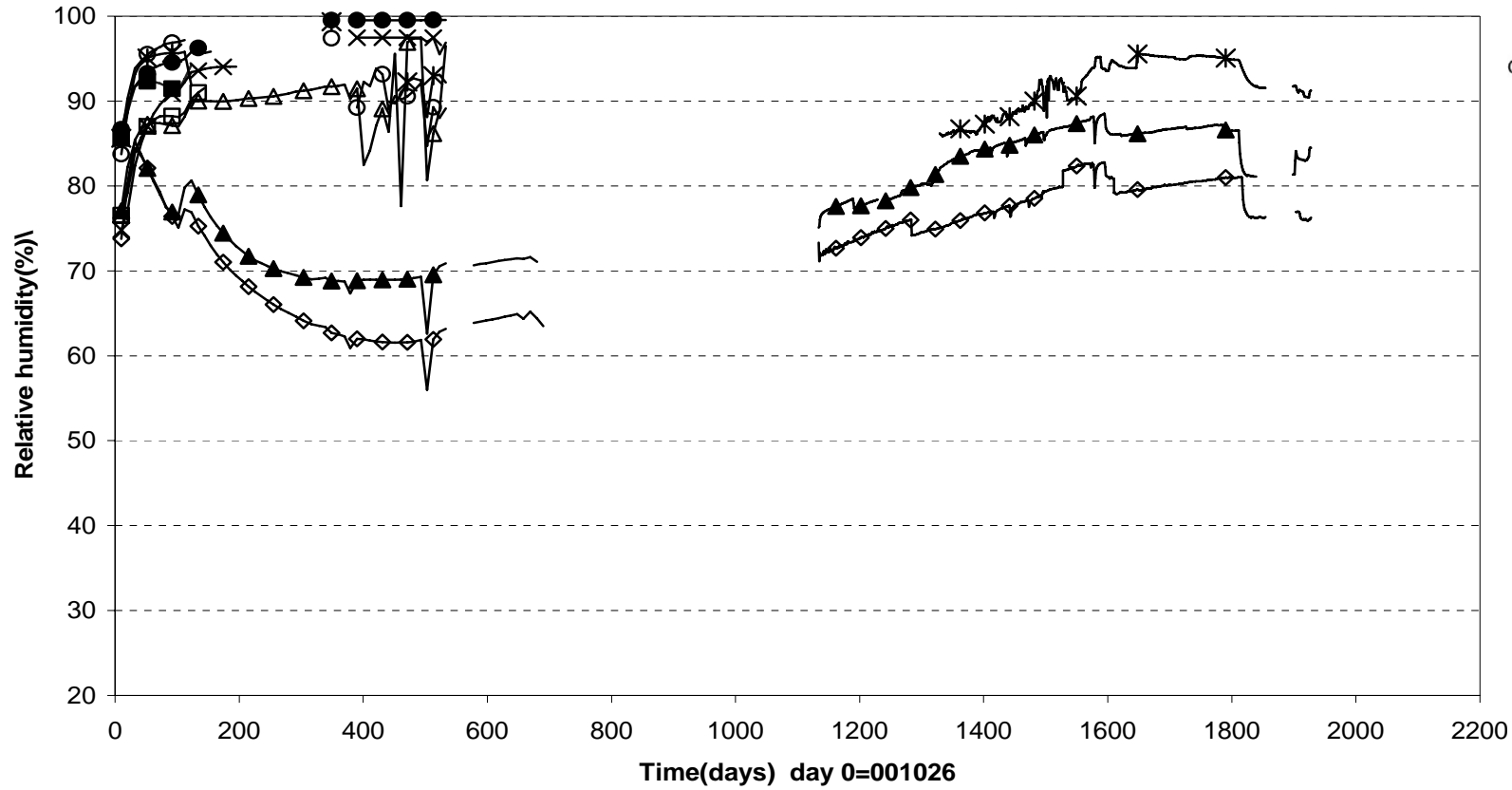
◇ W101(Cyl.1\Center\50)	◇ W101T	▲ W103(Cyl.1\Center\50)	▲ W103T
□ W104(Cyl.1\A\585)	□ W104T	× W105(Cyl.1\A\685)	× W105T
✱ W106(Cyl.1\A\785)	✱ W106T	● W111(Cyl.1\B\785)	● W111T
○ W118(Cyl.1\C\785)	○ W118T		

Relative humidity- Ring 5 (001026-060501)  
Vaisala

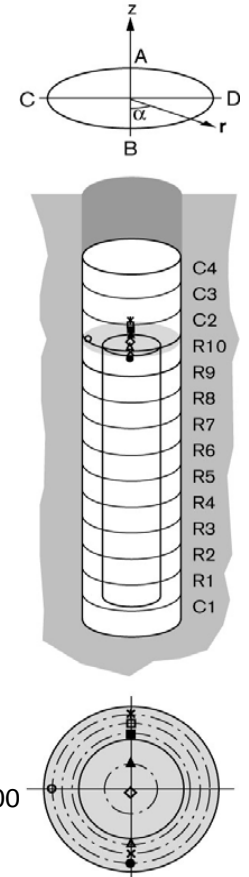


◇ W119(Ring5A\585)	◇ W119T	▲ W120Ring5A\685)	▲ W120T	■ W126(Ring5B\685)
■ W126T	△ W121(Ring5A\785)	△ W121T	□ W127(Ring5B\785)	□ W127T

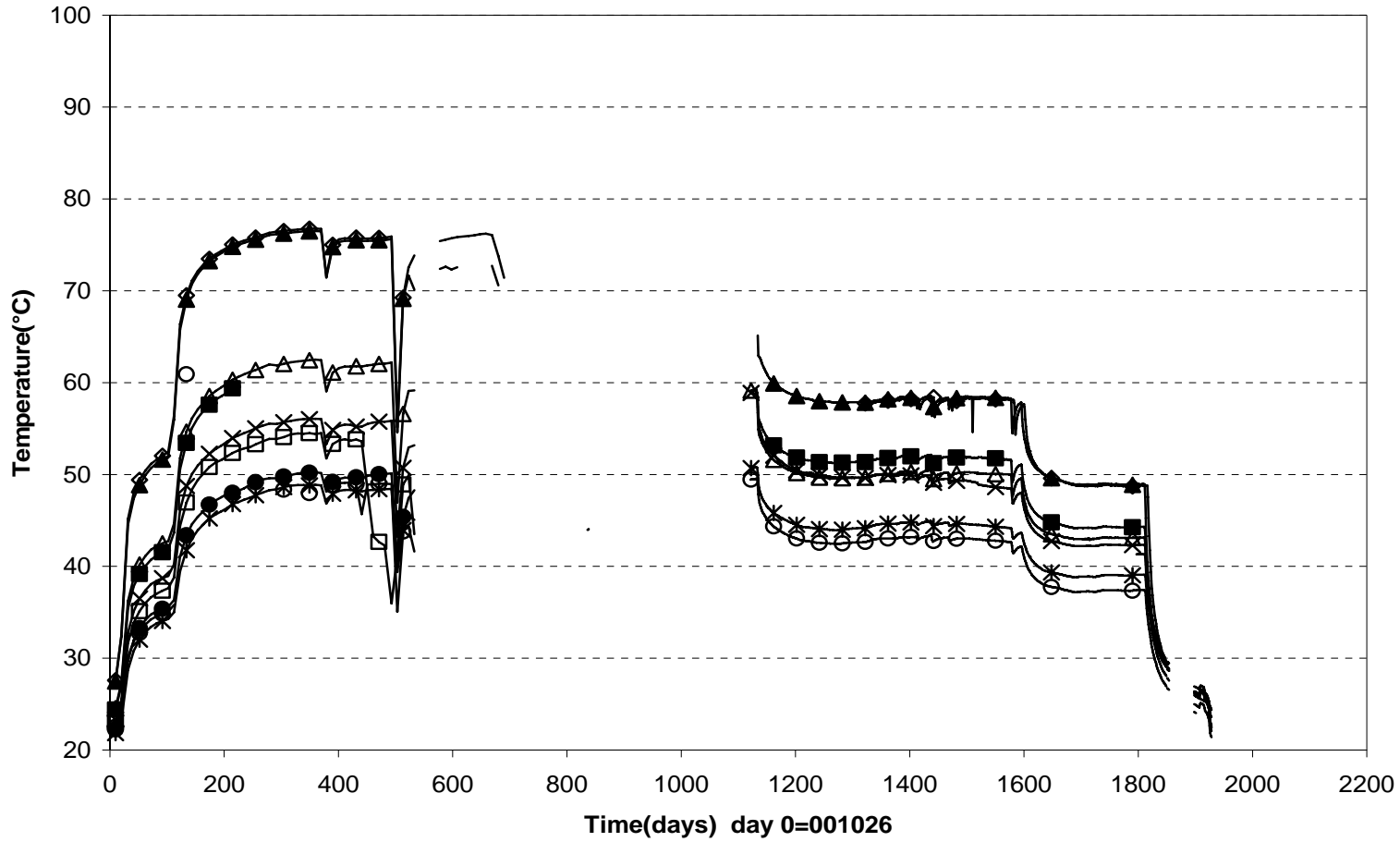
Relative humidity - Ring 10 (001026-060501)  
Vaisala



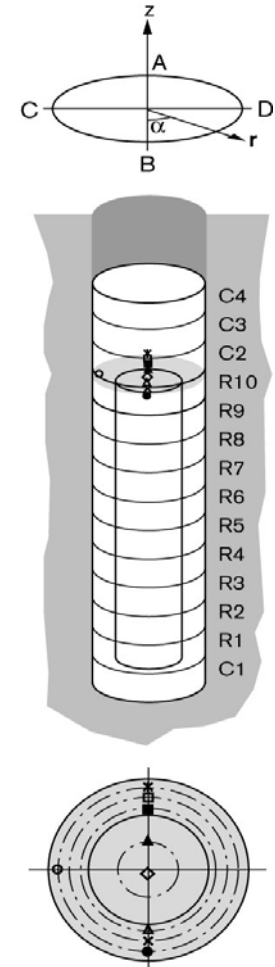
◇ W134(Ring.10\center\50)	▲ W135(Ring.10\A\262)	■ W136(Ring.10\A\585)
△ W142(Ring.10\B\585)	□ W137(Ring.10\A\685)	× W143(Ring.10\B\685)
✱ W138(Ring.10\A\785)	● W144(Ring.10\B\785)	○ W150(Ring.10\C\785)



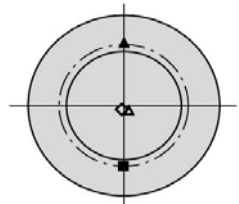
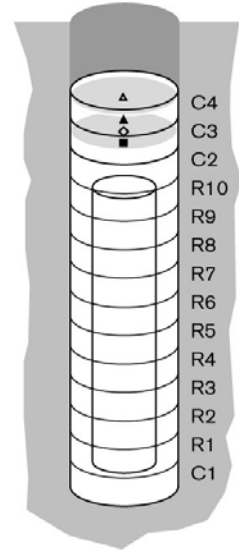
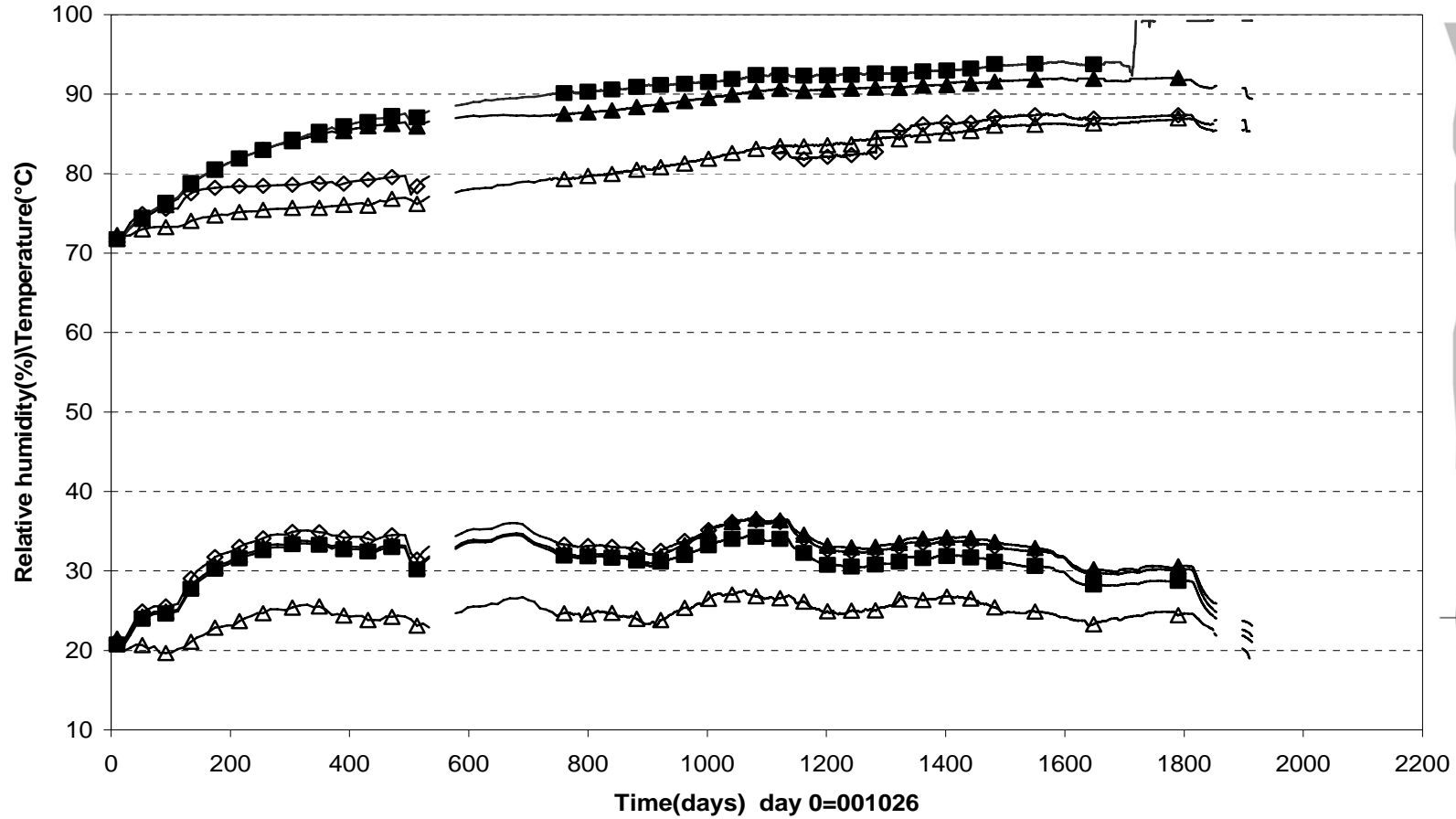
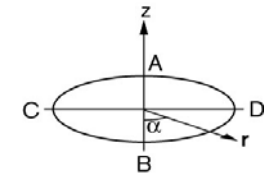
Relative humidity - Ring 10 (001026-060501)  
Vaisala



◇ W134T    ▲ W135T    ■ W136T    △ W142T    □ W137T    × W143T    ✖ W138T    ● W144T    ○ W150T



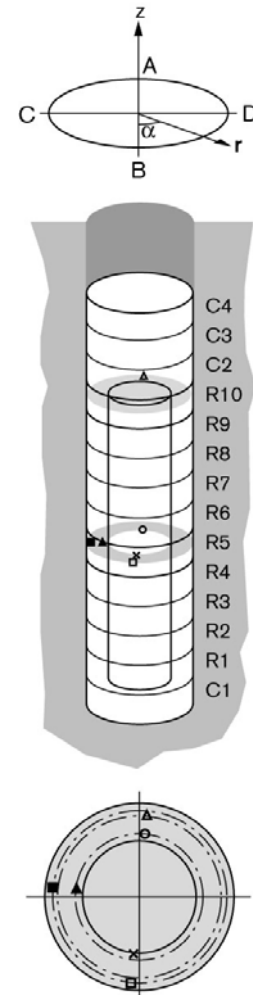
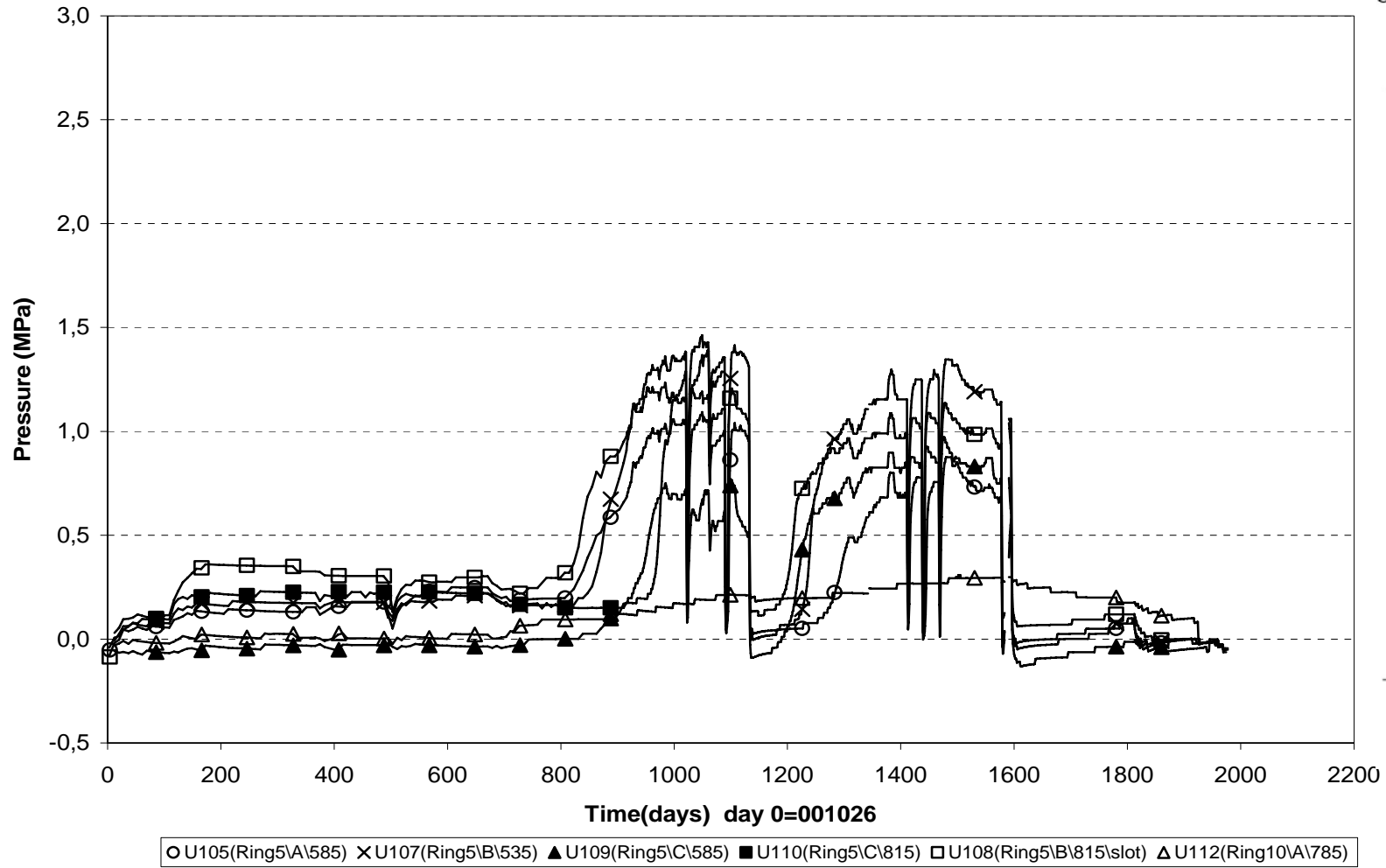
Relative humidity - Cylinder 3 and Cylinder 4 (001026-060501)  
Vaisala



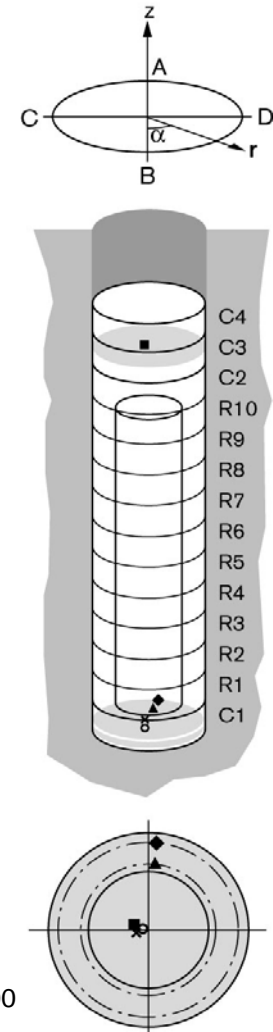
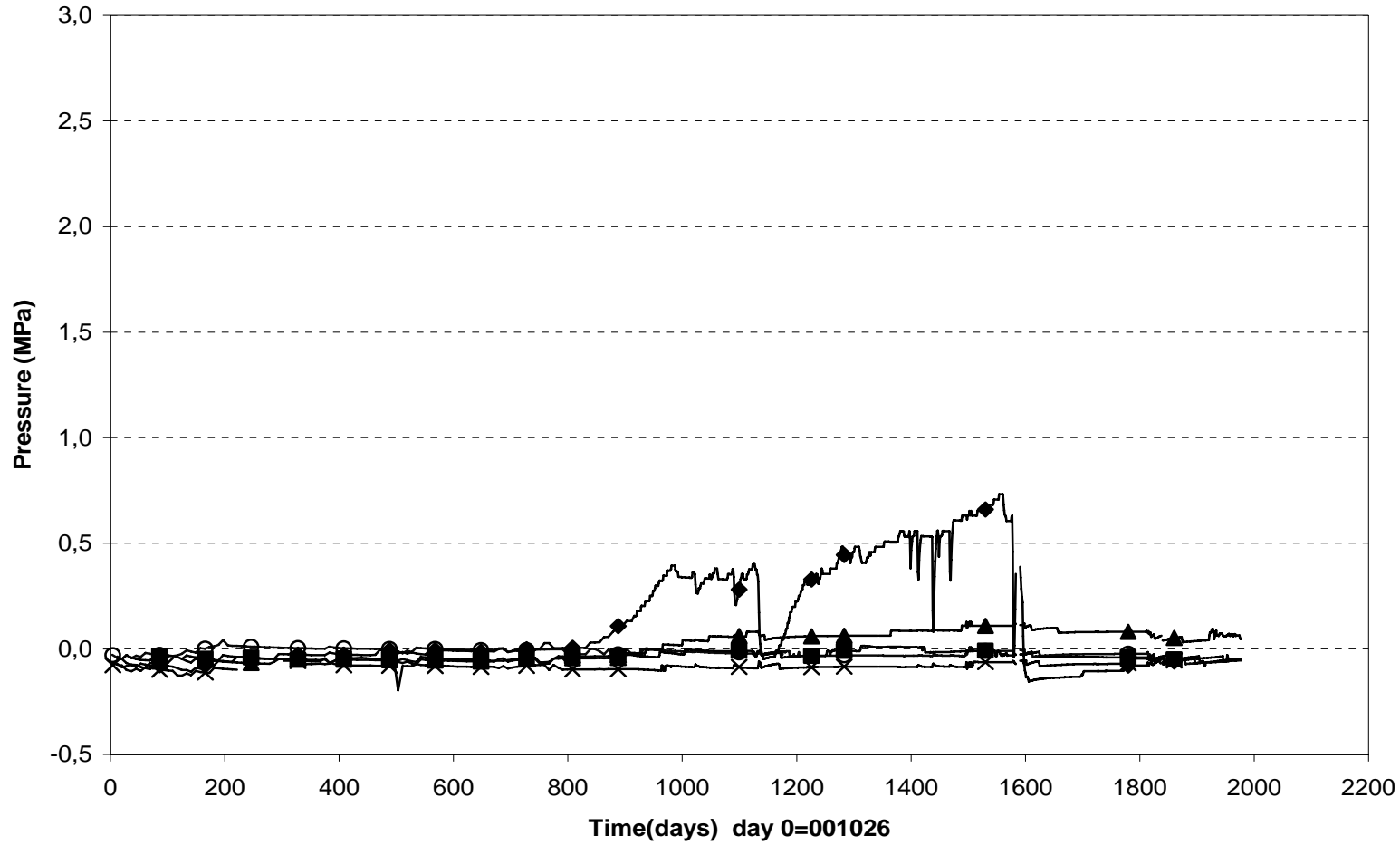
◇ W151(Cyl.3\Center\50)    ◇ W151T    ▲ W152(Cyl.3\A\585)    ▲ W152T    ■ W153(Cyl.3\C\585)    ■ W153T    △ W155(Cyl.4\center\50)    △ W155T



**Pore water pressure - Ring 5 and Ring 10 (001026-060501)  
Geokon**

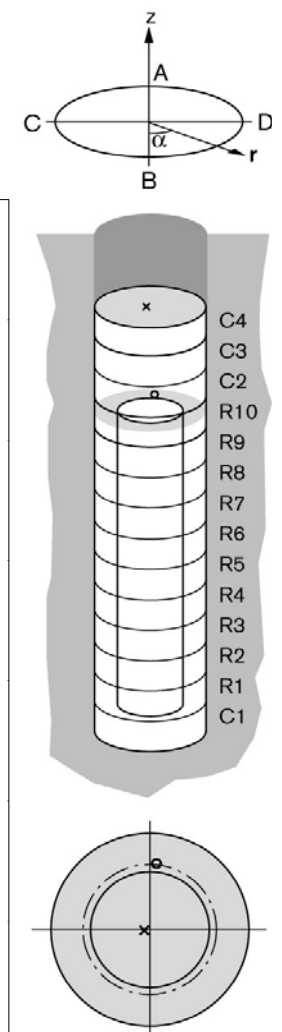
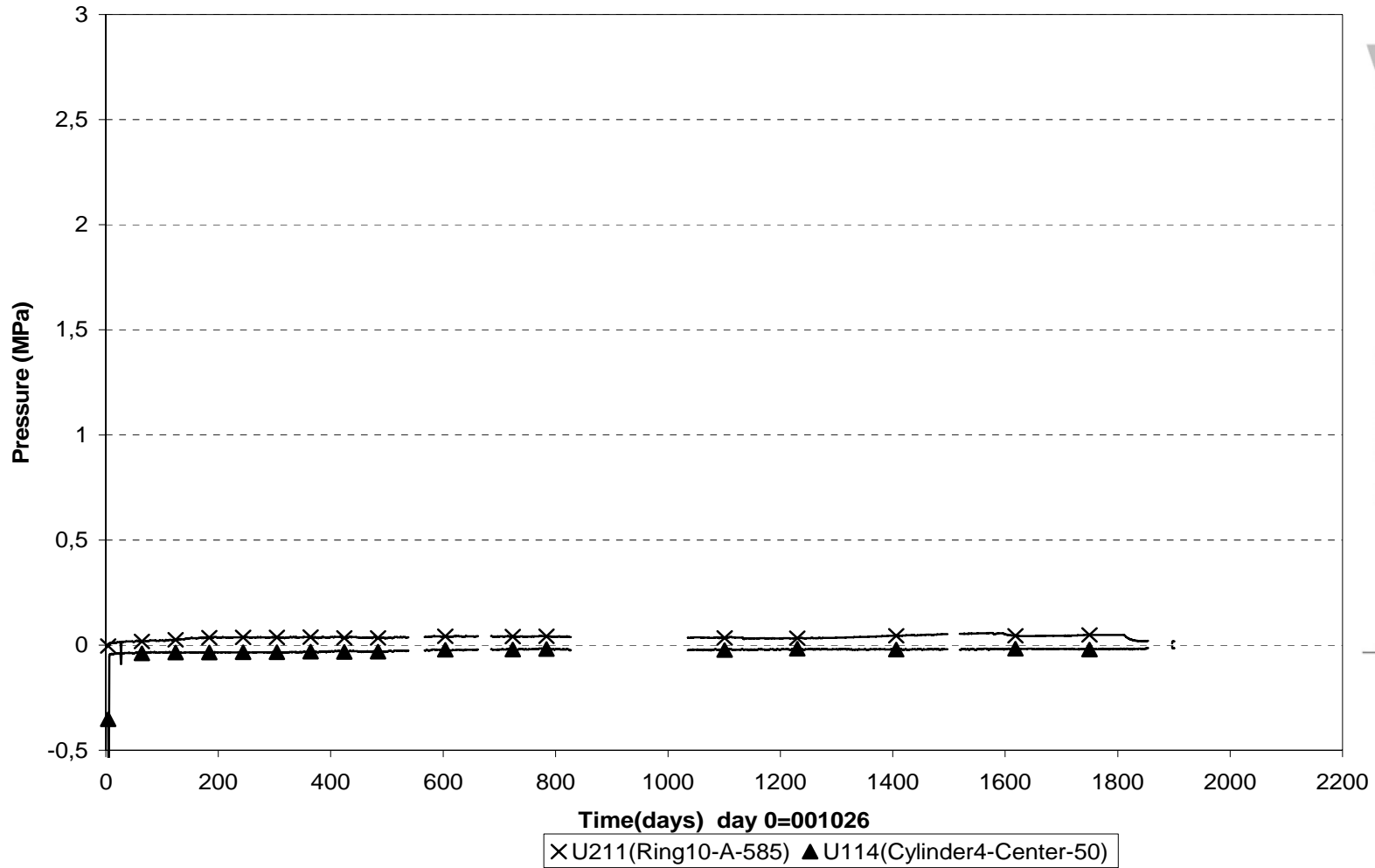


Pore water pressure - Cylinder 1 and Cylinder 3 (001026-060501)  
Geokon

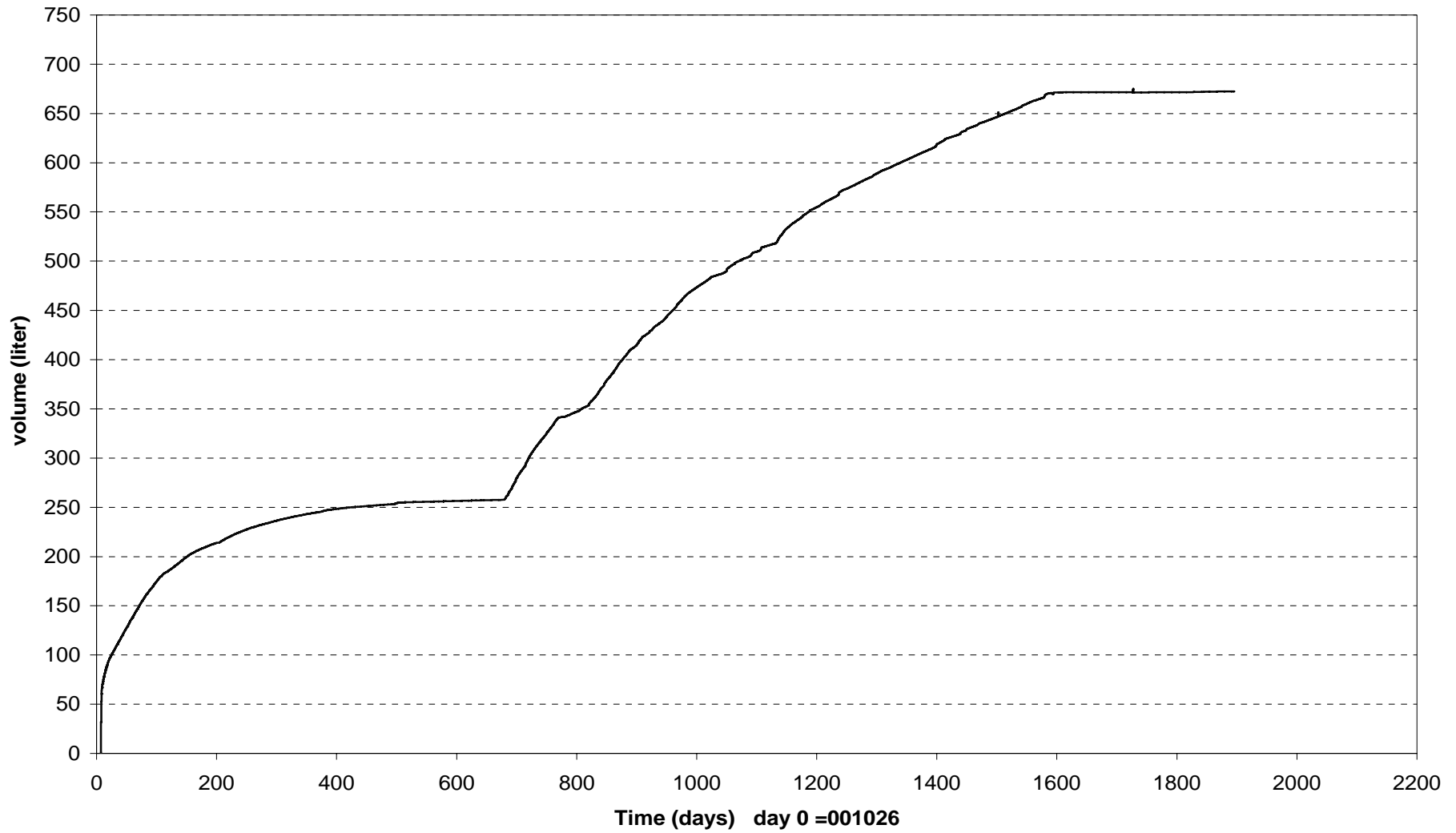


○ U101(Cyl.1\center\50) × U102(Cyl.1\center\50) ▲ U103(Cyl.1\A\585) ◆ U104(Cyl.1\A\785) ■ U113(Cyl.3\center\50)

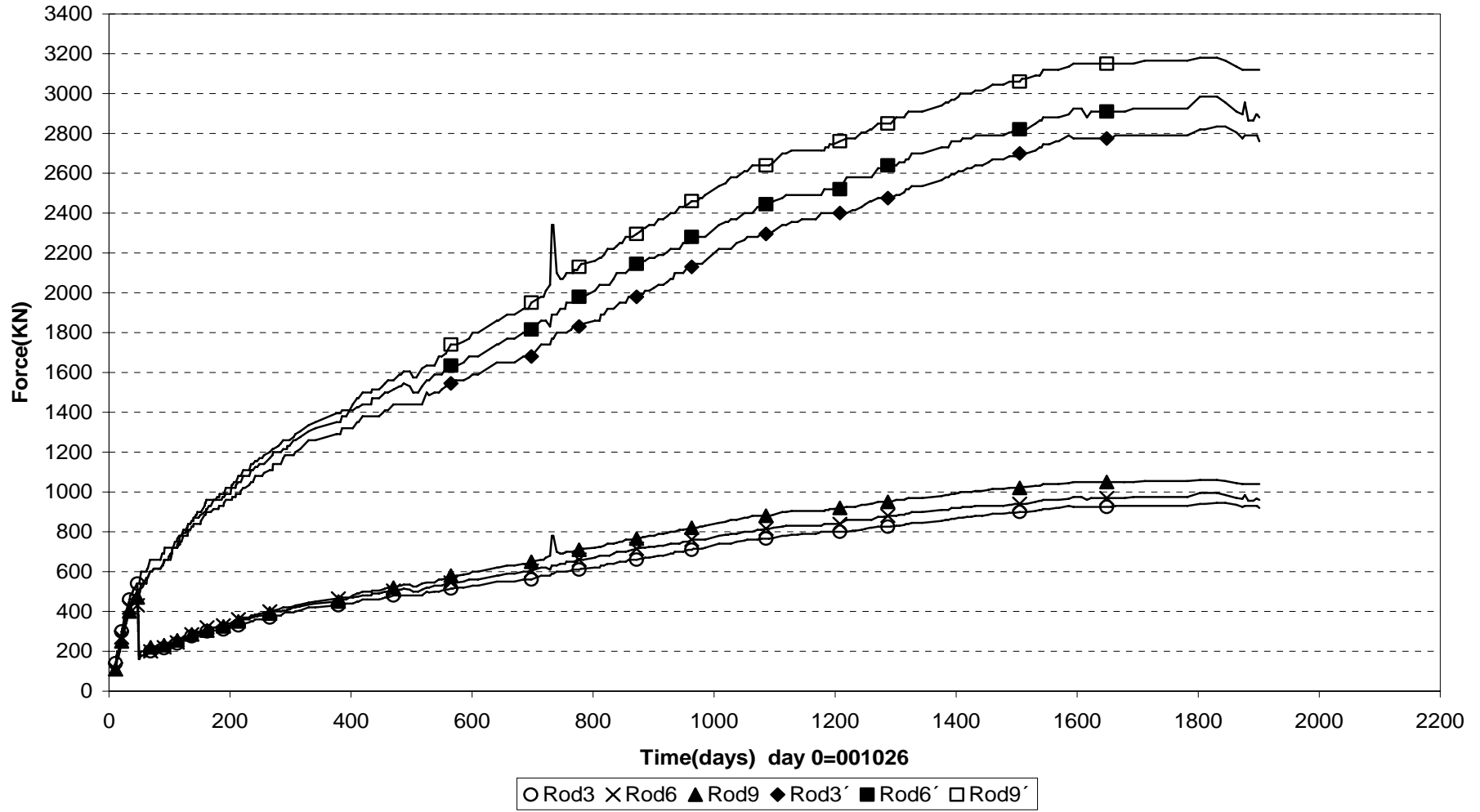
Pore water pressure - Ring 10 & Cylinder 4 (001026-060501)  
Kulite



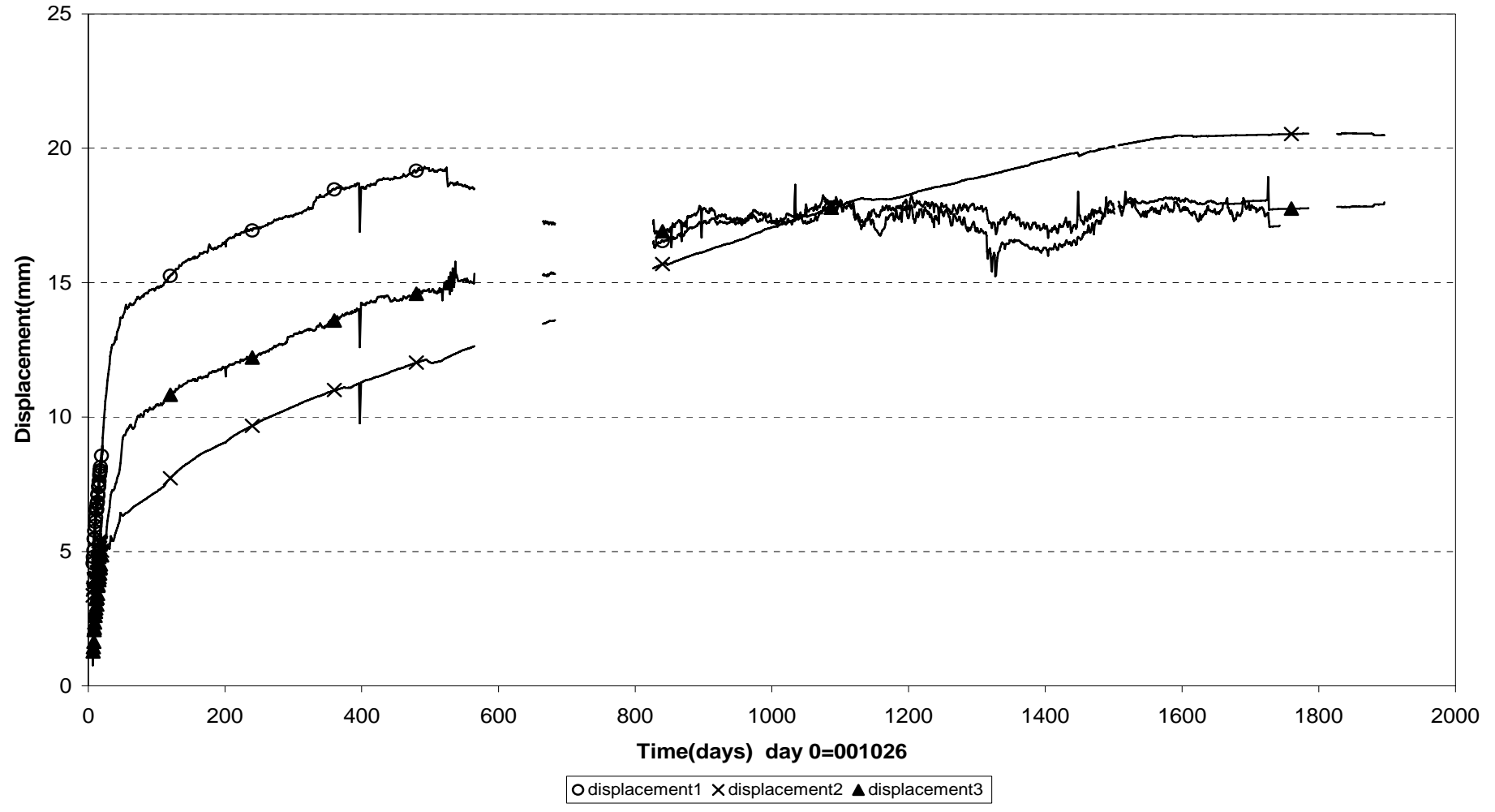
### Inflow into filter (001026-060501)



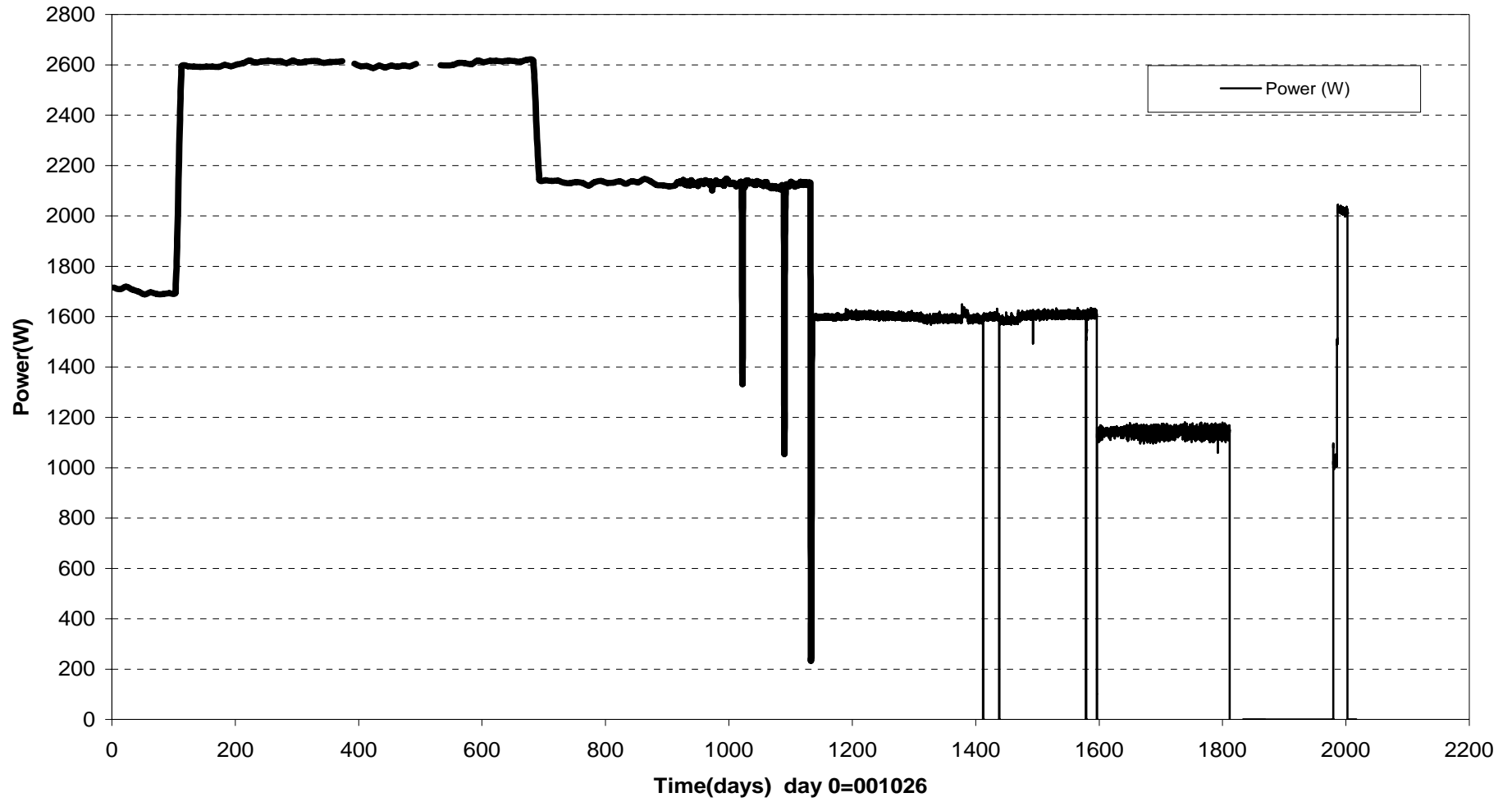
### Forces on plug (001026-060109)



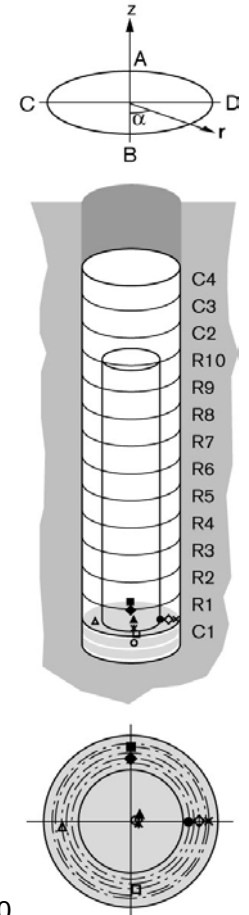
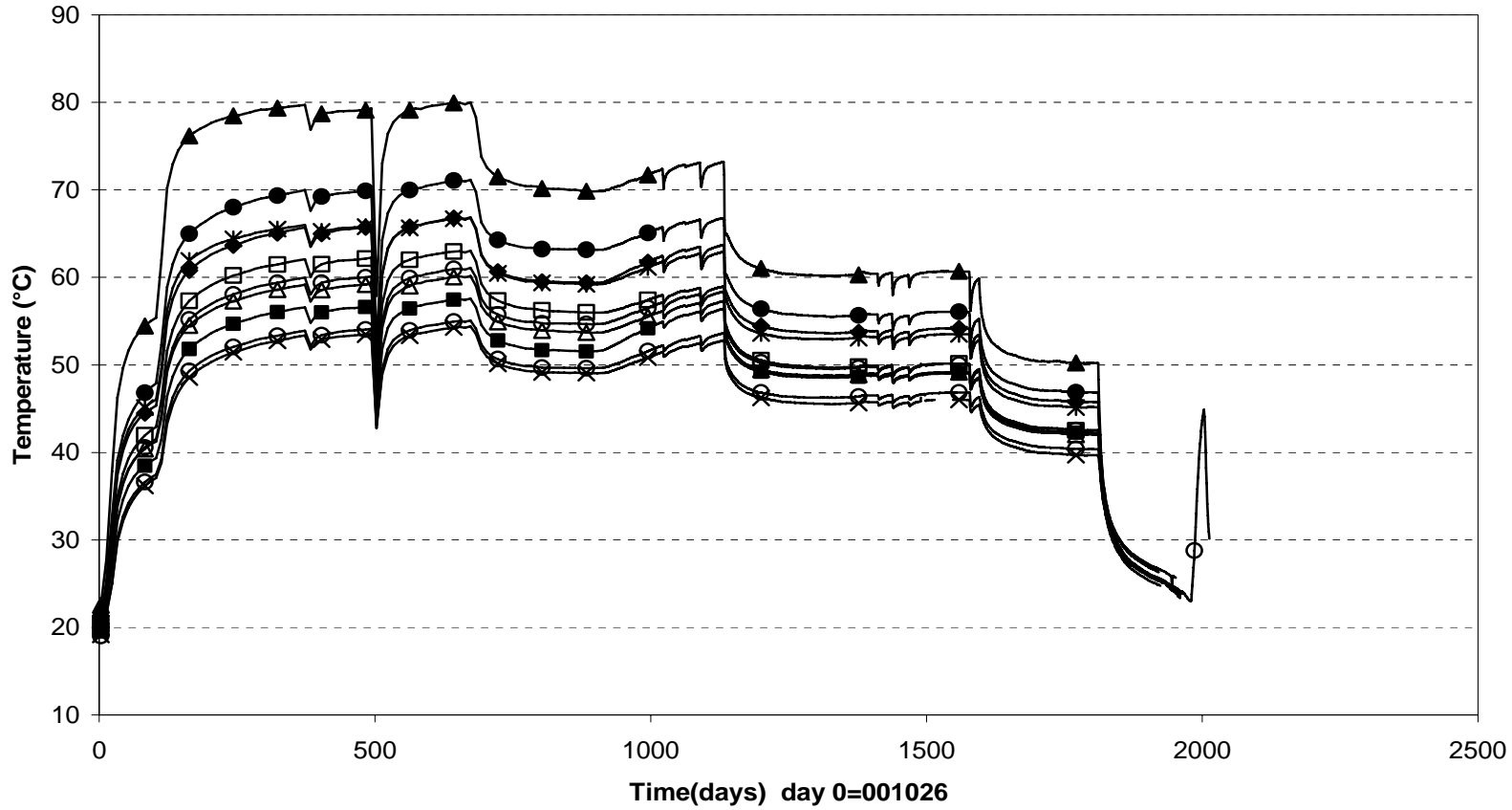
### Displacement of plug (001026-060501)



Canister power (001026-060501)



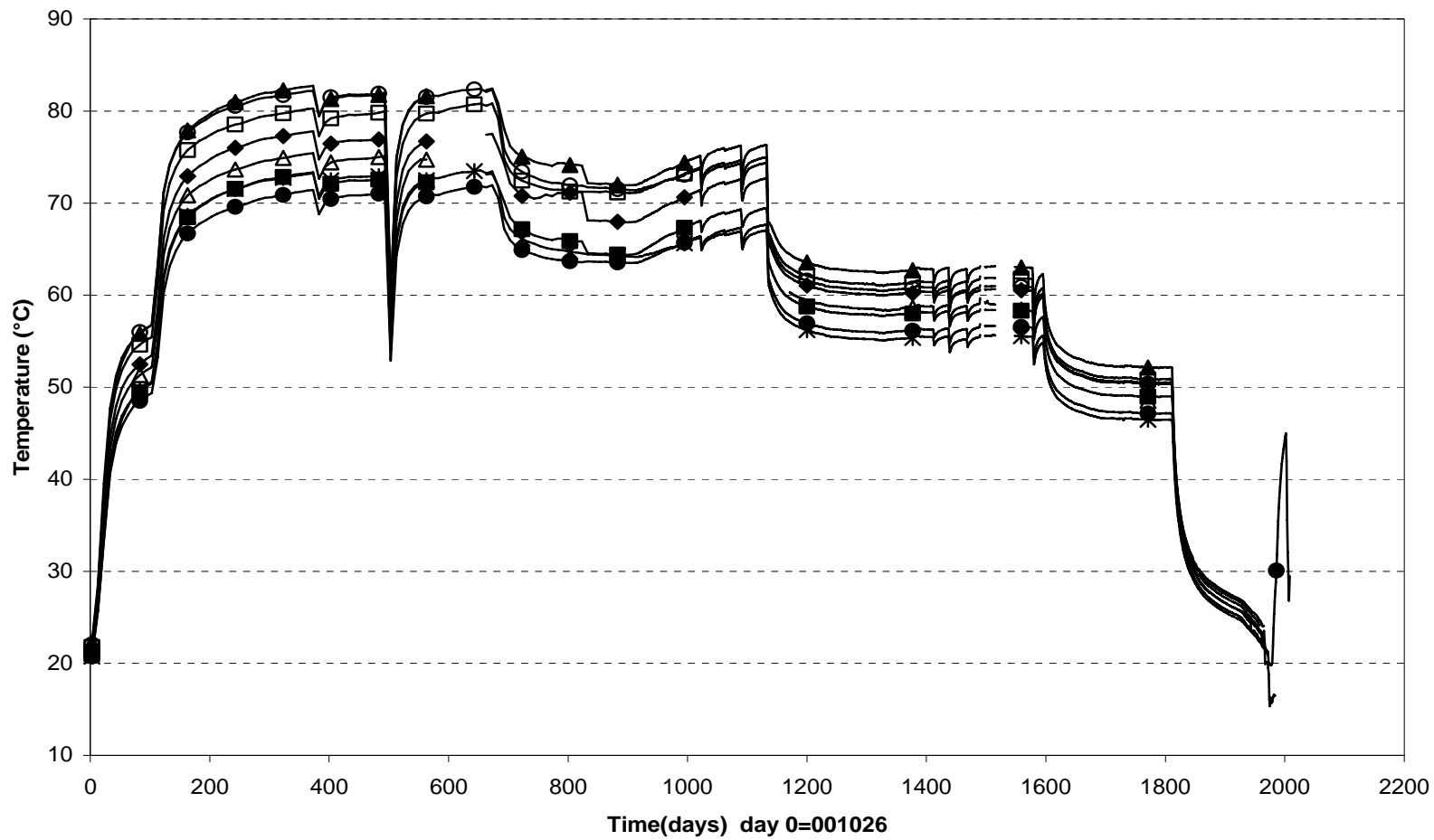
### Temperature in the buffer - Cylinder 1 (001026-060501) Thermocouple



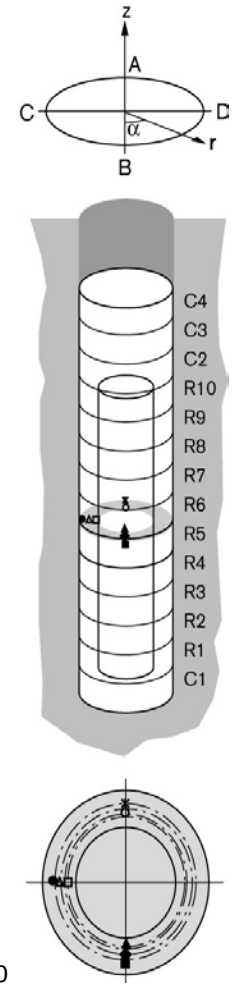
○ T101(Cyl.1\center\50)	✖ T102(Cyl.1\center\50)	▲ T103(Cyl.1\center\50)	◆ T104(Cyl.1\A\635)
■ T105(Cyl.1\A\735)	□ T106(Cyl.1\B\685)	△ T107(Cyl.1\C\685)	● T108(Cyl.1\D\585)
○ T109(Cyl.1\D\685)	× T110(Cyl.1\D\785)		



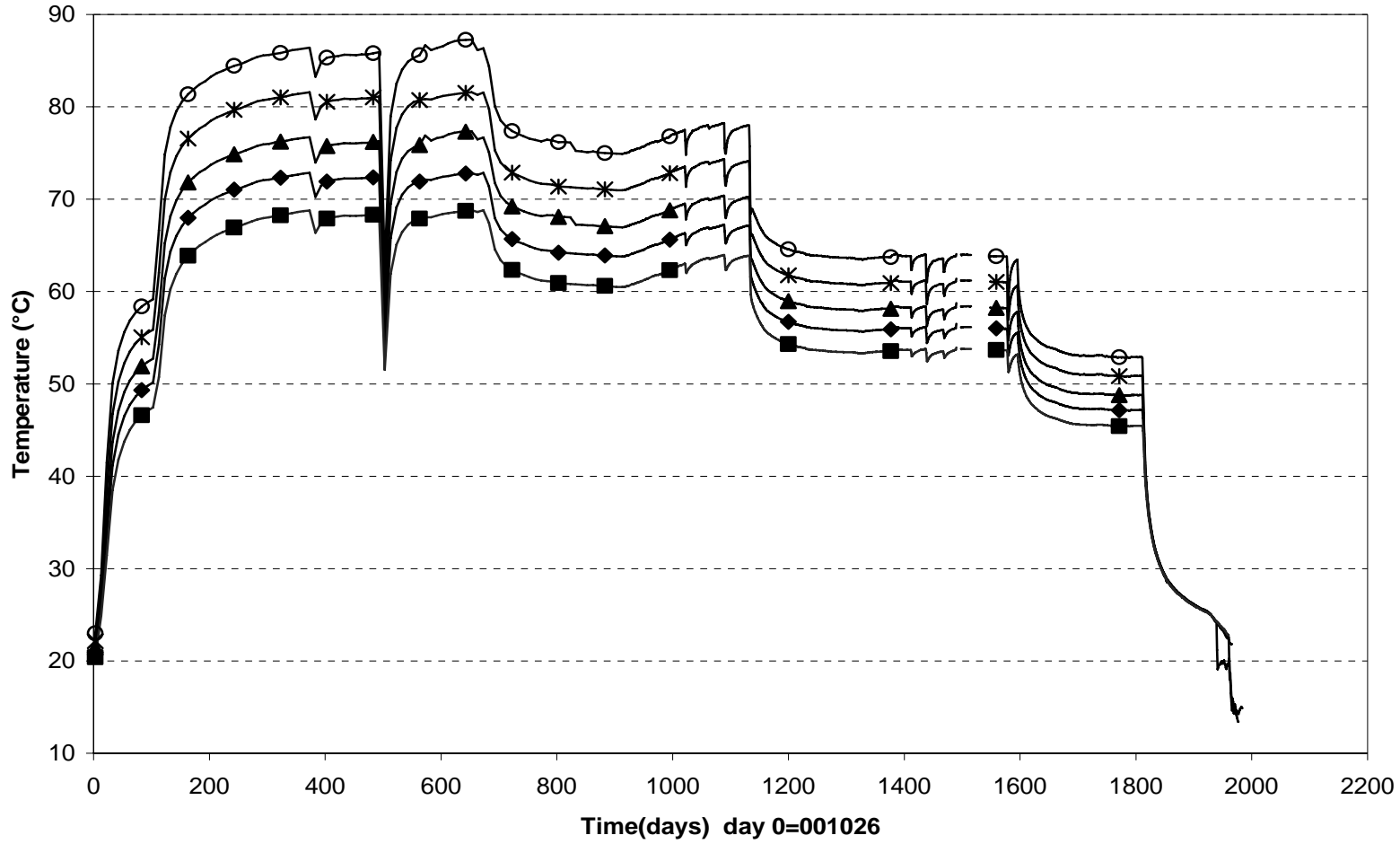
**Temperature in the buffer - Ring 5 (001026-060501)**  
**Thermocouple**



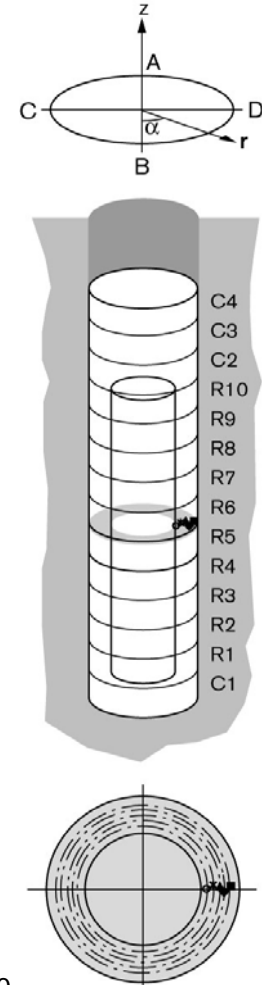
○ T111(Ring5\A\635)	✱ T112(Ring5\A\735)	▲ T113(Ring5\B\610)	◆ T114(Ring5\B\685)
■ T115(Ring5\B\735)	□ T116(Ring5\C\610)	△ T117(Ring5\C\685)	● T118(Ring5\C\735)



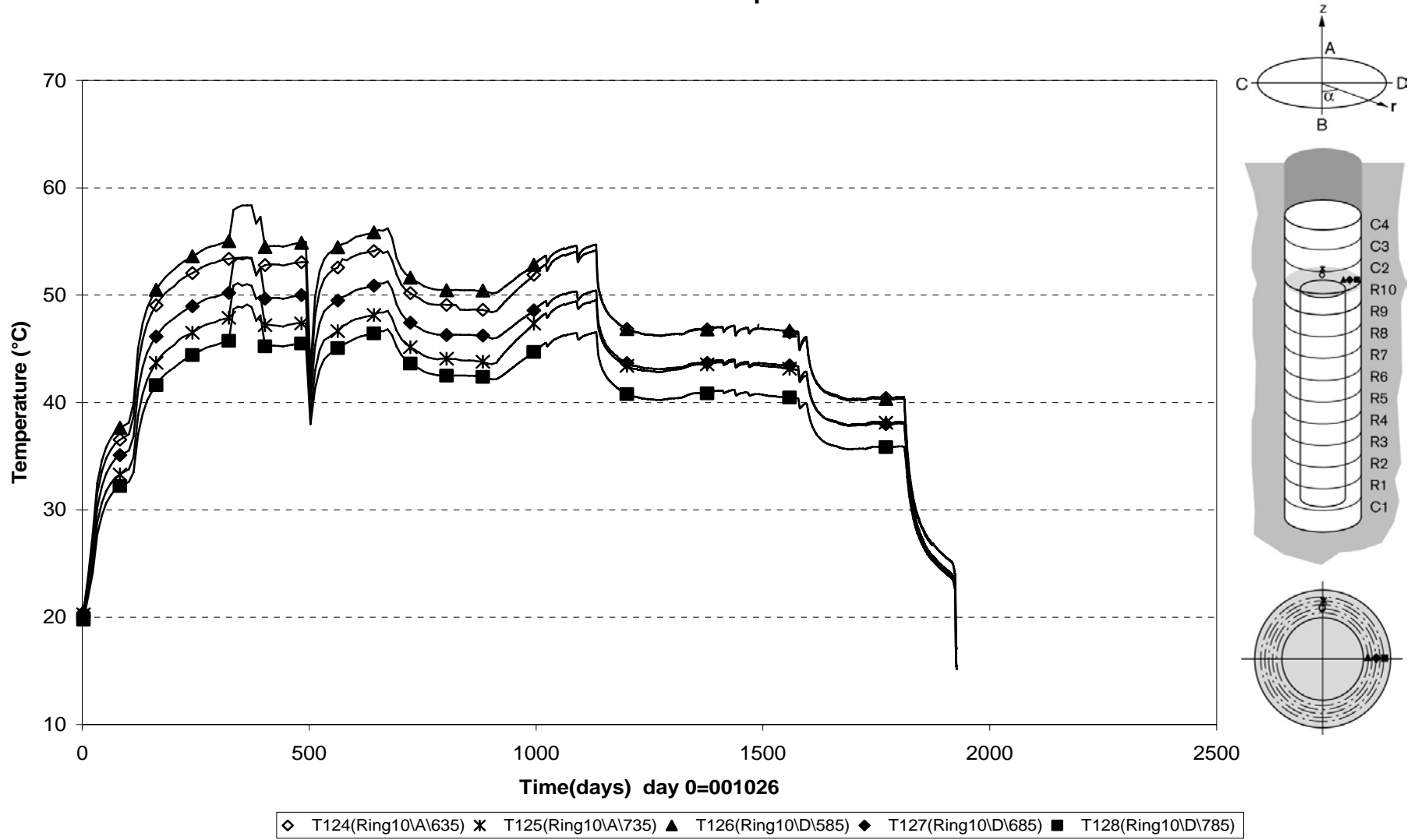
**Temperature in the buffer - Ring 5 (001026-060501)  
Thermocouple**



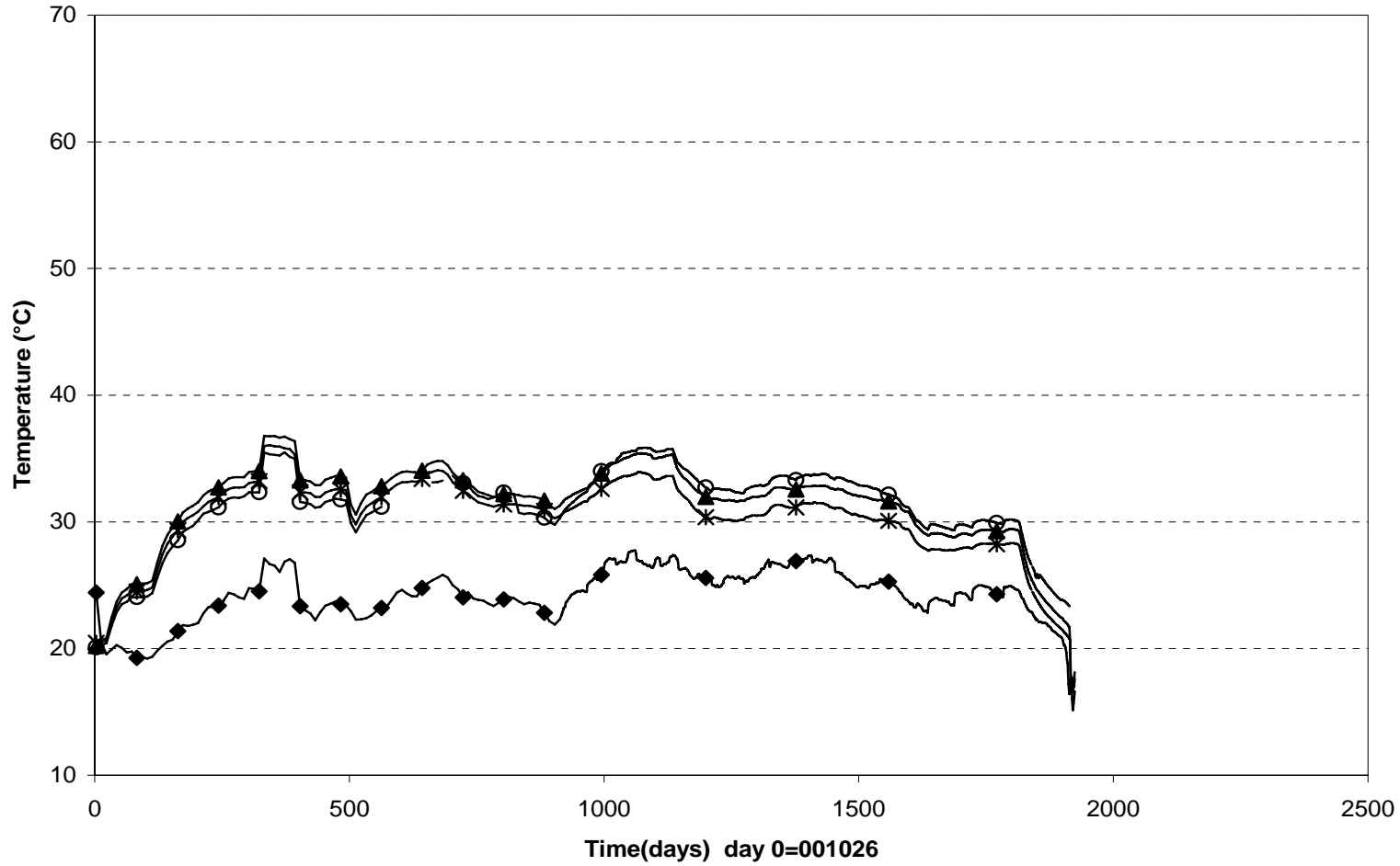
○ T119(Ring5\D\585) \* T120(Ring5\D\635) ▲ T121(Ring5\D\685) ◆ T122(Ring5\D\735) ■ T123(Ring5\D\785)



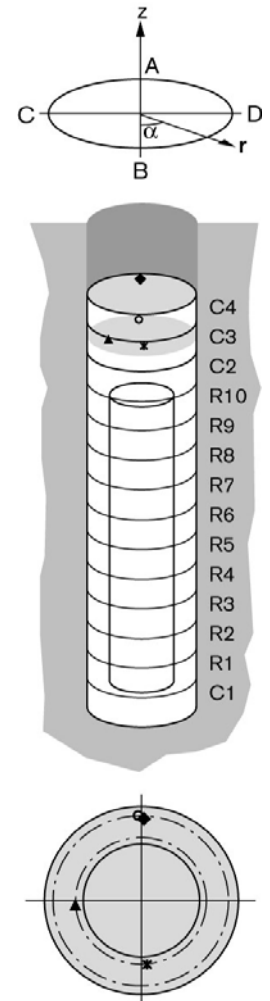
### Temperature in the buffer - Ring 10 (001026-060501) Thermocouple



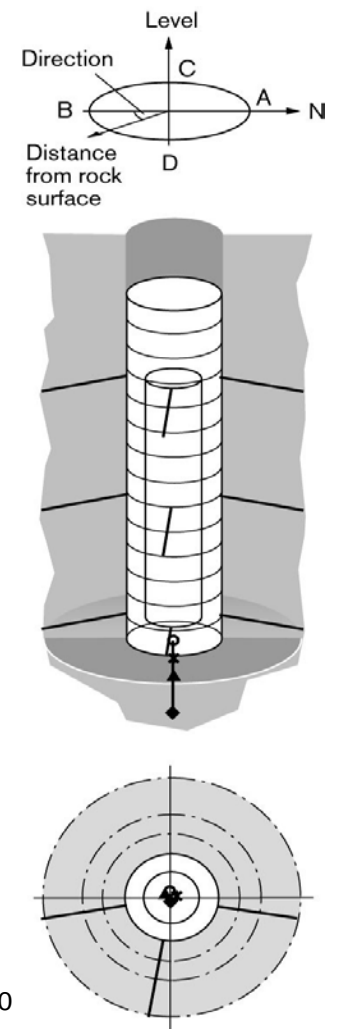
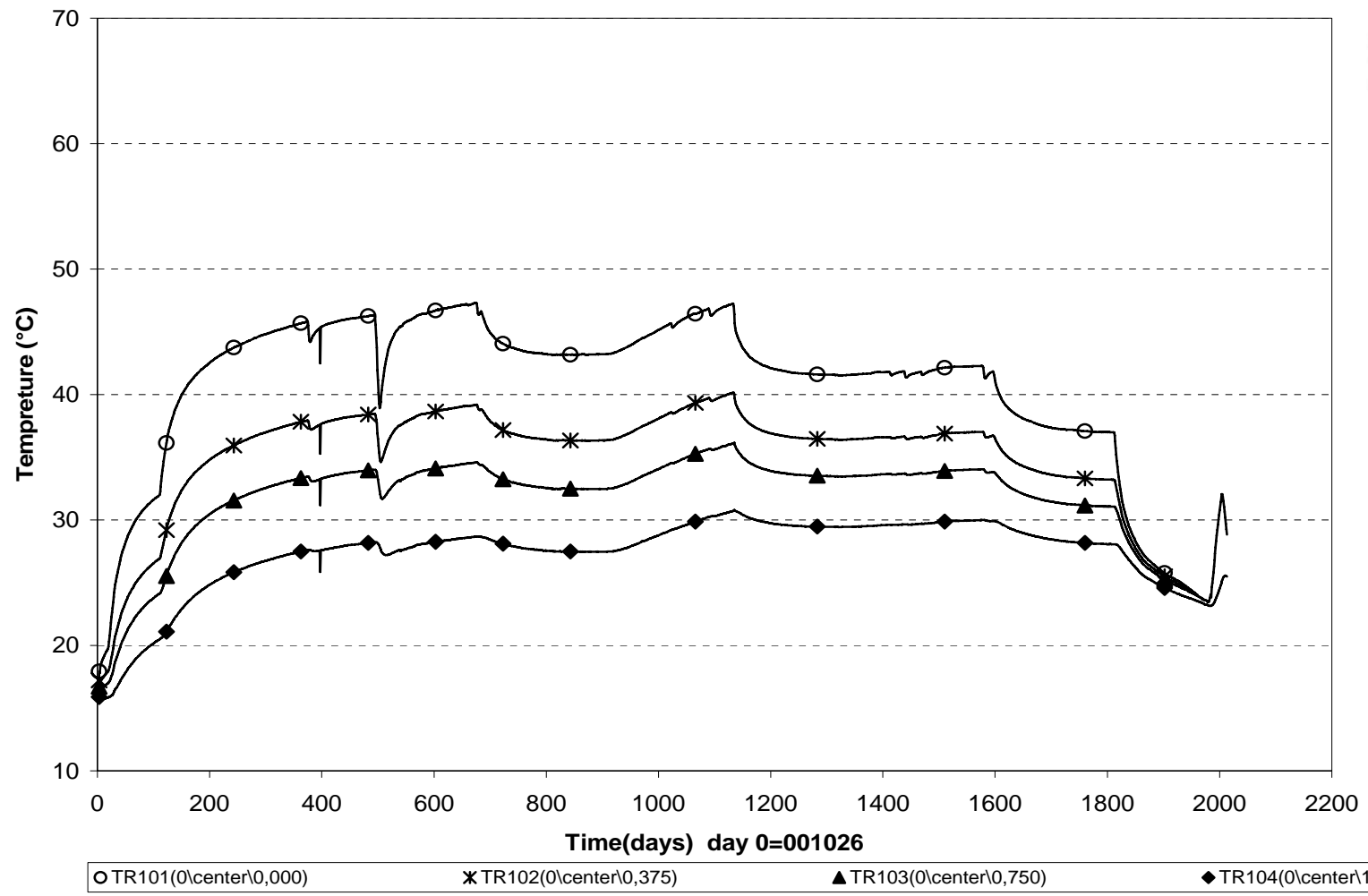
### Temperature in the buffer - Cylinder 3 and Cylinder 4 (001026-060501) Thermocouple



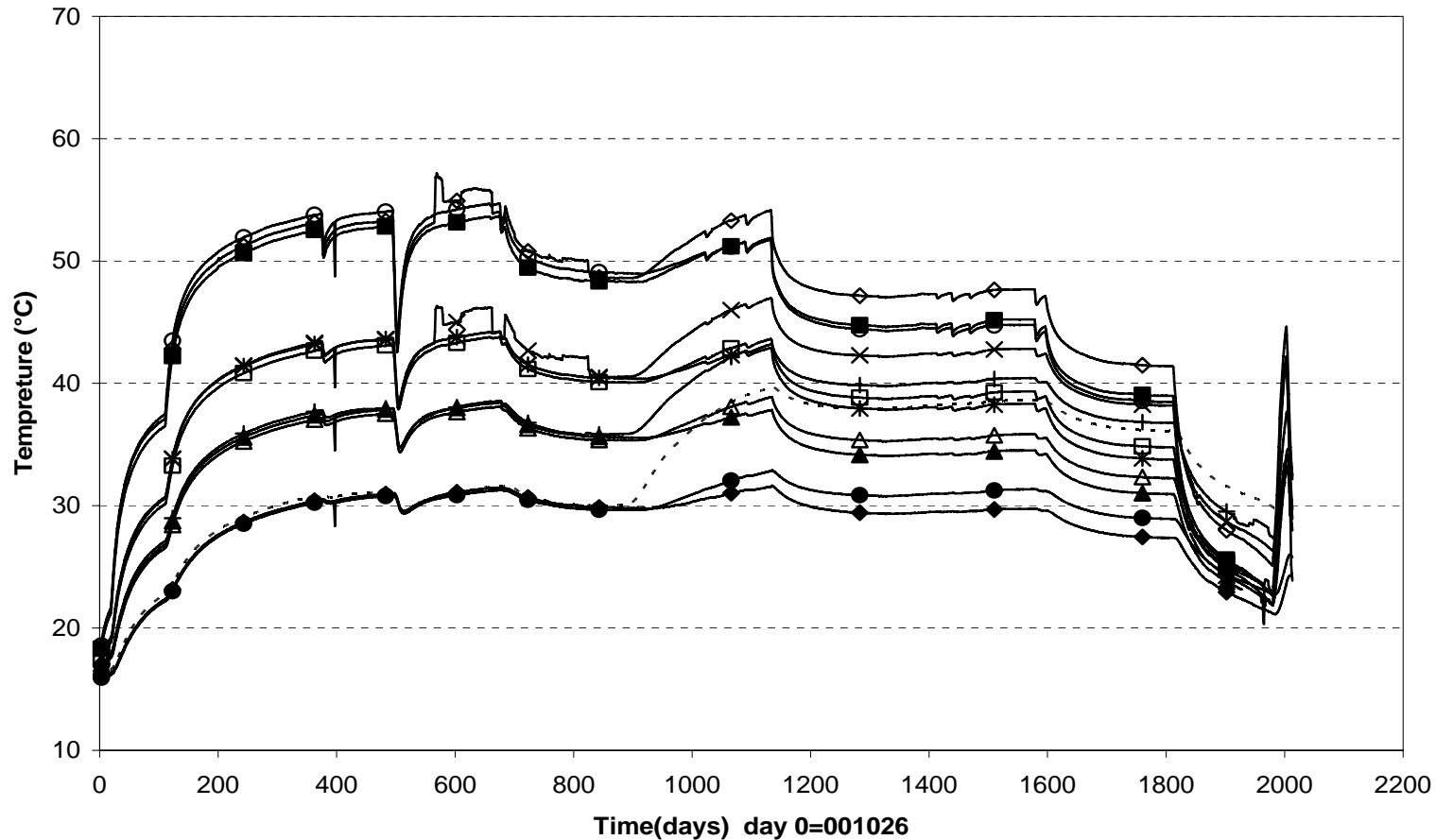
○ T129(Cyl.3\A\785) ✕ T130(Cyl.3\B\585) ▲ T131(Cyl.3\C\585) ◆ T132(cyl 4\A\785)



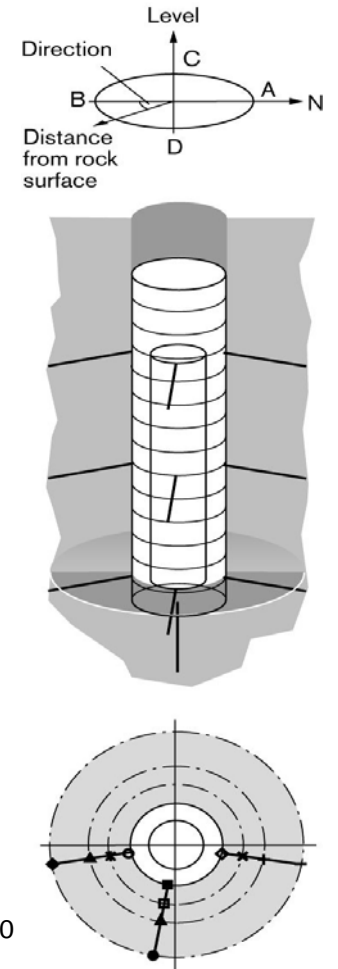
**Temperature in the rock - below the dep. hole (001026-060501)  
Thermocouple**



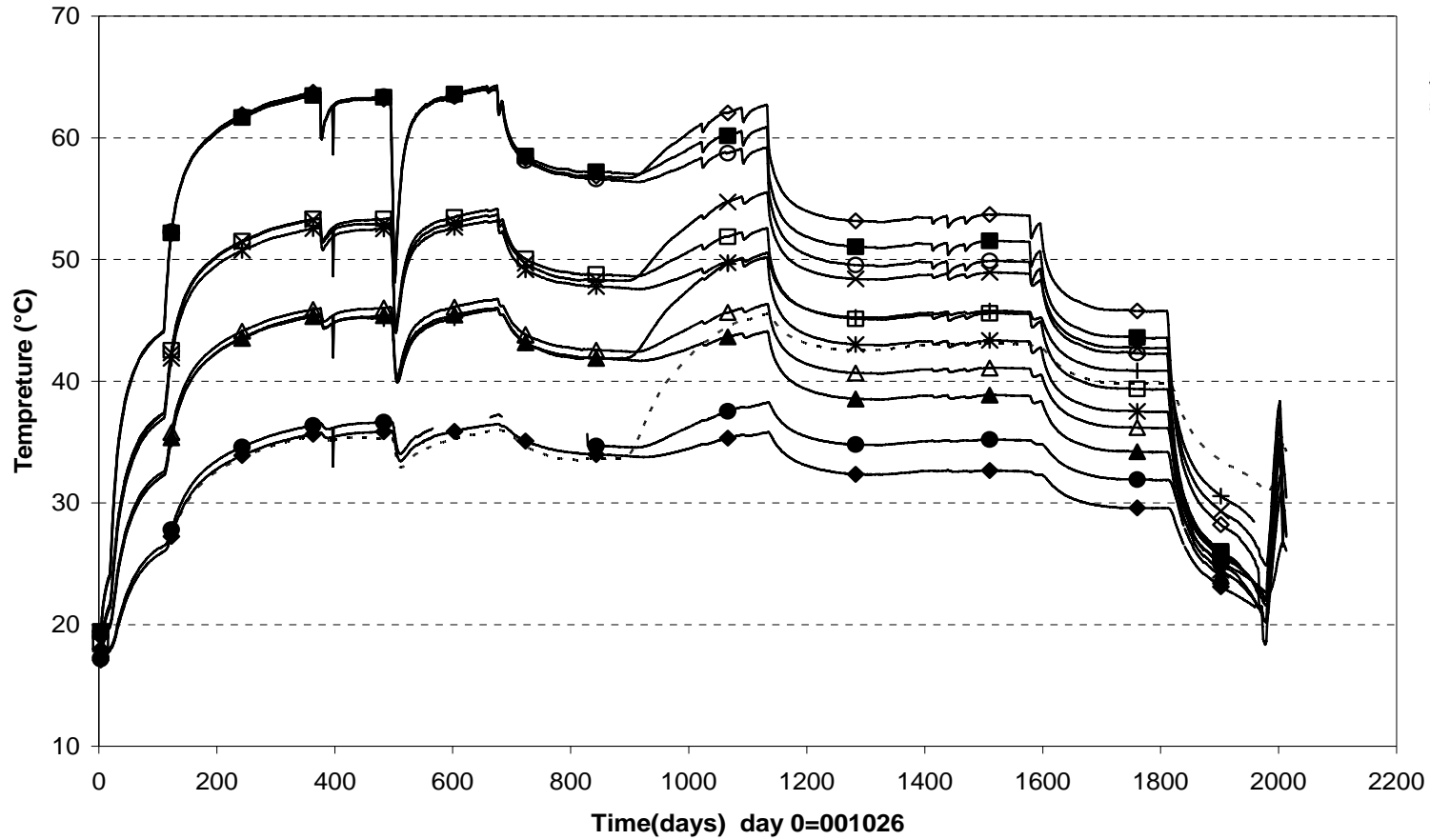
**Temperature in the rock - level 0,6 m (001026-060501)**  
**Thermocouple**



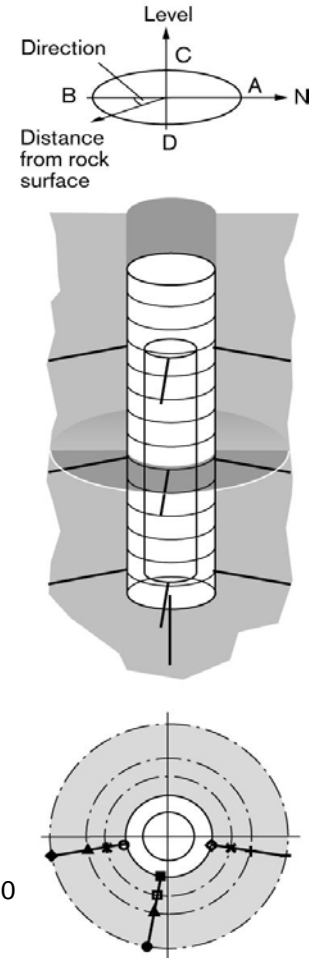
○ TR105(0,61\10°\0,000)	✱ TR106(0,61\10°\0,375)	▲ TR107(0,61\10°\0,750)	◆ TR108(0,61\10°\1,500)
■ TR109(0,61\80°\0,000)	□ TR110(0,61\80°\0,375)	△ TR111(0,61\80°\0,750)	● TR112(0,61\80°\1,750)
◇ TR113(0,61\170°\0,000)	✕ TR114(0,61\170°\0,375)	+	TR115(0,61\170°\0,750) - - - - TR116(0,61\170°\1,500)



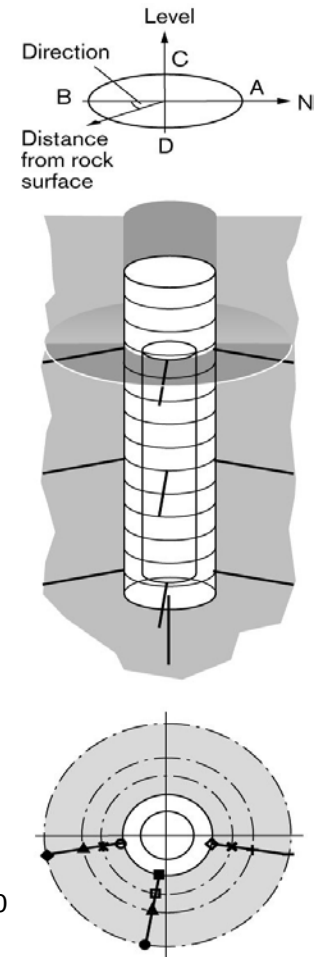
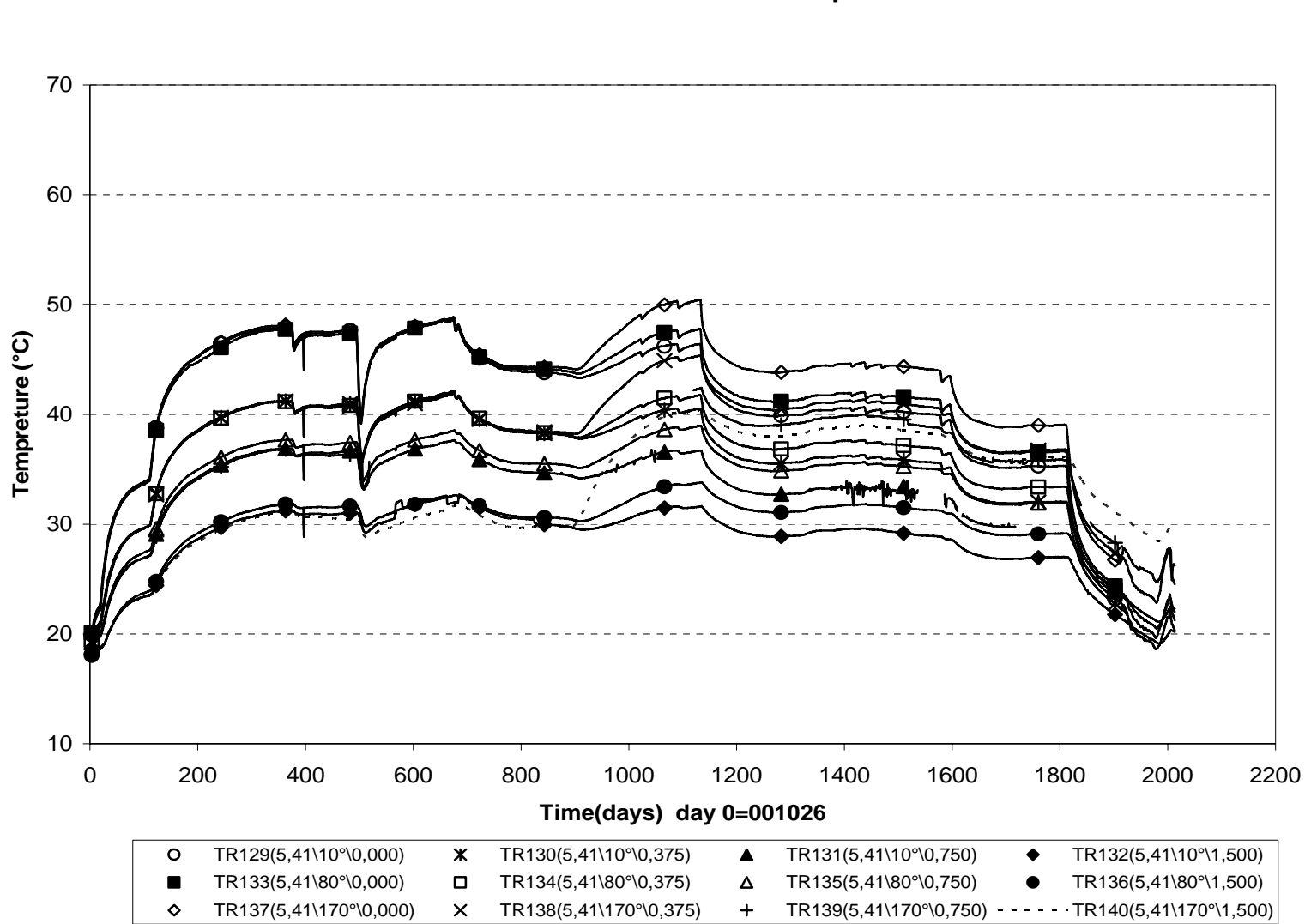
**Temperature in the rock - level 3,01 m (001026-060501)  
Thermocouple**



○ TR117(3,01\10\0,000)	✱ TR118(3,01\10\0,375)	▲ TR119(3,01\10\0,750)	◆ TR120(3,01\10\1,500)
■ TR121(3,01\80\0,000)	□ TR122(3,01\80\0,375)	△ TR123(3,01\80\0,750)	● TR124(3,01\80\1,500)
◇ TR125(3,01\170\0,000)	✕ TR126(3,01\170\0,375)	+	TR127(3,01\170\0,750) - - - - TR128(3,01\170\1,500)

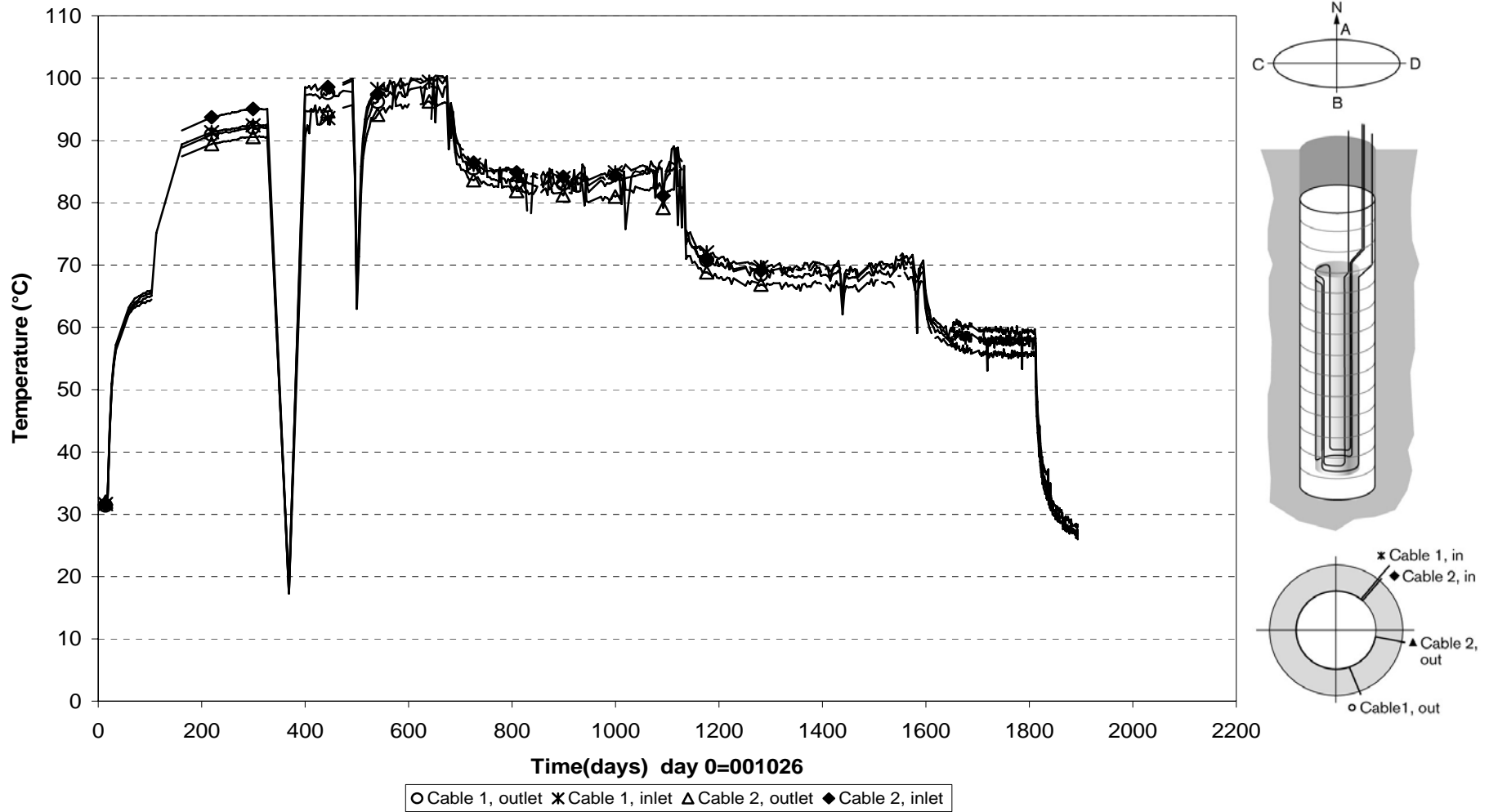


**Temperature in the rock - level 5,4 m (001026-060501)**  
**Thermocouple**

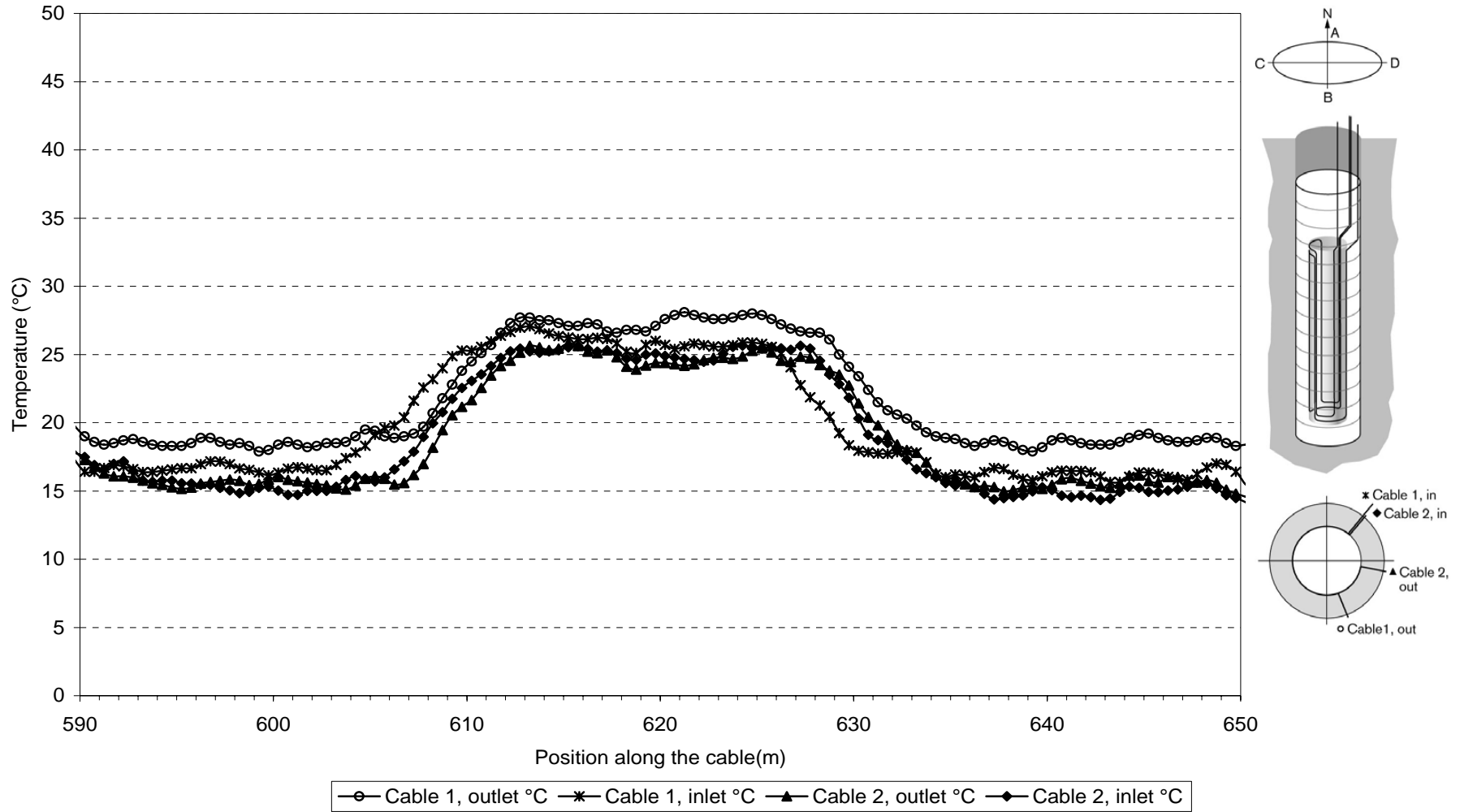




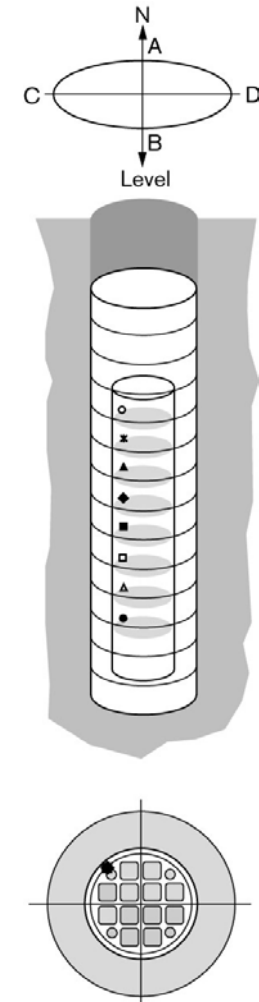
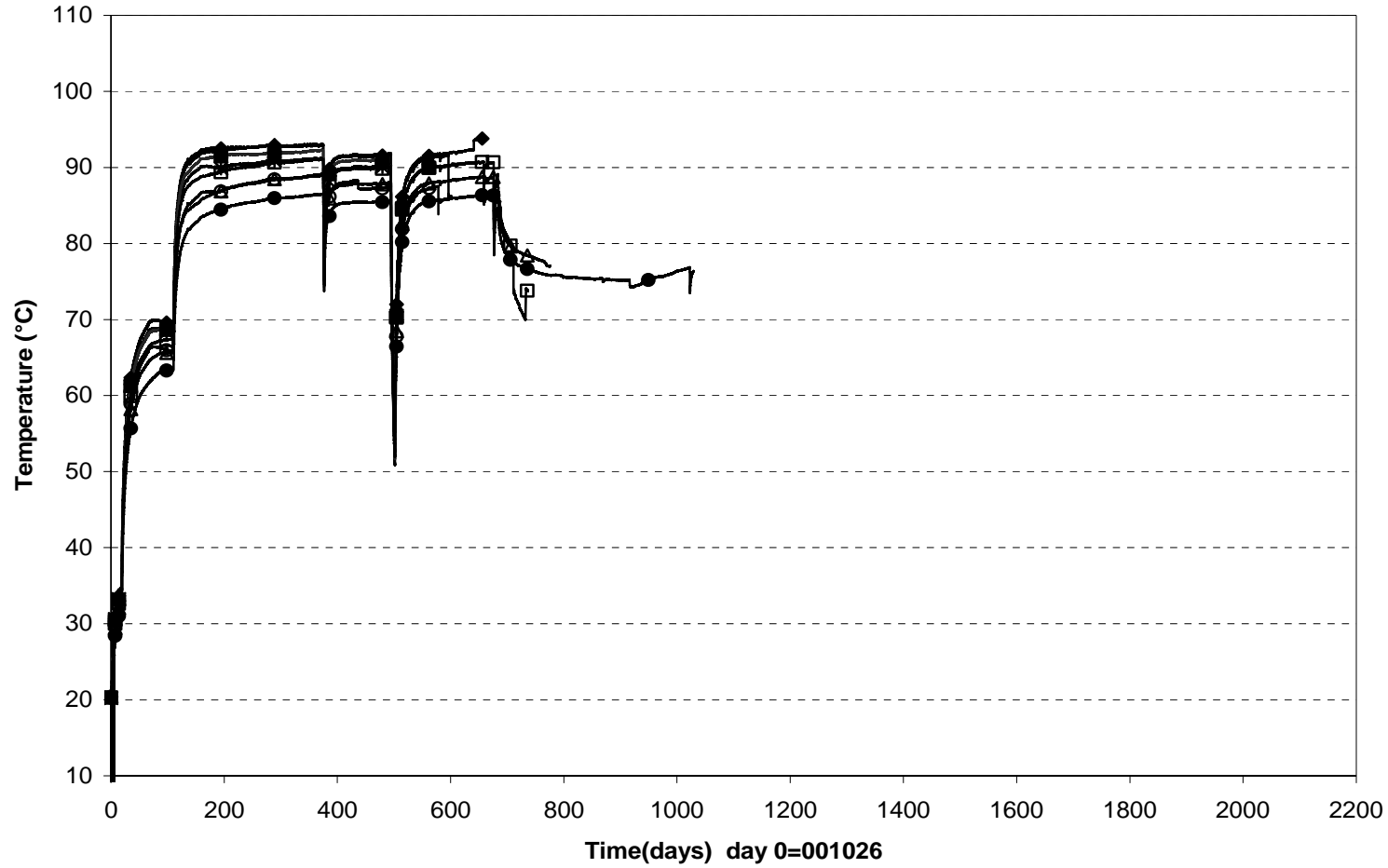
**Max.temperature on the canister surface (001026-060208)  
Optical fiber cables**



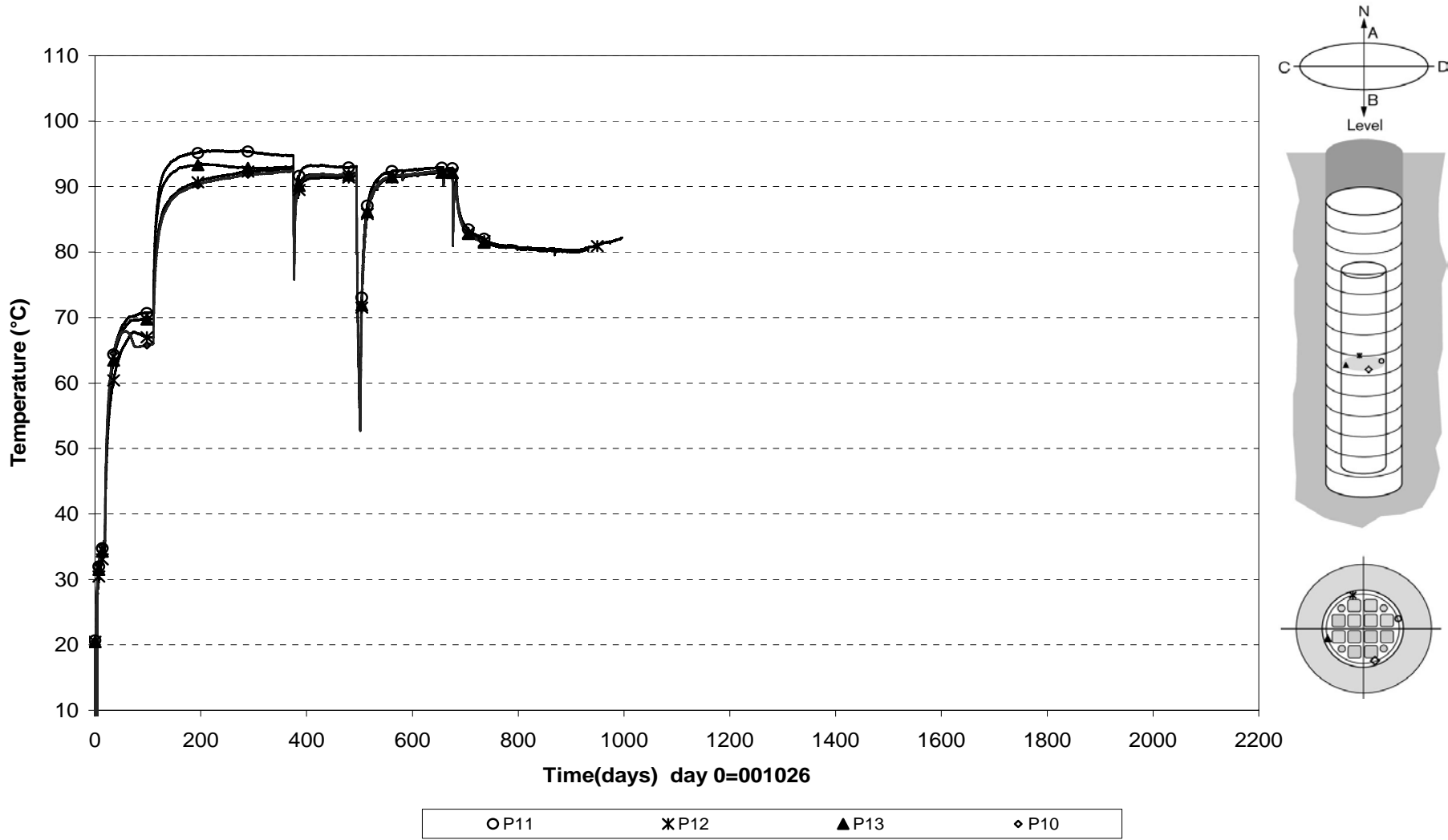
**Temperature profile on the canister surface (060207)  
Optical fiber cables**



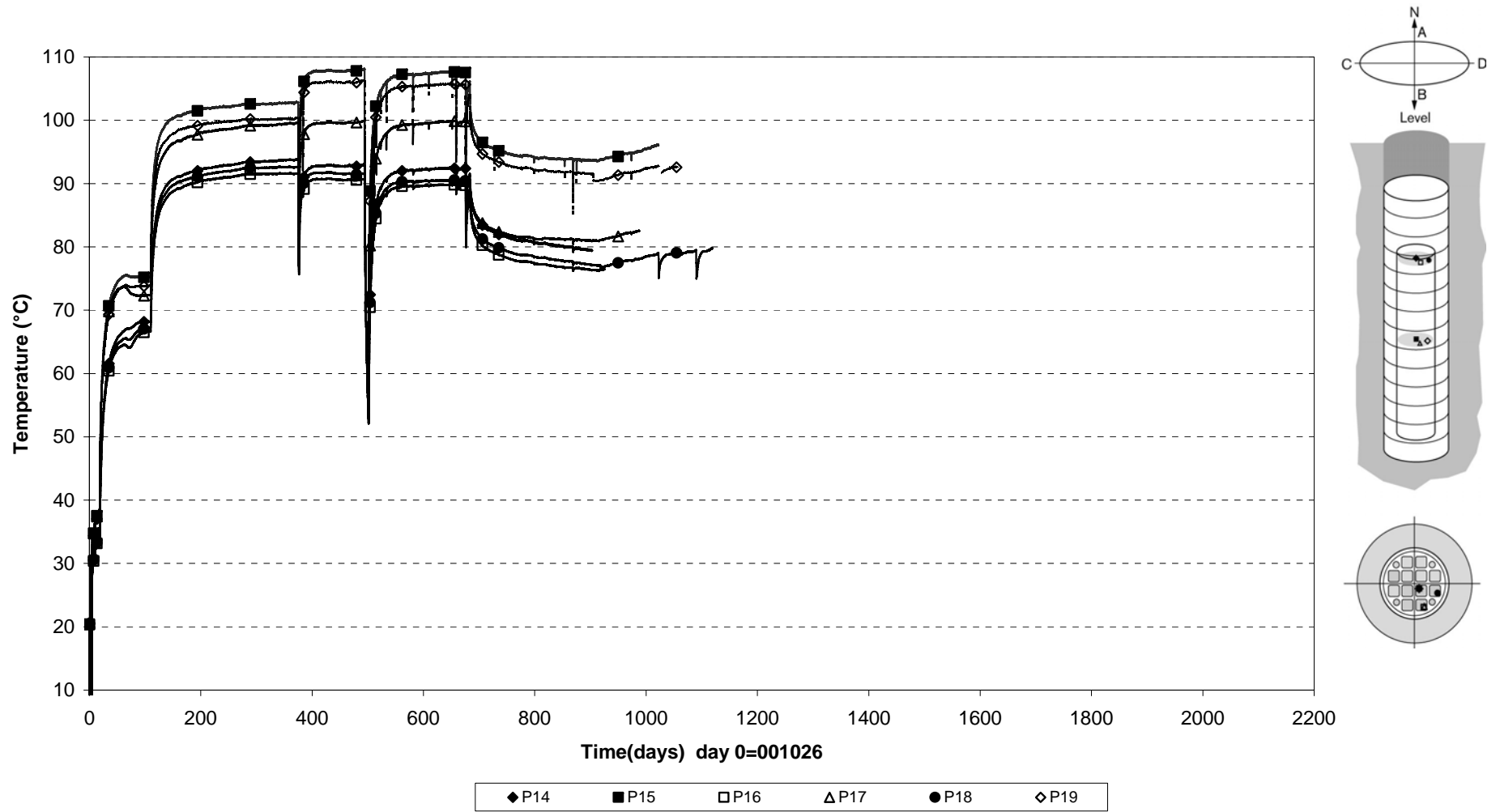
**Temperature inside the canister (001026-060501)  
PT-100**



**Temperature inside the canister (001026-060501)  
PT-100**



Temperature inside the canister (001026-060501)  
PT-100





## Appendix B







**STRESS AND STRAIN MEASUREMENT OF THE ROCK MASS  
RETRIEVAL TEST AT ÄSPÖ**

Measuring period  
2005-11-01 – 2006-04-30

Martin Edelman  
Kennert Röshoff

2006-06-07



# Contents

<b>1</b>	<b>Extent</b>	<b>83</b>
<b>2</b>	<b>Technical background</b>	<b>85</b>
2.1	Vibrating wire embedment biaxial stressmeters	85
2.2	Embedded strain meters	85
2.3	Cement	85
<b>3</b>	<b>Field measurement</b>	<b>87</b>
3.1	Installation work	87
3.2	Location of instruments	87
3.3	Registration	87
<b>4</b>	<b>Computer processing of field data</b>	<b>91</b>
4.1	Evaluation of stresses	91
4.1.1	Radial deformations	91
4.1.2	Calculation of deformation to stresses	91
4.2	Evaluation of strain	92
4.2.1	Calculation of strain	92
4.3	Material parameters	92
4.4	Processing	92
<b>5</b>	<b>Results</b>	<b>93</b>
5.1	Results of canister hole 1	99
5.1.1	Stress change for each biaxial stressmeter	99
	Biaxial stressmeter A1 uncompensated for temperature	99
	Biaxial stressmeter B1 uncompensated for temperature	100
	Biaxial stressmeter C1 uncompensated for temperature	101
	Biaxial stressmeter D1 uncompensated for temperature	102
5.1.2	Strainmeter A1:1, B1:1, C1:1, D1:1, D1:2 (temperature compensated)	103
5.1.3	Strainmeter C1:2 (temperature compensated)	103
5.2	Results of canister hole 2	104
5.2.1	Stress change for each biaxial stressmeter	104
	Biaxial stressmeter A2 uncompensated for temperature	104
	Biaxial stressmeter B2 uncompensated for temperature	105
	Biaxial stressmeter C2 uncompensated for temperature	106
	Biaxial stressmeter D2 uncompensated for temperature	107
5.2.2	Strainmeter B2:1, C2:1, C2:2 (temperature compensated)	108



# 1 Extent

BBK AB and NCC Teknik have, on commission of SKB, Äspö hard rock laboratory, performed rock mechanical measurements in the CRT (Återtaget) tunnel at Äspö. The measurement program comprises of registration of the stress and the strain response around the two canister holes during drilling and heating of the rock mass.

In the first phase, the response of the rock mass was monitored during the drilling of the two canister holes (QPTD F69-00-21). This second phase includes the response registered during a heating phase. The heating experiment started on 2000-10-27 and will continue for about five years.

The aim of the instrumentation is to monitor the stress changes due to heating of the rock mass in a canister hole. The strain meter is used to monitor the relative changes of strain of the intact rock and across fractures.

The commission extends over field measurement and evaluation.

BBK AB is responsible for measuring equipment, the mobilization, field measurement, the computer processing. BBK AB and NCC Teknik are responsible for the interpretation and report of the measurements.

This report presents the measurement results during the period of the heating phase from 2005-11-01 to 2006-04-30.



## **2 Technical background**

### **2.1 Vibrating wire embedment biaxial stressmeters**

The biaxial stressmeter, Geokon model 4350, is designed to measure compressive stress changes in rock, salt, concrete or ice. Principal stress changes are measured in the plane perpendicular to the borehole axes. The stressmeter consists of a high-strength steel cylinder that is grouted into a 60 mm borehole. Stress changes in the host material cause the cylinder to deform.

The radial deformation of the cylinder is measured by means of three pairs of vibrating wire sensors spaced at 60° intervals. Changes of stress produce corresponding changes in the resonant frequency of the sensors. These changes of frequency can be related to stress changes using factory-supplied calibrations. Longitudinal strain sensors and temperature sensors are also included in the stressmeter.

### **2.2 Embedded strain meters**

The vibrating wire strain gages are designed for direct embedment in concrete. The strainmeter is 15 cm long and commonly used for strain measurement in foundations, piles, bridges, dams, tunnel liners etc.

The strain is measured using the vibrating wire principle. A length of a steel wire is tensioned between two end blocks that are embedded directly in concrete. Deformation (i.e. strain changes) of the concrete mass will cause the two end blocks to move relative to one another, thus altering the tension in the steel wire. The tension is measured by excitation of the wire and measuring its resonant frequency of vibration using an electro magnetic coil.

### **2.3 Cement**

Special expansive grout was used to insure that the gage is in complete contact with the surrounding rock. The instruments are grouted in special cement from Denmark named Densitop T2. This cement is chosen to have as similar properties as the rock as possible. The compression strength is 150 MPa. The coefficient of expansion is approximate 8.5 microstrain/C° that is similar to hard rock as granite and as 85 % of common concrete.

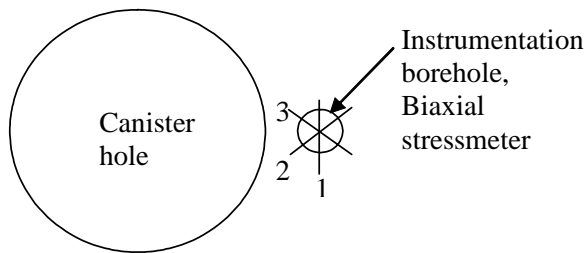




## 3 Field measurement

### 3.1 Installation work

Installation of the stressmeter gage is accomplished by inserting the gage into a grout-filled borehole using a setting tool and self-aligning setting rod.



The stress cell is orientated so that the first vibrating wire is orientated tangentially to the canister hole. The second string is orientated  $60^\circ$  from tangential direction and the third string is orientated  $120^\circ$  from tangential direction.

The strainmeters were fixed to a 6 mm glasfiber rod and pushed into the grout after the stress cell was installed.

### 3.2 Location of instruments

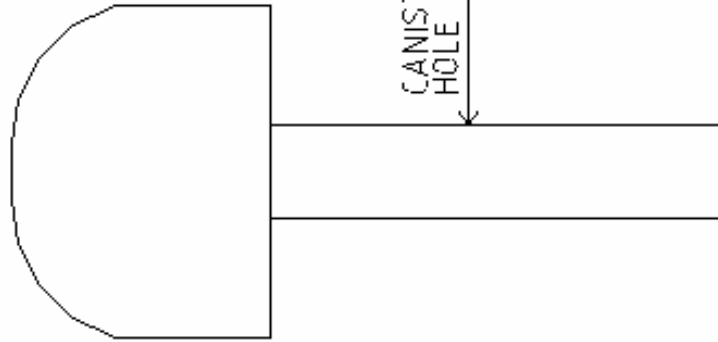
See figure 3.1 and figure 3.2.

### 3.3 Registration

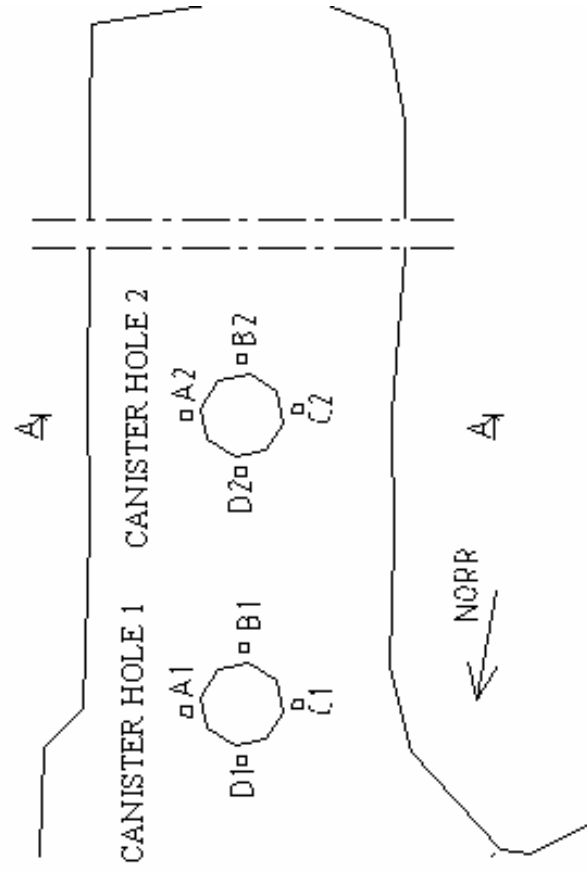
A datalogger type Campbell CR10X has captured the measurements, which have been recorded once every hour during the period 2000-10-01 to 2001-01-01, and once every six hours during the period 2001-01-03 to 2006-04-30.

MEASUREMENT LAYOUT

SECTION A-A



PLAN



□ BOREHOLE LAYOUT

Figure 3.1. Measurement Layout.

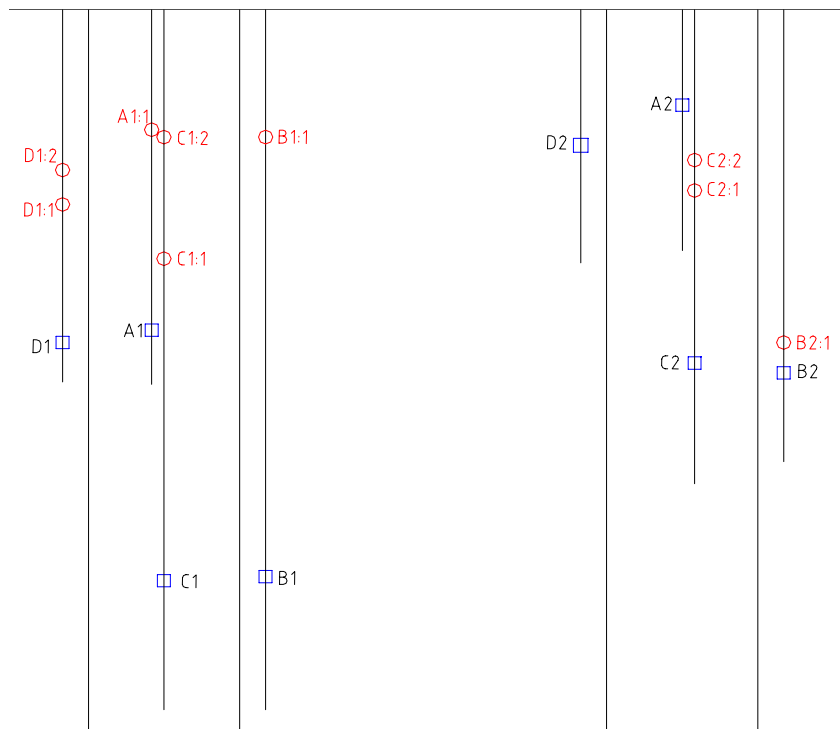
Canister Hole 1

Canister Hole 2

PLAN



SECTION A-A



□ Biaxial stressmeter

○ Deformationmeter

**Figure 3.2.** Location of instruments



## 4 Computer processing of field data

### 4.1 Evaluation of stresses

The stress changes are evaluated from the measured deformations registered by the vibrating wires.

#### 4.1.1 Radial deformations

Radial deformation for each of the strings are calculated with the equation:

$$V_r = (R_1 - R_0) * Gagefactor \quad (in. \text{ or } mm)$$

$V_r$  = Radial deformation for each of the strings

$R_1$  = Deformation reading in digits (= frequency<sup>2</sup> / 1000)

$R_0$  = Deformation zero reading in digits (= frequency<sup>2</sup> / 1000)

#### 4.1.2 Calculation of deformation to stresses

The magnitude and the direction of the stress changes are determined from the measured radial deformation of the sensor in three directions.

The equations below give the magnitude and the direction of the maximum stress increase and reduction in a plane perpendicular to the borehole axes:

##### Maximal stress increase

$$p = \frac{1}{2} \left[ \frac{1}{3B} \left( (2V_{r_1} - V_{r_2} - V_{r_3})^2 + 3(V_{r_2} - V_{r_3})^2 \right)^{1/2} + \frac{1}{3A} (V_{r_1} + V_{r_2} + V_{r_3}) \right]$$

$V_{r_1}$  = Radial deformation for string 1

$V_{r_2}$  = Radial deformation for string 2

$V_{r_3}$  = Radial deformation for string 3

$A, B$  = Coefficients depending on the sensor geometry and the material properties

##### Maximal stress reduction

$$q = \left[ \frac{1}{3A} (V_{r_1} + V_{r_2} + V_{r_3}) - p \right]$$

### The angle of the maximal stress increase

The angle in the plane perpendicular to the borehole axes is measured clockwise from the tangential direction of the canister hole.

$$\theta = \frac{1}{2} \cos^{-1} \left[ \frac{V_r - A(p+q)}{B(p-q)} \right]$$

## **4.2 Evaluation of strain**

Nine strain gages were installed in the same boreholes as the biaxial stressmeters.

### **4.2.1 Calculation of strain**

Strain measurement were calculated as temperature compensated load related strain with the following equation:

$$\mu_{true} = (R_1 - R_0) * B + (T_1 - T_0)(C_1 - C_2)$$

$\mu_{true}$  = temperature compensated microstrain

$R_1$  and  $R_0$  =Digits reading

$B$  = batch calibration factor

$C_1$  and  $C_2$  are the coefficients of expansion of steel and concrete, 12.2 microstrain/ $C^\circ$  and 8.5 microstrain/ $C^\circ$ .

## **4.3 Material parameters**

Material parameters used in the calculations are as the following:

- Young's modulus of intact rock 69 Gpa
- Poisson's ratio of intact rock 0.25
- Coefficients of expansion of steel 12.2 microstrain/  $C^\circ$
- Coefficients of expansion of concrete 8.5 microstrain/ $C^\circ$

## **4.4 Processing**

The raw data registered have been processed in Microsoft Excel software. The calculation and evaluation gathered from the deformations in the plane perpendicular to the borehole axes are presented as:

Temperature

Radial deformation of the three pairs of wires in plane perpendicular to borehole axes

Maximal stress increases and stress reduction in plane perpendicular to borehole axes

Orientation of maximal stress increase in plane perpendicular to borehole axes

Strain measurement

## 5 Results

A summary of the results of the stress changes is presented in Table 1. These values represent total changes in stress magnitude and stress orientation during each reporting period during phase 2 (heating) together with maximum changes in stress magnitude and orientation recorded during phase 1 (drilling). Figure 5.1 presents graphically the maximum typical changes in stress magnitude and orientation during this reporting period from 2005-11-01 to 2006-04-30. These results are not compensated for temperature changes, nor are they compensated for longitudinal stress changes.

Although the measurements of stress meters are affected by temperature, the temperature compensated results of stress meters are not presented in this report because a further detailed study of the relationship between temperature and stress meter measurements will be required in order to quantify these effects. In addition, the longitudinal stress changes are affected by temperature changes and for this reason these longitudinal measurements are not currently used for determination of radial stresses. Results of the biaxial stress meters without temperature or longitudinal stress compensation, and the strain meters with temperature compensation from each borehole for the period 2005-11-01 to 2006-04-30 are summarized on the diagrams in section 5.1 and 5.2.

The diagrams in section 5.1 and 5.2 for each borehole display:

- Maximum stress increases and stress reductions in plane perpendicular to borehole axes.
- Orientation of maximum stress increase in plane perpendicular to borehole axes.
- Strain measurements presented in the diagrams are temperature-compensated with the unit of micro strain. Positive values represent elongation.

The data during this reporting period indicate that:

- The temperature is inhomogeneous around these two canister holes.

### Hole 1

The temperature around canister hole 1 varies with values from 65°C to 71°C towards the end of the period. The temperature is stable or somewhat decreasing with a few degrees.

There are no values from either set of vibrating wires (1-3) or (4-6) in stress meter A1, B1, C1 or D1 during the complete period. Due to this there are no values for maximum stress increase, reduction, or change in orientation of maximum stress around canister hole 1. Sensor Vr1 in biaxial stress meter A1 stopped displaying values in early April. However, sensor Vr2 in the same stress meter (A1) that stopped showing values in October 2004 started displaying values over a year later, in the beginning of December 2005. Due to this the stress increase and decrease, and the orientation of maximum stress increase for stress meter A1 can be seen during a part of the measuring period, from early December to early April. During this time the readings were stable. The stress increase displayed a small decrease and the orientation of maximum increase increased from 2 to 2.5 degrees.

Measurements taken at the strain gauge locations generally display steady values in micro strain as well as in temperature. There is a tendency of a small decrease in temperature. The strain values decreased with 20 micro strains at strain gauge C1:1 and increased with 10 micro strains at strain gauge B1:1. The value at D1:2 have been unchanged throughout the period. Strain gauge D1:1 stopped giving values in mid November.

At strain gauge C1:2 the increase have been 40 micro strains with a small overall decrease in temperature of only 2°C.

## Hole 2

The temperature around canister hole 2 varies from 23°C to 28°C towards the end of the period. The tendency is somewhat unstable and decreasing temperature with about 3-4°C around stress meter A2 and D2. For stress meters B2 and C2 the temperature decreases with 8°C throughout the period. An increase in temperature can also be seen during most of April for these two sensors. However, towards the end of the measuring period the temperature decreases dramatically.

The variations in stresses around canister hole 2 are none or very small. The orientation ranges from -9,5 degrees to 38,6 degrees between the different sensors. The variation for each sensor is very small.

The strain gage readings show some disturbances from mid January. The measurements vary from 20 micro strains to 65 micro strains increase. The readings for strain gauge B2:1 display a dramatically drop of over 80 micro strains during most part of April, but the strain quickly decreases again about 40 micro strains during the last part of the period. The same tendency can be seen for the other strain gages as well. The correlations between the changes in strain and temperature for these sensors are magnificent. The changes seem to continue into next period.



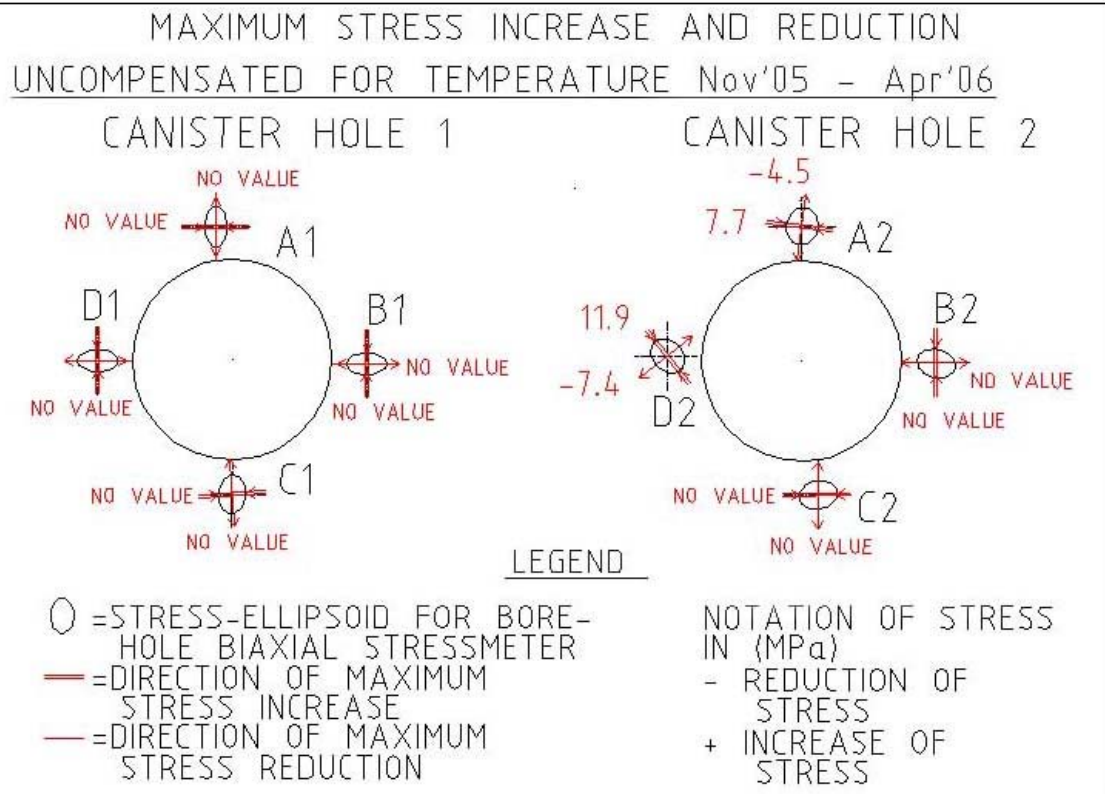


**Figure 5.1.** Maximum stress changes uncompensated for temperature.

Stress-meter	Measuring period								
	Phase 1: Drilling phase			Phase 2: Heating phase					
				Period: 2000-10-01 to 2001-11-30			Period: 2000-10-01 to 2001-11-30		
	Typical max. stress increase (Mpa)	Typical max. stress reduction (Mpa)	Orientation of max. Stress increase (degree)	Typical max. stress increase (Mpa)	Typical max. stress reduction (Mpa)	Orientation of max. Stress increase (degree)	Typical max. stress increase (Mpa)	Typical max. stress reduction (Mpa)	Orientation of max. Stress increase (degree)
A1	17.0	-10.0	11.5	22.7	-10.9	10.3	22.6	-10.8	10.3
B1	15.0	-11.0	17.0	21.1	-10.3	16.8	26.9	-10.5	16.8
C1	12.0	-7.4	0	21.9	-9.9	5.4	21.9	-9.8	5.4
D1	22.0	-11.0	0	25.8	-9.1	0	26.3	-9.4	0
A2	5.0	-4.0	-11.0	4.4	-3.3	-18.3	3.7	-3.3	-17.7
B2	11.0	-7.3	-7.5	31.1	-4.6	-14.1	57.9 (*)	-4.6	-21.3
C2	11.0	-7.7	29.5	29.1	-6.6	31.2	33.7 (*)	-7.6	30.2
D2	9.3	-7.2	38.5	16.5	-9.9	38.7	16.2	-9.9	38.3

Stress-meter	Measuring period			Measuring period			Measuring period		
	Phase 2: Heating phase con't (see Note 5)			Phase 2: Heating phase con't			Phase 2: Heating phase con't		
	Period: 2002-05-01 to 2002-10-31			Period: 2002-11-01 to 2003-04-30			Period: 2003-05-01 to 2003-10-31		
	Typical max. stress increase (Mpa)	Typical max. stress reduction (Mpa)	Orientation of max. Stress increase (degree)	Typical max. stress increase (Mpa)	Typical max. stress reduction (Mpa)	Orientation of max. Stress increase (degree)	Typical max. stress increase (Mpa)	Typical max. stress reduction (Mpa)	Orientation of max. Stress increase (degree)
A1	23.3	-11.0	10.4	34.7(*)	-17	5.7	38.7	-13.7	6.1
B1	21.1	-10.6	15.9	34(*)	-9.6	17.1	51 to 68	5 to 34	5 to 19
C1	22.3	-10.4	5.3	34(*)	-9.1	5.7	41.5	-5.2	5.2 to 6.6
D1	27.3	-9.7	-2.9	45(*)	-5.6	-4.3	60.3	4.8	-3.2 to -4.9
A2	4.3	-3.9	-13.9	3.5	-3.5	-9(*)	6.9	-4.3	-7.4
B2	34 to 57	4 to 21	-0.6 to -8	32 to 54	6 to 22	-1 to -10	53.2	23.2	-10.7
C2	50 to 71	5.3 to 22.7	22 to 33	48 to 70	6 to 26	19 to 33	53 to 74	8 to 31	16 to 32
D2	16.0	-10.1	38.7	15	-9	38	12.4	-8.1	38

**Notes:**

1. Positive values of stress indicate compression, negative values of stress indicate extension.
2. Positive values of orientation indicate anti-clockwise rotation, negative values of orientation indicate clockwise rotation.
3. Typical maximum stress increases and reductions represent maximum stabilised readings during the measuring period.  
(\*) indicates that the reading had not stabilised during the measuring period.
4. Orientation of maximum stress increase is the orientation that corresponds to the typical maximum stress increase.
5. Calculation and processing methods revised during this reporting period to eliminate compensation for both temperature and longitudinal strains until further studies on these effects are carried out.

Stress-meter	Measuring period			Measuring period			Measuring period		
	Phase 2: Heating phase con't			Phase 2: Heating phase con't			Phase 2: Heating phase con't		
	Period: 2003-11-01 to 2004-04-30			Period: 2004-05-01 to 2004-10-31			Period: 2004-11-01 to 2005-04-30		
	Typical max. stress increase (Mpa)	Typical max. stress reduction (Mpa)	Orientation of max. Stress increase (degree)	Typical max. stress increase (Mpa)	Typical max. stress reduction (Mpa)	Orientation of max. Stress increase (degree)	Typical max. stress increase (Mpa)	Typical max. stress reduction (Mpa)	Orientation of max. Stress increase (degree)
A1	47,3	1,3	4,0 to 4,7	no value	no value	no value	no value	no value	no value
B1	no value	no value	-89,7 to 0,1	no value	no value	no value	no value	no value	no value
C1	46,0	10,0	4,3 to 9,4	48,2	3,1	3,8	46,7	3,2	3,8
D1	82,0	31,7	-9,5 to 0,6	no value	no value	no value	no value	no value	no value
A2	6,7	-4,3	-7,0	6,9	-4,8	-7,2 to -7,7	6,6	-4,5	-7,8 to -8
B2	50,8	23,0	-4,9 to -59,7	52,0	23,8	-11,2	55.9(**)	27.2(**)	-16.1(**)
C2	51,5	32,7	14,1 to 59,3	52,2	34,0	13,3	50,9	33,7	12,5
D2	12,1	-7,7	37,9	12,3	-7,8	38,1 to 38,8	10,8	-6,8	38,1 to 33,8

Stress-meter	Measuring period			Measuring period			Measuring period		
	Phase 2: Heating phase con't			Phase 2: Heating phase con't (Note 7)			Phase 2: Heating phase con't		
	Period: 2005-05-01 to 2005-10-31			Period: 2005-11-01 to 2006-04-30					
	Typical max. stress increase (Mpa)	Typical max. stress reduction (Mpa)	Orientation of max. Stress increase (degree)	Typical max. stress increase (Mpa)	Typical max. stress reduction (Mpa)	Orientation of max. Stress increase (degree)	Typical max. stress increase (Mpa)	Typical max. stress reduction (Mpa)	Orientation of max. Stress increase (degree)
A1	no value	no value	no value	45	3,5	2,1			
B1	no value	no value	no value	no value	no value	no value			
C1	no value	no value	no value	no value	no value	no value			
D1	no value	no value	no value	no value	no value	no value			
A2	8,3	-4,6	-6,1 to -6,7	7,5	-4,6	-9,5			
B2	no value	no value	no value	no value	no value	no value			
C2	no value	no value	no value	no value	no value	no value			
D2	12,0	-7,2	38,6 to 40,0	12,0	-7,2	38,6			

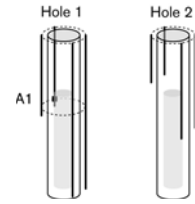
**Notes:**

1. Positive values of stress indicate compression, negative values of stress indicate extension.
2. Positive values of orientation indicate anti-clockwise rotation, negative values of orientation indicate clockwise rotation.
3. Typical maximum stress increases and reductions represent maximum stabilised readings during the measuring period.  
(\* ) indicates that the reading had not stabilised during the measuring period.
4. Orientation of maximum stress increase is the orientation that corresponds to the typical maximum stress increase.
5. Calculation and processing methods revised during this reporting period to eliminate compensation for both temperature and longitudinal strains until further studies on these effects are carried out.
6. (\*\* ) indicates that the sensor stopped giving values in April 2005.
7. Measurements for stress meter A1 can be seen for part of the period.

**Table 1. Summary of results for stress measurements**

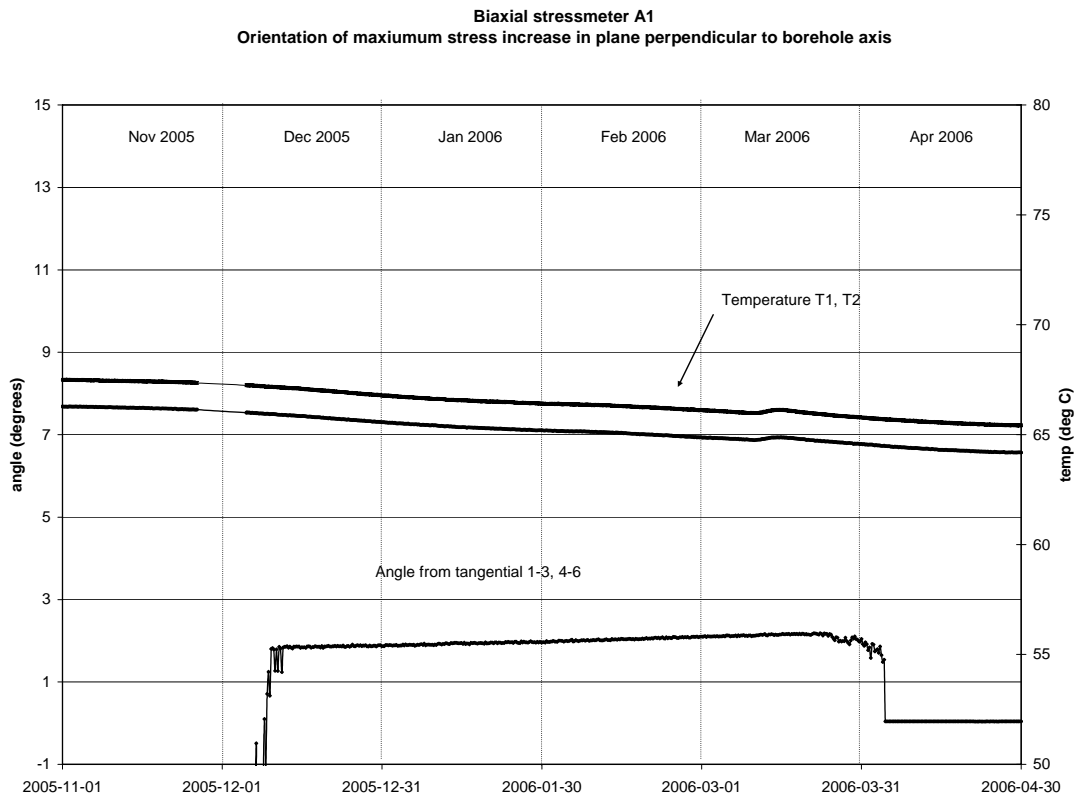
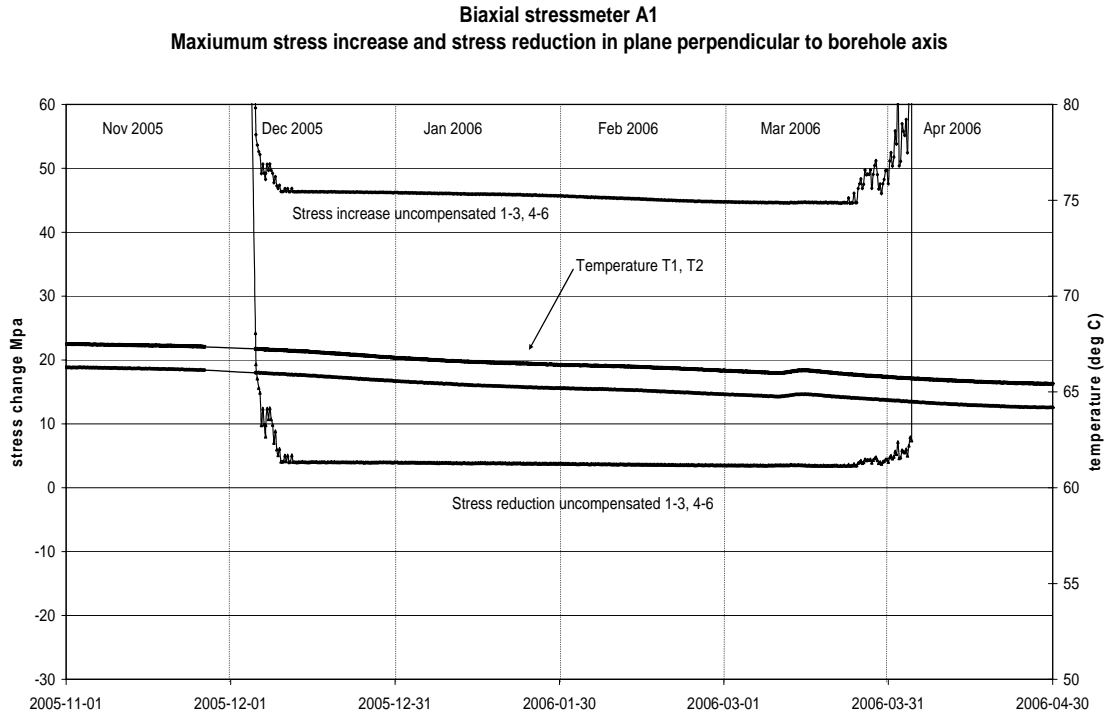


## 5.1 Results of canister hole 1

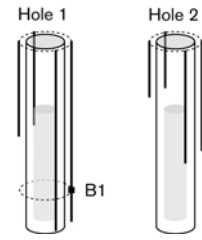


### 5.1.1 Stress change for each biaxial stressmeter

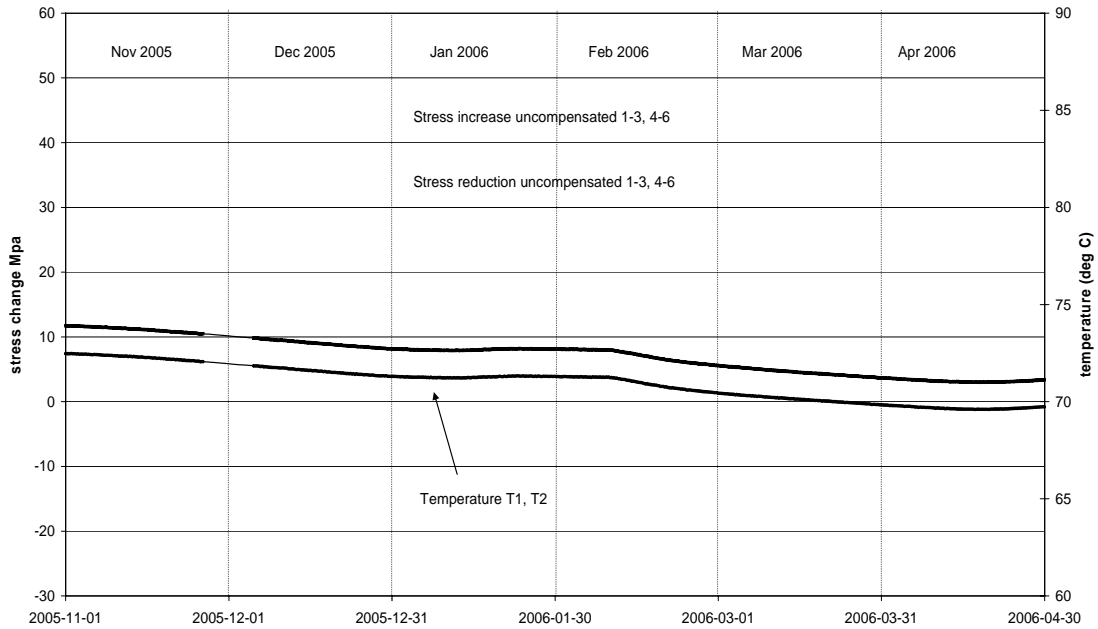
#### Biaxial stressmeter A1 uncompensated for temperature:



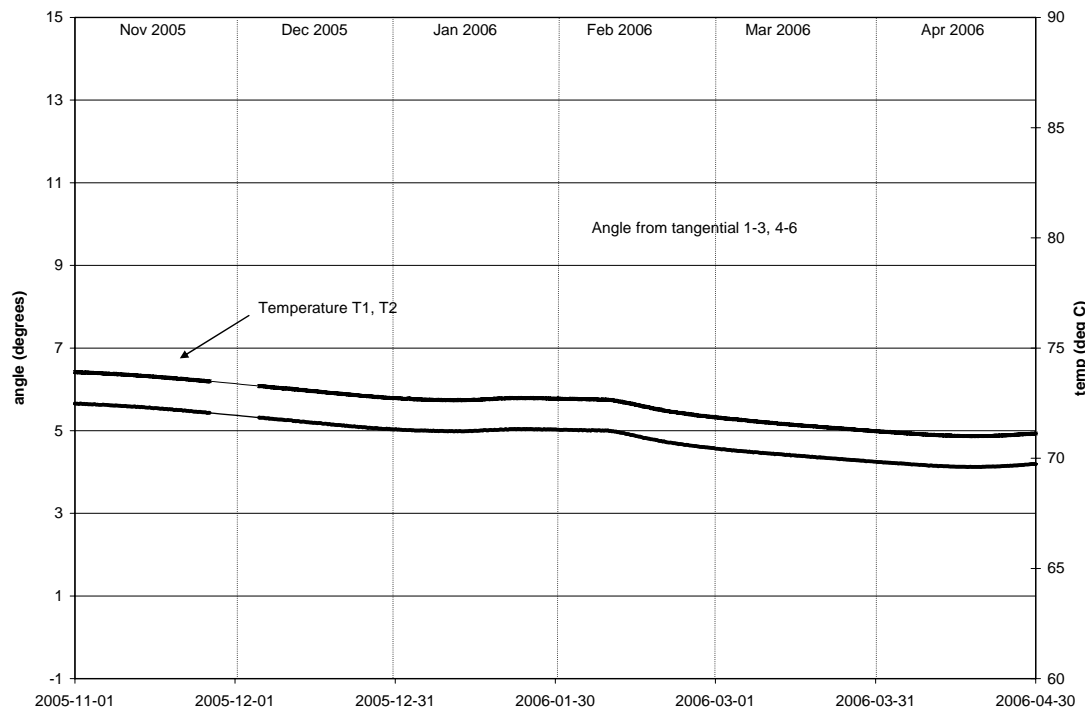
**Biaxial stressmeter B1 uncompensated for temperature:**



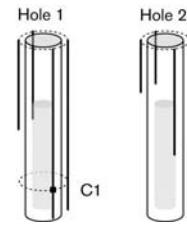
**Biaxial stressmeter B1**  
**Maximum stress increase and stress reduction in plane perpendicular to borehole axis**



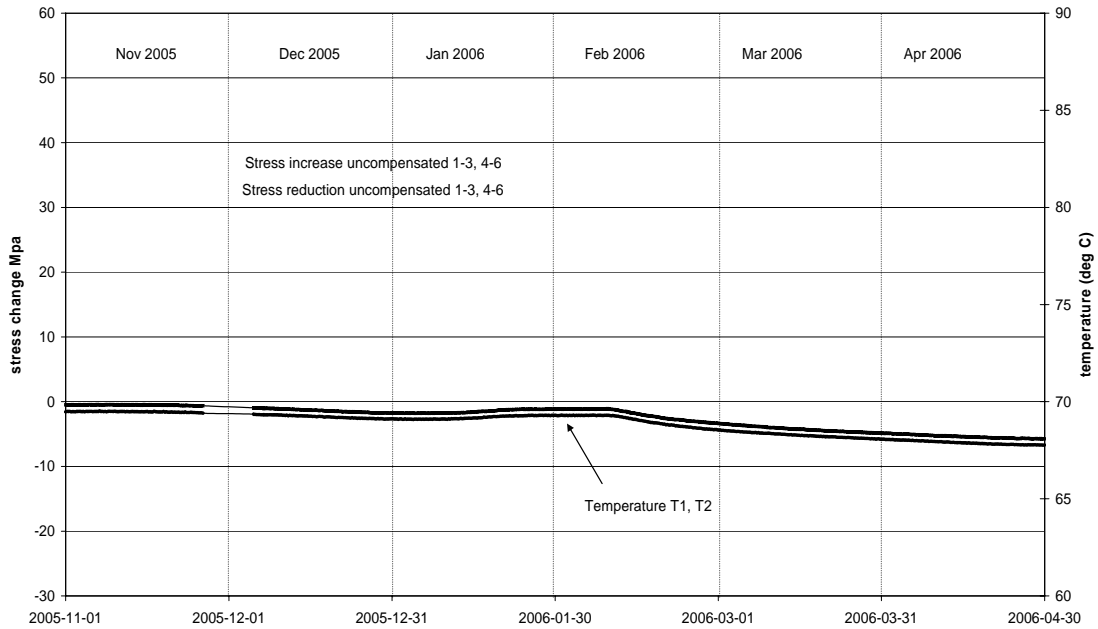
**Biaxial stressmeter B1**  
**Orientation of maximum stress increase in plane perpendicular to borehole axis**



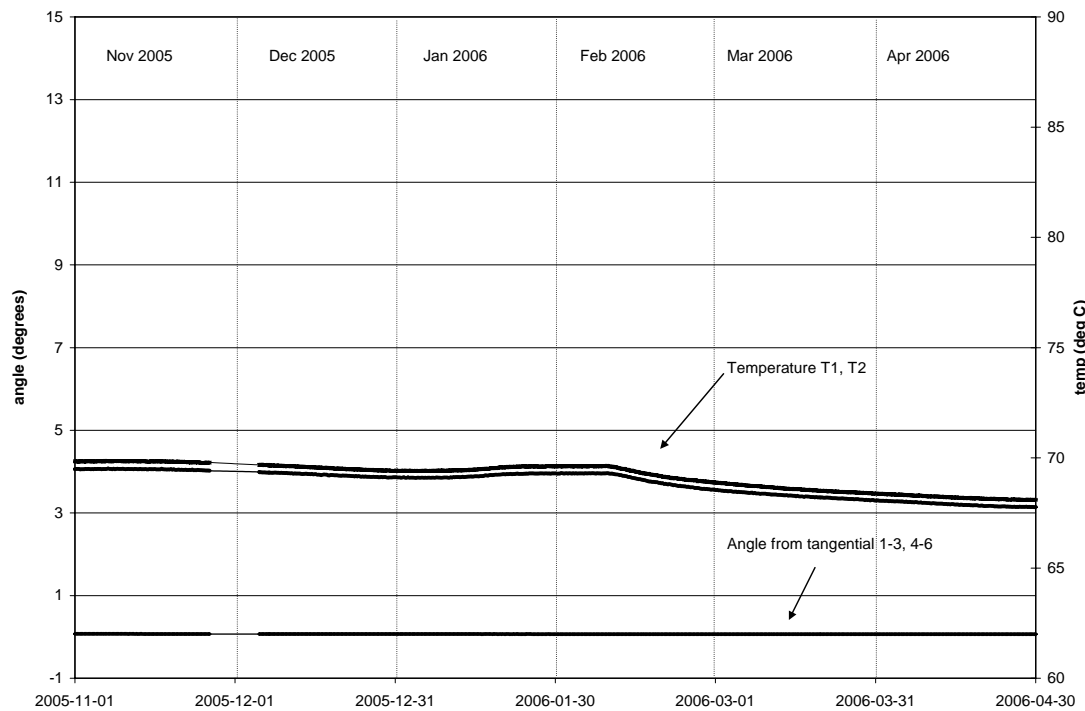
**Biaxial stressmeter C1 uncompensated for temperature:**



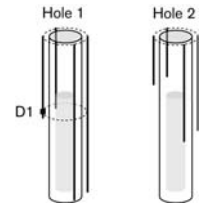
**Biaxial stressmeter C1**  
**Maximum stress increase and stress reduction in plane perpendicular to borehole axis**



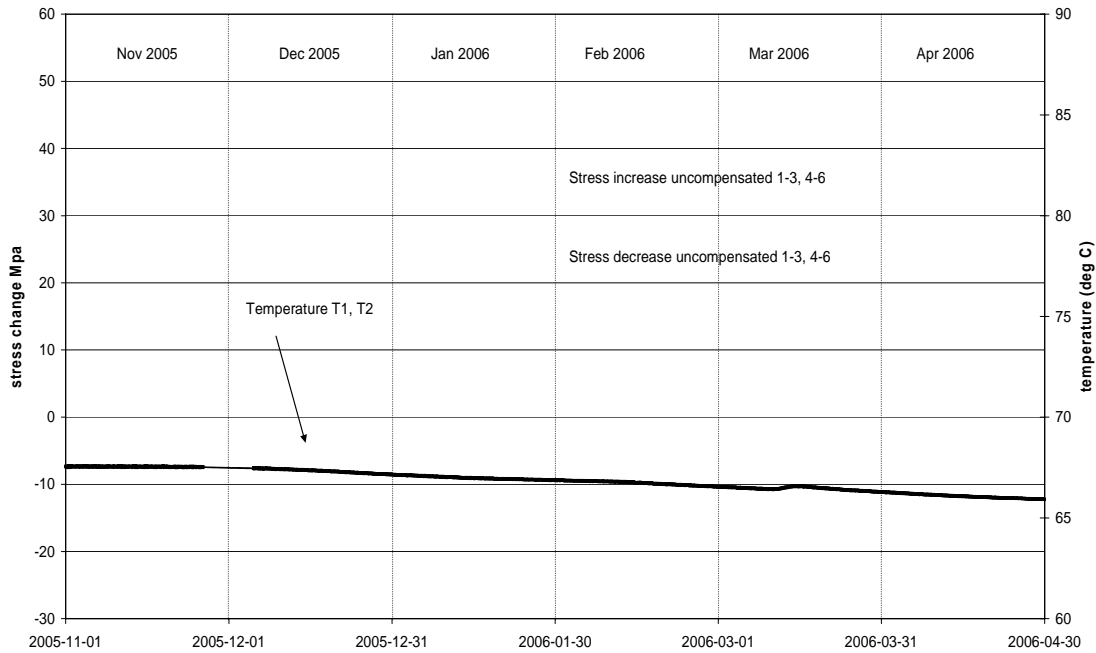
**Biaxial stressmeter C1**  
**Orientation of maximum stress increase in plane perpendicular to borehole axis**



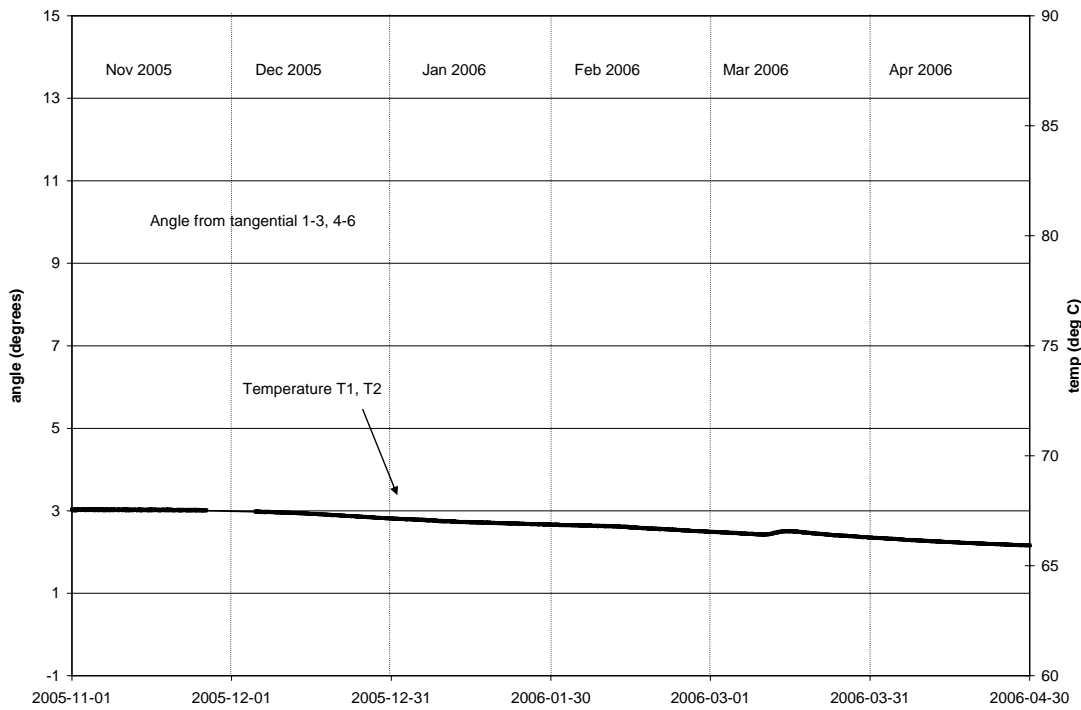
**Biaxial stressmeter D1 uncompensated for temperature:**



**Biaxial stressmeter D1**  
**Maximum stress increase and stress reduction in plane perpendicular to borehole axis**

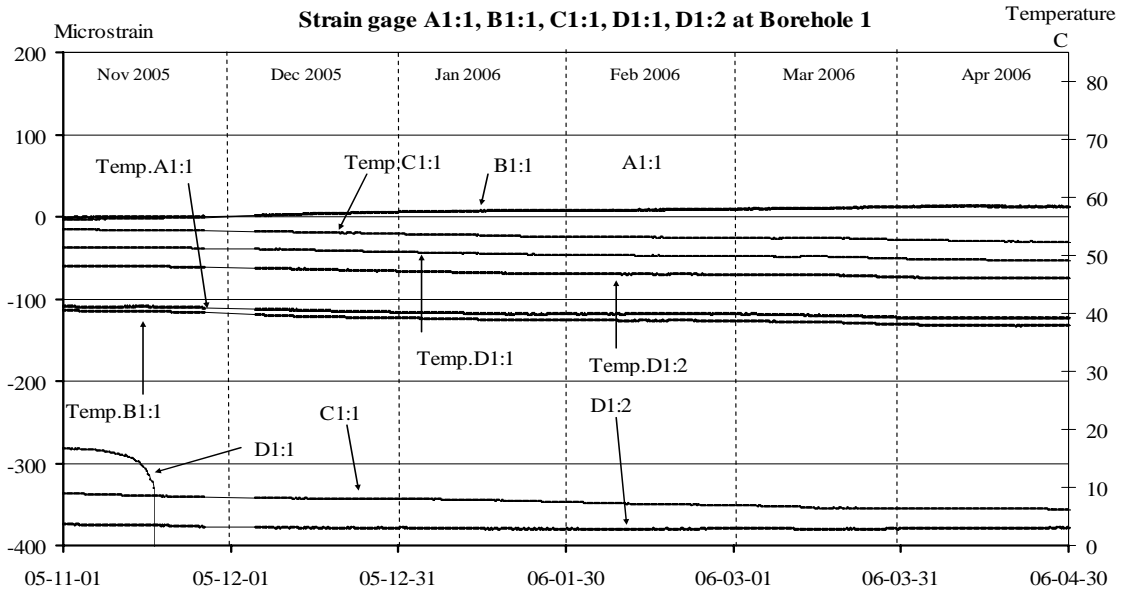
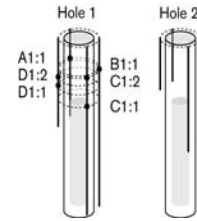


**Biaxial stressmeter D1**  
**Orientation of maximum stress increase in plane perpendicular to borehole axis**



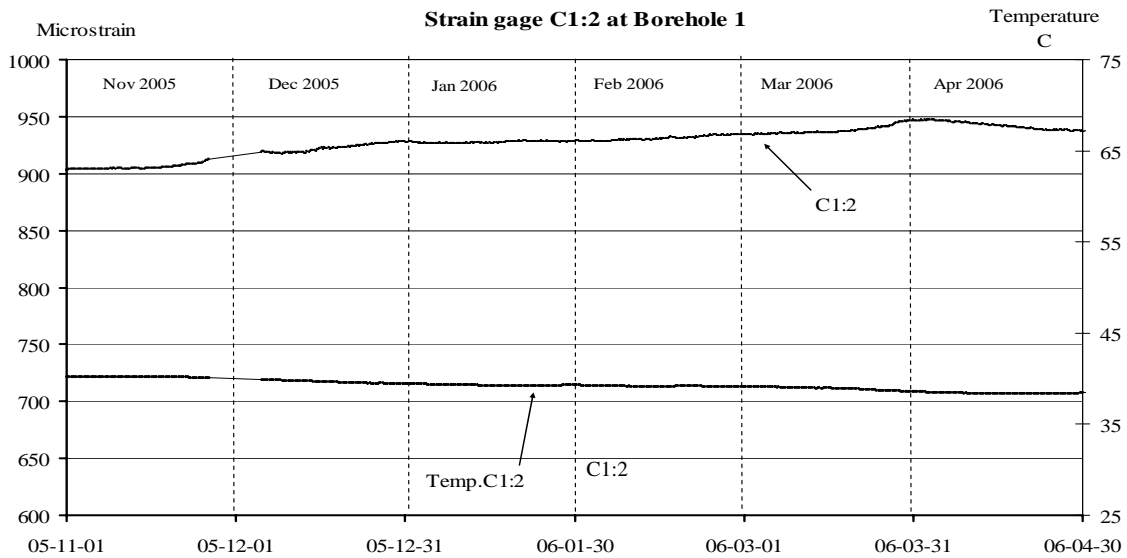


### 5.1.2 Strainmeter A1:1, B1:1, C1:1, D1:1, D1:2 (temperature compensated)



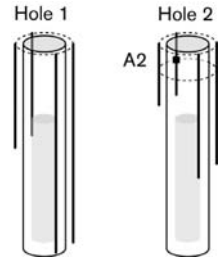
Positive values of microstrain represent elongation

### 5.1.3 Strainmeter C1:2 (temperature compensated)



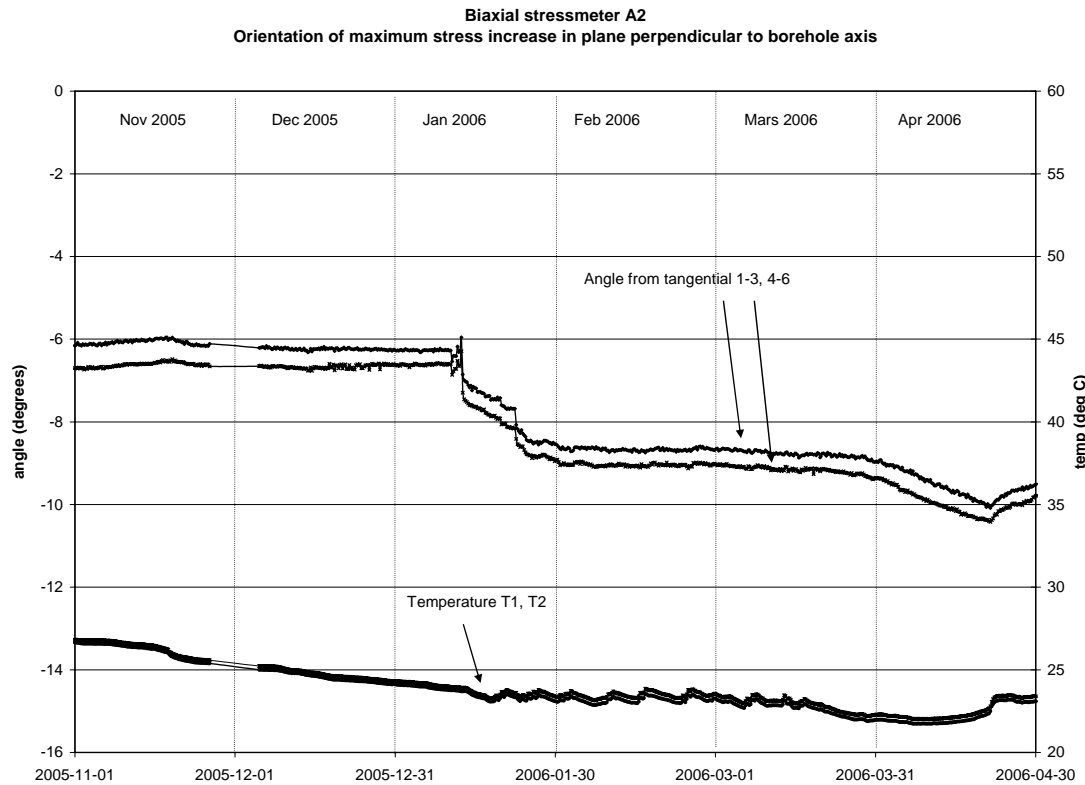
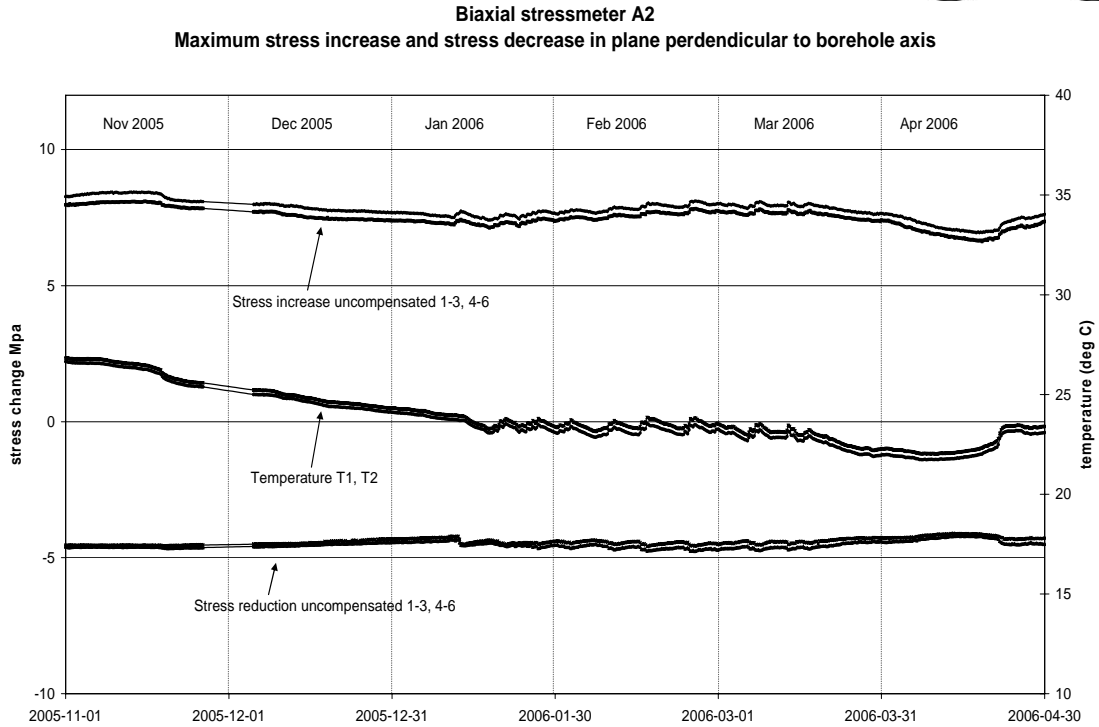
Positive values of microstrain represent elongation

## 5.2 Results of canister hole 2

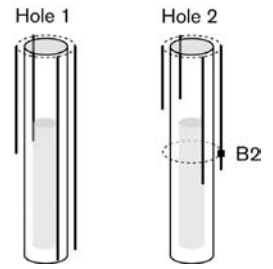


### 5.2.1 Stress change for each biaxial stressmeter

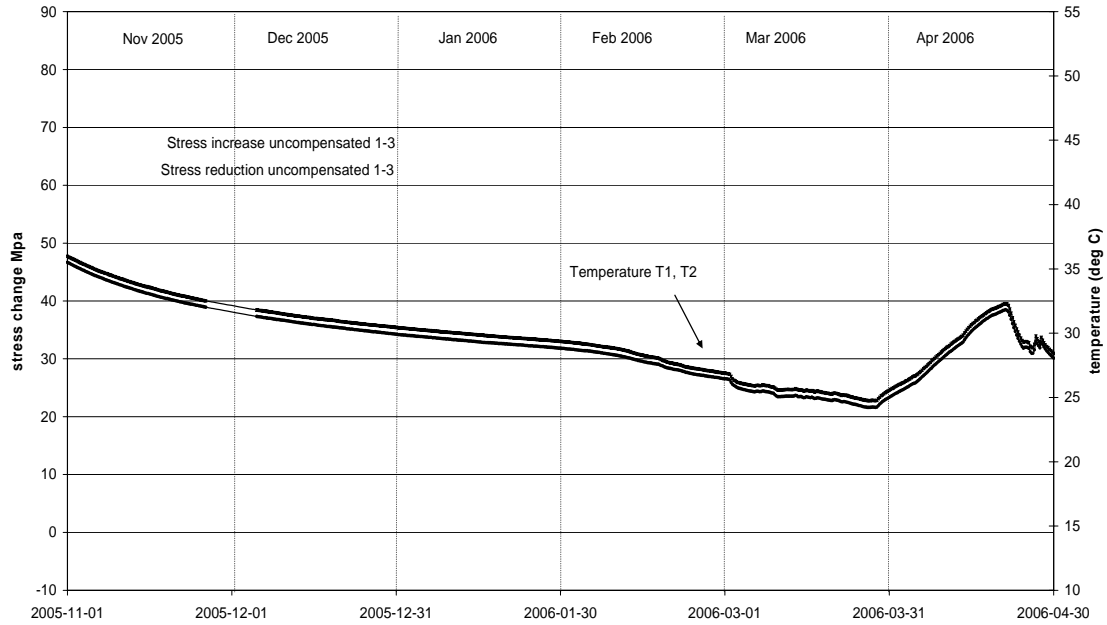
#### Biaxial stressmeter A2 uncompensated for temperature:



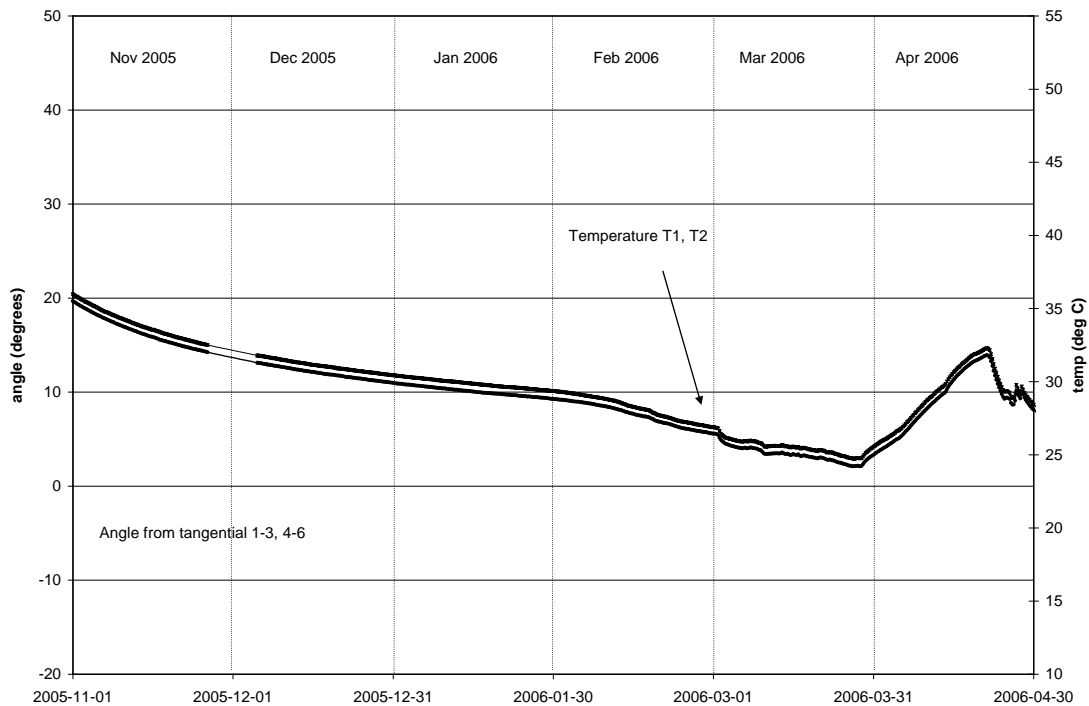
**Biaxial stressmeter B2 uncompensated for temperature:**



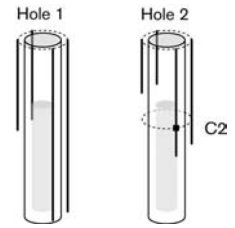
**Biaxial stressmeter B2**  
**Maximum stress increase ( $\sigma_1$ ) in plane perpendicular to borehole**



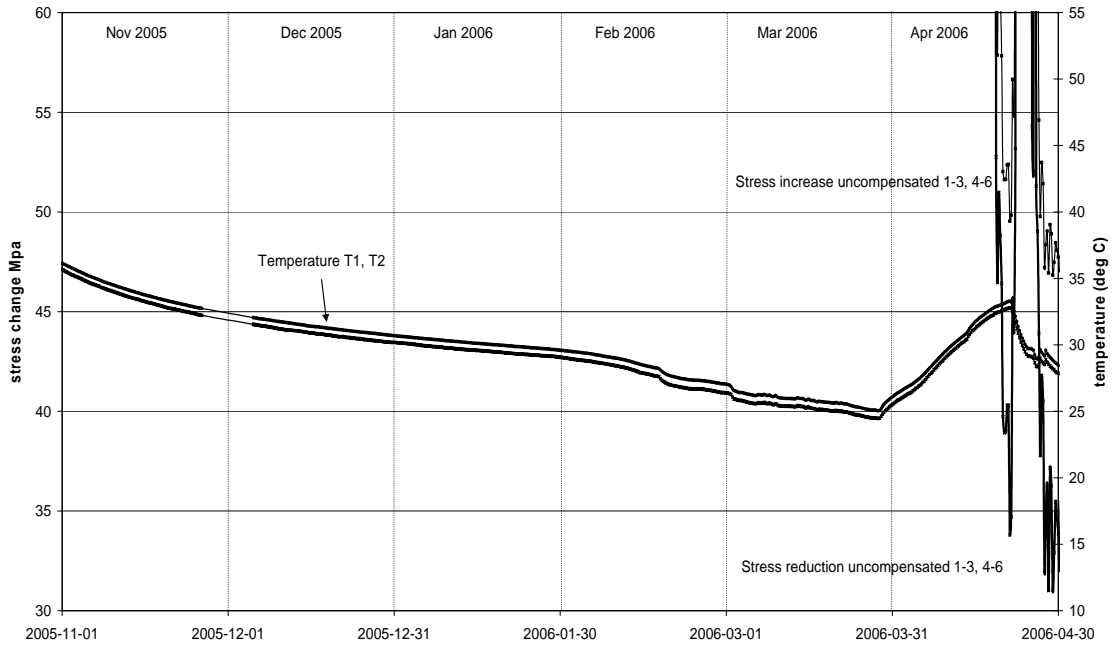
**Biaxial stressmeter B2**  
**Orientation of maximum stress increase ( $\sigma_1$ ) in plane perpendicular to borehole**



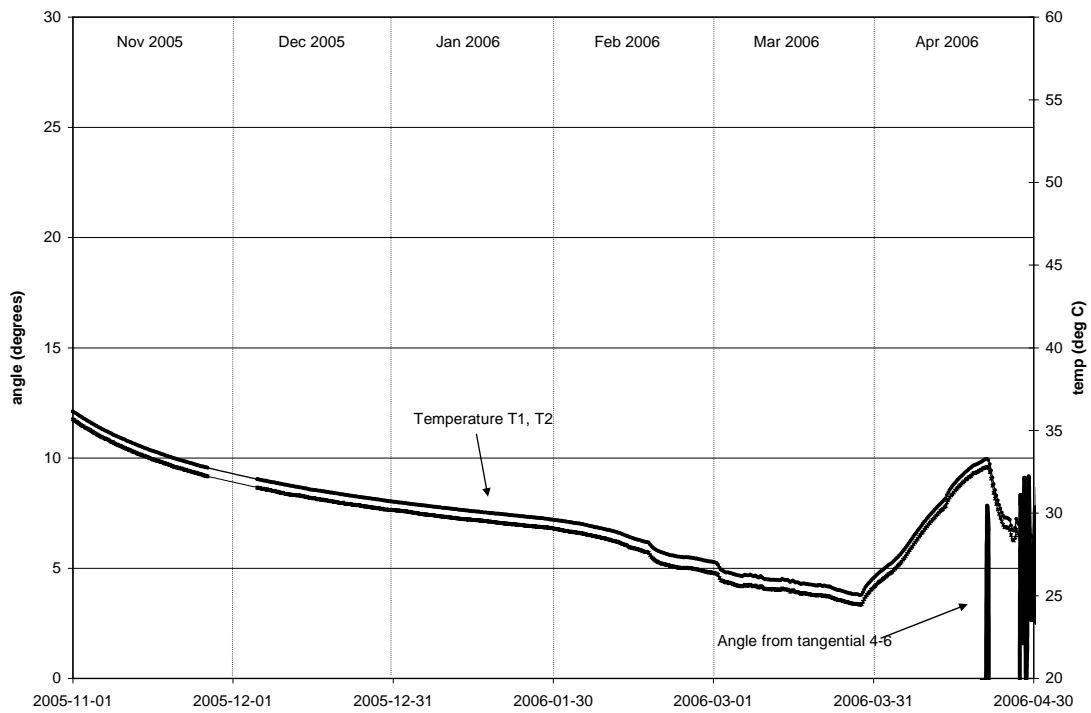
**Biaxial stressmeter C2 uncompensated for temperature:**



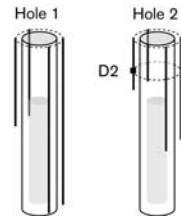
**Biaxial stressmeter C2**  
**Maximum stress increase and stress reduction in plane perpendicular to borehole axis**



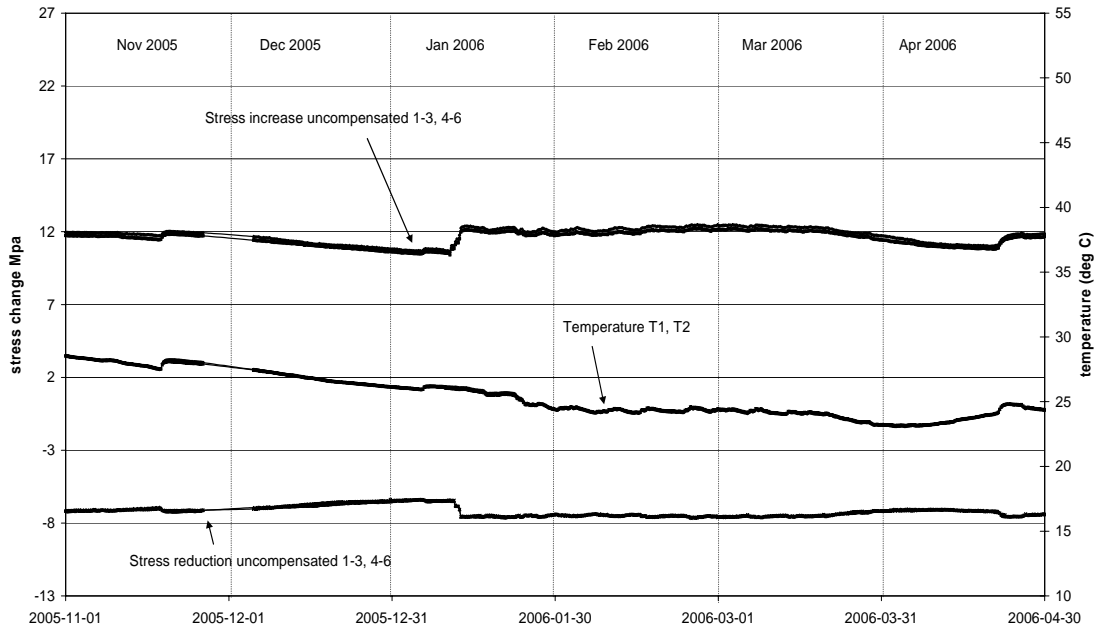
**Biaxial stressmeter C2**  
**Orientation of maximum stress increase in plane perpendicular to borehole axis**



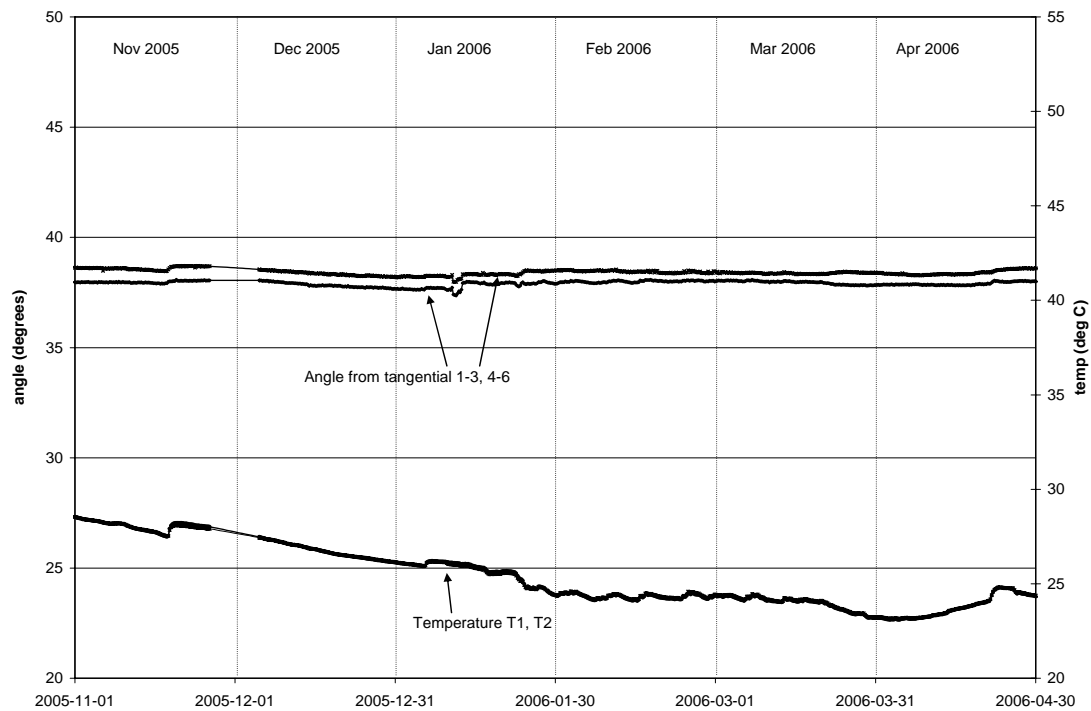
**Biaxial stressmeter D2 uncompensated for temperature:**



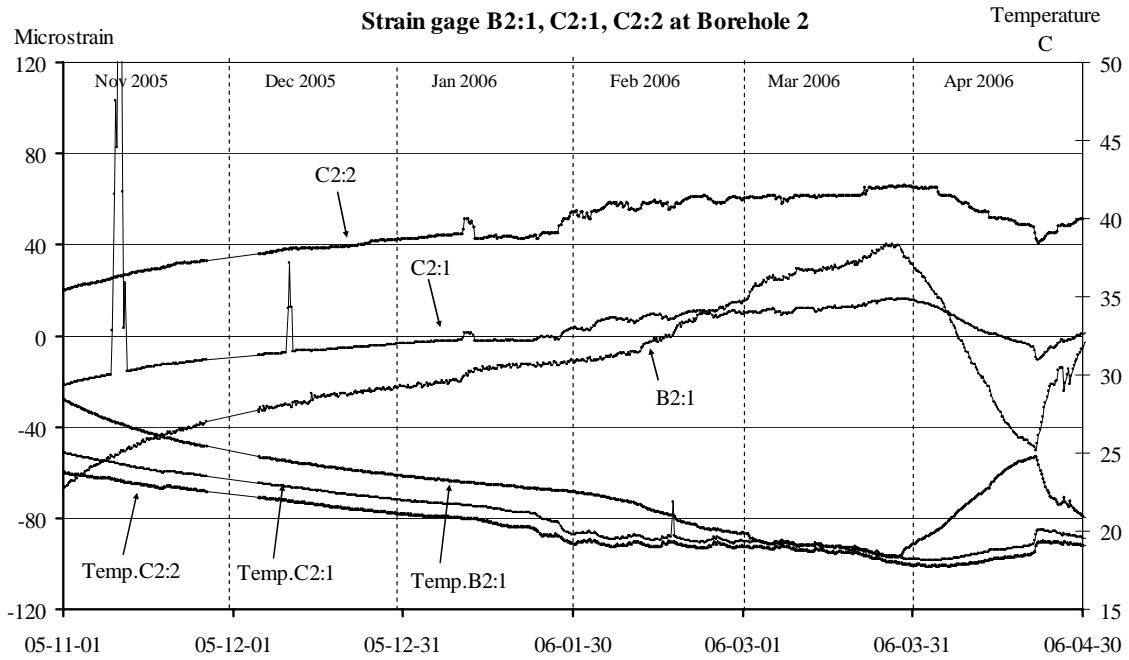
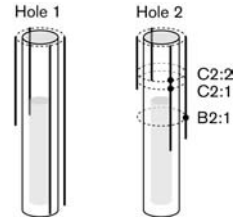
**Biaxial stressmeter D2**  
**Maximum stress increase and stress reduction in plane perpendicular to borehole axis**



**Biaxial stressmeter D2**  
**Orientation of maximum stress increase in plane perpendicular to borehole axis**



### 5.2.2 Strainmeter B2:1, C2:1, C2:2 (temperature compensated)



Positive values of microstrain represent elongation